Copy No. 9

NASA Project Apollo Working Paper No. 1100

ENVIRONMENTAL FACTORS INVOLVED IN THE CHOICE OF LUNAR OPERATIONAL DATES AND THE CHOICE OF LUNAR LANDING SITES

NATIONAL AERONAUTICS AND SPACE ADMINISTRATION
MANNED SPACECRAFT CENTER
~~Houston,~~ Texas

November 22, 1963

3307-63

NASA PROJECT APOLLO WORKING PAPER NO. 1100

ENVIRONMENTAL FACTORS INVOLVED IN THE CHOICE OF LUNAR OPERATIONAL DATES AND THE CHOICE OF LUNAR LANDING SITES

Prepared by: Staff of Space Environment Division

John M. Eggleston
Assistant Chief
Space Environment Division

Authorized for Distribution:

Maxime A. Faget
Assistant Director for
Engineering and Development

NATIONAL AERONAUTICS AND SPACE ADMINISTRATION

MANNED SPACECRAFT CENTER

HOUSTON, TEXAS

NOVEMBER 22, 1963

TABLE OF CONTENTS

LIST OF TABLES

LIST OF FIGURES

LIST OF FIGURES

LIST OF FIGURES

LIST OF FIGURES

ENVIRONMENTAL FACTORS INVOLVED IN THE CHOICE OF LUNAR OPERATIONAL DATES AND THE CHOICE OF LUNAR LANDING SITES

SUMMARY

Environmental factors that may influence the choice of Apollo operational launch dates are covered and recommendations made on the basis of the present state of knowledge. The present state of knowledge of large scale topography of the lunar surface is briefly reviewed and the best estimate of small scale topography given. Based on criteria for selection, ten lunar landing areas are recommended as most likely to contain acceptable landing sites. It is not intended that this paper serve as a detailed description of any single factor but rather to provide a sufficient appreciation of most of the environmental factors which will affect the operational planning of Apollo missions.

INTRODUCTION

The Apollo program is scheduled to land a man and over 200 pounds of scientific equipment on the lunar surface prior to 1970. However, many of the factors which will influence the choice of the exact date and the exact landing area must be chosen well beforehand for the purposes of mission planning, vehicle design, and space suit considerations. This paper, prepared by the Space Environment Division of the Manned Spacecraft Center, is intended to present, in a useful form, some of these factors. The paper first covers the variations in the environmental conditions: solar radiation, meteoroid streams, the heating and lighting conditions on the lunar surface, et cetera. The latter portion of the paper covers some of the present restrictions placed on the choice of lunar landing sites, a criteria used for picking these sites, and several possible sites which appear to satisfy these criteria.

The cislunar space and lunar surface environmental conditions are affected by those factors which are dependent on the phase of the lunar month, those conditions which occur on an annual cycle, and those conditions which appear at this time to be random. For the purposes of uniformity, a coordinate system has been used to define the phase of the lunar month. The system is shown in figure 1, along with a list of the factors considered in this paper. The reference line is chosen as the projection of the earth-sun line onto the earth-moon plane. The counterclockwise rotation of the moon about the earth is measured from this line by the angle, θ. Thus, "first quarter" occurs at the end of the first quandrant ($\theta = 90°$), full moon at $\theta = 180°$, et cetera. The view depicted

in this figure shows all motions to be counterclockwise: the earth's rotation about its polar axis, the moon's rotation about its polar axis, the moon about the earth (or, to be more exact, the earth and moon about their common center of gravity), and the earth-moon system about the sun, are all counterclockwise. Using the proposed "free-return" trajectory, the Apollo spacecraft will leave its earth-orbit with the rotation of the earth and will enter the lunar orbit opposite to the rotation of the moon about its polar axis. When it leaves this orbit, the Apollo spacecraft will return to earth with the rotation of the earth. As a rule-of-thumb, injection into translunar flight, injection into and out of lunar orbit, and entry into the earth's atmosphere will occur at a point very close to where the earth-moon line passes through each planet, but on the back side of each planet.

No inference should be given to the relative importance of the factors listed in figure 1 due to order of presentation or the length of discussion. All of the factors are important and most of them will require further investigation before the full mission plan for the Apollo spacecraft is firmly established.

ENVIRONMENTAL FACTORS

Meteoroids

In the earth-moon system, the meteoroid environment appears in two forms: (1) sporadic and (2) stream meteoroids. The sporadic meteoroids are individual particles having random orientation and no known relation with any other particle. Meteoroid streams consist of particles in relatively close proximity, each particle having a similar, but independent orbit about the sun. The particles are usually scattered rather uniformly along the entire length of the stream orbit and a predictable meteoroid influx is encountered each time the earth and stream orbits intersect. The dates and time duration of our passage through the major streams are predictable. The intensity (flux-mass and flux vs. time variation) is not well established.

Sporadic Meteoroids.- The sporadic meteoroid flux has been defined by Whipple (ref. 1) from measurements of meteors occurring within a known boundary surface. The original flux-mass relation has been modified to exclude earth shielding and to incorporate a constant density of 0.5 gm/cc. The number of particles/ft^2-day for a meteoroid mass, m, and greater at an average velocity of 30 km/sec is expressed as follows:

$$\log N = -1.34 \log m - 10.423 \qquad (1)$$

and is depicted in figure 2. It is to be noted the prescribed sporadic flux is a daily average for any month of any year and does not take into consideration the month-to-month variation that will be discussed subsequently.

It has been postulated in reference 2 that for particles less than 10^{-8} grams the particle concentration decreases with distance from the earth's surface at a rate inversely proportional to the distance to the 1.4 power to a minimum value at 10^5 km. However, this postulation has not been generally accepted nor evident in the measurements according to reference 3. This decrease has not been applied to the MSC meteoroid environment. The aforementioned flux-mass relation will define the primary sporadic meteoroid flux for near-earth, cislunar and lunar operations.

The sporadic meteoroids appear to be the scattered remains of ancient meteoroid streams and consequently do not display a symmetrical distribution in intercepting the orbit of the earth-moon system. As most observers will note, more meteors (meteoroids passing through the earth's atmosphere) are seen between midnight and dawn than are seen from dusk to midnight. The significance of this observation is that more meteoroids are intercepted on the earth's leading face than on its trailing face. This qualitative observation was quantitatively measured by Hawkins (ref. 4), and the results are plotted in figure 3. The observed results, labeled "apparent", are plotted in polar form in the top half of the figure and in a cartesian plot at the bottom. In the polar plot the moon is superimposed for reference since the same measurement will apply to the moon during a lunar month. A man standing on the lunar surface will "see" the same flux as a man standing on the same relative position on earth. Thus, a landing at the center of the visible face of the moon (0λ, 0β) will experience as much as $\frac{1}{5}$ less sporadic meteoroids (at $\theta = 270°$) during the last half of the lunar cycle ($180 < \theta < 360$) than the first half ($0 < \theta < 180$).

The dashed curve on these plots marked "stationary" indicates that the majority of the sporadic meteors are in a posigrade orbit about the sun and were overtaken by the earth-moon system. Starting with the observed or apparent distribution, astronomers have assumed all meteors have a velocity of 40 km/sec at a distance of one astronomical unit, and have subtracted (vectorally) the earth's heliocentric velocity of approximately 30 km/sec. If one accepts the assumptions, the result, shown on figure 3, indicates that an observer standing on an earth that was not rotating about the sun would see ten times as much flux moving in a posigrade as in a retrograde orbit (relative velocity = 42 km/sec).

Regardless of how valid such assumptions are, qualitatively we can

say that at the center of the visible face of the moon, during the phase from $\theta = 180°$ to $\theta = 360°$, the sporadic meteoroid flux will be significantly less and the velocity of the meteoroids that are seen will be significantly less (10 km/sec as opposed to 70 km/sec) than the opposite case. During this phase, the subject point on the moon is first in sunshine and then in earthshine.

The month to month variation of the sporadic meteors is indicated in figure 4 by the clear or open blocks. It may be seen that, on the average, sporadic meteors produce a maximum flux during June, July, and August and a minimum flux during January thru April. In figure 4, the sporadic flux monthly variation has been compared to the MSC meteoroid flux model. The MSC flux represents a cumulative flux of the sporadic meteoroids of visual magnitude +5 and greater. Note that each unit of the ordinate has been normalized to the MSC average sporadic flux of 48.5 meteors/hr.

Meteor Showers.- Noticeable increases in the average hourly rate of meteor activity occur at regular intervals during the calendar year. This increase is due to the earth's passage through streams of particles traveling in parallel heliocentric orbits and generally assumed to be cometary debris. To the observer on earth, these streams of meteors appear to originate in various well-known constellations that serve as a means of classification.

The orbits of 9 major streams (18 major streams have been tabulated in the SED meteoroid environment, reference 5) are superimposed on the earth's orbit in figure 5. The flux rates of some of the 18 major streams have been added to the monthly distribution of the sporadic meteoroids in figure 4. The flux-mass relation has been determined for only a few streams and in a limited visual magnitude range; therefore, the total meteoroid flux at any mass has been defined as:

$$(f_{total})_m = f_{stream} + f_{MSC\ sporadic} = 48.5N \qquad (2)$$

N = ordinate of figure 4

m = mass

This graphical interpretation assumes all stream flux-mass variations follow the same distribution law as was given in figure 2 for sporadic meteors. The stream flux is at a minimum January thru April and the last of August thru September. It is to be noted that although the number per unit time of the stream meteoroids greatly exceeds the sporadic meteoroids, the integrated total of streams is only 20 to 30 percent of the total measured meteors.

The meteoroid stream radiants have been used in conjunction with the lunar phases to illustrate the shielding provided by the moon to a man

standing on the lunar surface at the position of the zero latitude and zero longitude during the year 1963. In the simplified approach to this problem the inclination of the meteor stream has been considered in the ecliptic plane for all inclination equal to or less than 45°. The area of the moon intercepted by the stream is ±90° of the substream point as it moves with the rotation of the moon during the moon's passage thru the stream. The result is shown in figure 6. From January 5 thru April no meteoroid streams will be encountered. From May 1 thru December, the open areas of figure 6 indicate streams that will intercept the moon, but will not impinge at 0λ and 0β. The following table lists stream name, and date of activity of streams that do not intercept the lunar position 0λ, 0β during 1963:

O-Cetid	May 14 to 23
Arietid	June 13 to 19
Perseids	June 13 to 16
β Taurids	June 24 to 27
Northern Taurids	October 28
Southern Taurids	November 10
Geminid	November 27 December 10

The regions of the moon shielded for all of the major streams (taking into consideration the stream altitudes) for the years 1965 to 1970 will be presented in a working paper in the near future.

Secondary Ejecta.- The lunar surface meteoroid flux will have a primary meteoroid flux composed of the sporadic near-earth meteoroid flux, the stream meteoroid flux plus a secondary flux composed of ejecta as a result of primary impingement; the flux of secondary particles has been theoretically predicted in reference 6 to be 10^4 greater than the primary and to persist up to a lunar altitude as high as 30 km. The density of the ejecta is 3.5 gm, with a maximum velocity of 2.4 km/sec; however, reference 6 states that 99.75 percent of the ejecta has a velocity of 1 km/sec or less. The secondary flux presented in figure 2 includes a shielding factor of $\frac{1}{2}$, but does not take into consideration the percentage of the ejecta flux that have negligible velocities.

The flux-mass relation of secondary ejecta on the lunar surface can

be expressed as:

$$\log N_s = -1.34 \log m - 6.59 \qquad (3)$$

The hazard of the secondary meteoroid flux has been compared with the primary meteoroid flux by using a Summer's penetration equation for a skin of finite thickness for the primary flux and a Bohn and Fuchs, reference 7, low velocity penetration equation. When converted to penetrations/ft^2-day, the secondary flux of equation 3 produces one order of magnitude less penetrations than the primary flux.

RADIATION

There are three potential radiation hazards to Apollo: cosmic radiation, trapped (Van Allen) radiation, and solar flare radiation. The cosmic radiation and the trapped radiation do not affect the choice of a lunar landing site or time. Although the radiation dose received during exit through the belts is a function of the exact trajectory, which in turn is influenced by the lunar declination, in no case does the dose exceed the design limits. The solar flare radiation in the form of protons shows an apparent yearly variation and also has directional properties which make the shielding provided by the moon a function of the landing site.

Yearly Variations.- It appears that certain months in the year produce more solar proton events than others. Figure 7 shows all of the recorded events during the last two solar cycles on a polar plot. It is apparent that the events tended to occur in the spring and fall and not to occur in June and December. The favorable launch periods, shown in the figure as shaded regions, coincide almost exactly with the crossing of the solar equator by the earth in its orbit. A fairly acceptable physical interpretation of the coincidence between the absence of events and the crossing of the solar equator is given by considering the proton streams as following the solar magnetic field lines. If at the solar equator the lines are perpendicular to the equatorial plane, the proton streams in this plane would have difficulty in propagating out to the earth's orbit.

Long-Term Variation.- There is a connection between the occurrence of solar proton events and the sunspot cycle, in that solar proton events tend to occur during the half of the cycle when sunspots are numerous and not to occur during the half when sunspots are rare. Figure 8 shows the last sunspot cycle projected into the next cycle. The region in which events occur is shaded.

Monthly Variation.- The effect of landing site choice on the solar proton environment depends upon the orbital position of the moon within the lunar month. This is because of the moon's position in relation to the directionality of some solar proton events. It is estimated that for two-thirds of the proton events (including all of the large events) about 10 percent of the proton flux is highly directional, coming from a directional, coming from a direction 50° to the west of the sun. The remaining 90 percent is omnidirectional. If the phase of the moon is such that the moon is between the landing site and the direction of the radiation, then the moon provides complete shielding from the directional part of the radiation. Such directional radiation occurs during the early part of the proton event, with more and more of the flux becoming isotropic, until at a time ranging from 5 to 20 hours after the beginning of the proton event, the flux is completely isotropic. This is largely because the early high energy particles tend to move directly down the magnetic field lines connecting the sun and the earth while the low energy particles are scattered and diffused. The more indirect a particle's motion, the longer it takes to arrive, and the more randomly oriented its direction will be when it arrives. Figure 9a shows that the high energy particles arrive earlier in an event, with the spectrum becoming "softer" as the event progresses. The actual dose reduction is complicated by the fact that even for the nondirectional radiation, a vehicle in the vicinity of the moon is shielded from one-half the free-space radiation. With this nondirectional radiation consistuting 90 percent of the total, a vehicle or a man on the moon will receive either 45 percent or 55 percent of the free-space radiation dose, depending on whether he is on the side away from or the side toward the directional radiation. Figure 9b shows the percentage of the free-space dose to be received at various locations and lunar phases. It may be seen that an observer standing on the lunar surface at (0λ, 0β) would receive less radiation during phases of the lunar month from about $\theta = 220°$ to $\theta = 40°$. During most of this period the point (0λ, 0β) is in earthshine (Partial to full). Another consideration is that because the directional protons occur early in the event, the effective warning time of a proton event is increased. This is especially significant when one considers that the LEM and a space suit offer practically no radiation shielding. Basing the dose reduction on comparative LEM - C/S module shielding, one may obtain 20 - 40 percent reductions, depending on the final LEM design.

LUNAR TEMPERATURES

The temperature at any point on the lunar surface depends upon the following factors:

Incident Solar Radiation.- This quantity will vary from a maximum

value of 2.0 cal cm^{-2} min^{-1} (±5 percent) at the subsolar point to a minimum value of zero beyond the terminator. Due to the inclination of the moon's axis, (α), the subsolar point will range between 1.533° north and 1.533° south of the lunar equator. Thus, to a good approximation, if A_o represents the incident solar radiation at the subsolar point, then at any other level surface on the daylight hemisphere,

$$A(\lambda, \beta) = A_o \cos \lambda \cos (\beta \pm \alpha) \qquad (4)$$

$$270° \leq \lambda \leq 90°, \quad \beta \pm \alpha \leq 90°,$$

where λ and β are the longitude and latitude of the point measured from the center of the illuminated disk. The negative sign on α applies when the subsolar (SS) point lies on the same side of the lunar equator as the point (λ, β) while the positive sign holds when the subsolar point lies on the opposite side of the equator from the point. The angle α varies between 0° and 1.533°. Under the constraints imposed on λ and $\beta \pm \alpha$, the incident solar radiation drops to zero beyond the terminator.

The value of A_o is not constant, as the earth-moon orbit about the sun is elliptical, of eccentricity 0.01675. This distance variation produces a resultant variation in A_o of ±3.35 percent. The blackbody temperatures at the subsolar point are 397.6° K. at perihelion and 391.1° K. at aphelion. The remainder of the ±5 percent uncertainty in the solar constant, A_o, is due to measurement errors.

Local Surface Reflectance.- One needs to know what fraction of the incident solar radiation is reflected. Letting ρ be the local reflectance, we see that $A(\lambda, \beta)$ $1 - \rho$ represents the amount of incident solar radiation which is absorbed at the point (λ, β).

From data acquired in the visible region of the spectrum, (that is, $0.35\mu \leq \lambda_{sp} \leq 0.8\mu$), the reflectance of the lunar surface is found to vary from 0.05 to 0.17. The reflectance dependence upon the wavelength shows it is 2.5 times greater at 0.8 microns (μ) than at 0.35μ. One also needs to know the distribution of the incident solar radiation with wavelength. About 53.3 percent of the solar constant lies in the wavelength range $0.35\ \mu \leq \lambda_{sp} \leq 0.8\ \mu$. This is the region in which the visual reflectance of the moon has been measured. Since no detailed information on the lunar infrared reflectance is available, there is uncertainty as to what value should be used for the integrated solar reflectance of the lunar surface.

Calculations indicate that the integrated solar reflectance $\bar{P} = 0.053$. This value should be refined as more detailed knowledge becomes available.

The resultant subsolar point blackbody temperature for $\bar{P} = 0.053$ is 390° K. This is calculated with the following equation:

$$A_o = (1-\bar{P})\ \sigma\ T_{SS}^{4} \tag{5}$$

Regardless of this uncertainty, the fact remains that there is a variation of reflectance with position on the moon. The brighter areas (greater reflectance) absorb less of the incident solar radiation than the darker areas (smaller reflectance). Consequently, there will be local temperature variations on the moon due to differences in surface reflectance. The brighter areas will tend to be cooler than the darker areas, all other things being equal.

Local Surface Geometry.- The chief mechanism for heat transfer between local features of the lunar surface is radiation. A perfectly smooth spherical surface would not experience radiative heat transfer between any parts of its surface, since no part of the surface can "see" any other part. However, as the moon's surface is far from perfectly smooth on a scale of kilometers and possibly meters, there is appreciable radiation heat transfer going on. This mechanism will cause concave depressions, valleys and crevices to become focal points, as it were, for reflected and re-radiated solar energy. This is due to the fact that such features are "seen" by effectively more of their surroundings, and consequently less of the incident radiation is able to escape from such "heat traps". This has the obvious effect of causing the temperatures of such features to be higher than that of the surrounding level areas having the same reflectance and thermal properties.

Another geometrical factor is the inclination of the local surface relative to the local horizontal plane. Equation 4 is valid only when the local surface coincides with the local horizontal plane. When this is not the case, the insolation term becomes simply $(1-\bar{P})\ A_o \cos\theta$, where θ is the angle between the normal to the surface and the direction of the sun. Since the RMS slope on the moon is believed to be less than 12°, this factor will not alter the temperatures of smooth areas by more than 2 percent. However, in regions of sharp relief, there will be a considerable spread in the incident solar radiation about the value $A(\lambda, \beta)$ calculated from equation 4. However, this spread can never be so large as to cause $A(\lambda, \beta)$ to exceed A_o. Due to this effect, a surface feature located at

$$\lambda = 0°,\ \beta = 45° + \alpha$$

and tilted towards the sun by a local slope of $45° + \alpha$, would be at the same temperature as a horizontal surface at the subsolar point, assuming the reflectance and thermal properties to be the same in both cases.

Thus, it appears that localized "hot spots" can arise due to purely geometrical effects, namely, local slope causing tilting of the local surface toward the sun and local topography acting to trap the incident radiation.

Local Thermal Properties.- The incident solar radiation which is absorbed by the lunar surface is budgeted in the following manner:

1. Re-radiated at the local surface temperature,

2. Stored in the material on the lunar surface,

3. Conducted into the interior of the moon.

Thus, the significant parameters for determining the local surface temperature which will balance the absorbed solar radiation are ϵ, emissivity of the surface, ρ, bulk density of the surface material, C, the specific heat, and k, the thermal conductivity. The latter three of these parameters combine to form the quantity known as thermal inertia:

$$\gamma = (k\rho c)^{-\frac{1}{2}} \tag{6}$$

It is this quantity which is evaluated by fitting theoretical temperature curves to measurements of lunar thermal emission during eclipses and lunations. To date, the eclipse temperatures are best fitted by a value of γ = 1,000 (C.G.S. units), the lunation temperatures by γ = 500. The apparent contradiction between the value of γ obtained from eclipse temperatures and lunation temperatures would be overcome if the lunar midnight temperature were to drop as low as 98° K. (instead of 120° K. as reported by Pettit and Nicholson in reference 8). This would raise the value of γ (which is inferred from the lunation temperatures) to 1,000, the same as for the eclipse data. Increasing γ would not alter the maximum temperature at lunar midday by more than several degrees, while it would depress the night time temperatures by about 20° K. Such a solution may be justified as Murray, reference 9, has recently measured temperatures as low as 105° K. on the night side of the moon. Since this was the lowest temperature his instrumentation could detect, the actual temperatures may lie still lower.

The emissivity of the lunar surface is related to the surface reflectance. In fact, assuming the moon to behave as a grey-body radiator, one can let $\epsilon = 1-\rho$. This assumes thermal equilibrium, which probably exists only near the subsolar point. Emissivity also varies according to material composition. Until we have a sample of the lunar surface, we can only make approximations to the emissivity.

Calculated Lunar Surface Temperature Models.- Calculations of lunation temperatures have been made on the basis of two extreme models for the lunar surface. One model postulates granular material (10-300μ particle size range) at least 40 cm in depth with $\gamma = 1,292$. The other model consists of solid rock having $\gamma = 32.7$, with no overlying dust.

Both models are assumed to consist of a semi-infinite solid possessing homogeneous thermal properties everywhere on the surface and to a considerable depth as well.

The surface temperatures calculated could be interpreted as representing the temperatures along the meridian passing through the subsolar point.

Figure 10 shows the level surface temperatures along the parallel of latitude passing through the subsolar point during a complete lunation (29.53 days) for both of the assumed extreme models. The maximum temperature was taken to be 390° K. (measured values range from 370-407° K.). The temperature at lunar midnight is 94° K. for the granular model and 202.5° K. for the rock model. This is to be interpreted in light of reported measured values ranging from 105° K. to 123° K. Since the rock model remains quite warm into the lunar night, it does not correspond too well with the known facts. However, there may well be isolated bare spots which would remain distinctly warmer during the night. Such anomalous "hot spots" have been reported by Murray, reference 9.

The pre-dawn temperatures dip to 85° K. for Model I and 185° K. for Model II. The lowest recorded lunar temperature is 105° K., which would seem to favor the dusty insulating surface.

It is felt that these temperature curves represent the limits between which the lunar surface temperature at any point near the lunar equator will vary during a complete lunation (29.53 days), neglecting the focussing effect of local topography and any extreme variations in local surface reflectance.

In order to provide an idea of the range of variation possible in the local surface temperature due to variations in the incident solar radiation, local reflectance, slope, topography, and thermal properties, the following list of extreme variations for the daylight hemisphere has been computed.

Cause	Δ T (° K.)
1. Variation in amount of incident solar radiation	±3° K.
2. Variation in local surface reflectance	±10° K.

Cause	ΔT (°K.)
3. Variation in local surface slope	±2.5° K. (Assuming RMS slope less than 12°)
4. Variation in local surface	±30° K. (focusing) -100° K. (shadows)
5. Variation in local thermal properties	±40° K.

It should be noted that the variations in surface temperature due to causes 1, 2, 3, and 4 in this list will decrease during the lunar night. However, the ΔT produced by variations in local thermal properties is likely to perist through the lunar night. Variations in the local thermal properties could arise from differences in chemical composition, state of the material, and thickness of the overlying insulating surface layer of granular material. There is even the chance of a concentration of radioactive rock strata underlying a region causing local heating.

Figure 11 shows the change in surface temperature which occurs during successive 6.0 hour intervals of a lunation. The most severe temperature rate of change occurs in the case of the granular model, where the temperature soars 60° K. in the first 6.0 hours following sunrise.

In figure 12 is seen an isothermal scan made of the near full moon. This illustrates that the isothermal contours are essentially concentric circles about the subsolar point. The fine detail is produced by local differences in reflectance, surface slope, topography, and thermal properties.

Figure 13 shows the position dependence of the actual level of the surface temperature, upon the temperature at the subsolar point, where θ denotes either the longitude of a point located on the parallel of latitude passing through the subsolar point if $\alpha = 0$. In addition one can think of θ as the angle between the normal to the local surface and the direction of the sun's rays when this local surface does not coincide with the local horizontal plane. In this case the insolation term E is given by

$$E = (1 - \rho) A_o \cos \theta \qquad (7)$$

Therefore, it can be said that the average temperature of any locale on the moon can be calculated throughout a lunation to within an accuracy of 10 percent. However, any attempt to determine the temperature fluctuations about this average temperature must await the acquisition of detailed

information about local properties (such as reflectance and thermal constrants) and local geometry (such as slopes and small-scale topography).

Due to a negligible lunar atmosphere, heating by convection should be no problem to the Apollo astronaut. The problems of incident solar radiation can be calculated only if space suit and spaceship thermal parameters are known. The only heat criteria for the Apollo landing that can be discussed here with any authority are those concerning direct conduction from the lunar surface to the astronaut or to the LEM. At the subsolar point the surface has the temperature of boiling water; but it falls to about 130° F at 60° of phase on either side, a temperature not unknown on earth. It may be considered "safe" from here to the terminator where it falls very rapidly from the freezing point of water at a rate of about 10° F per hour. During the lunar night, temperature extremes below 100° K. may impose severe operational problems.

LUNAR LIGHTING ENVIRONMENT

Galileo Galilei in his "Dialogues on Two Systems of the World" was one of the first to write about the rather unusual photometric characteristics of the moon. Observed near the full moon phase no significant difference in brightness is detectable between the limb regions and the center when albedo differences are eliminated; yet, it is known that a diffusing sphere illuminated by a distance source should appear the brightest at the center. This strong back scattering characteristic of the moon, observed more than 300 years ago, is believed to be due to the structure of the surface. In order that the physical structure of the lunar surface could be assessed, studies have been carried out on the change of surface brightness throughout a lunation. The resulting data, properly interpreted, are a rich source of information for the derivation of a photometric model for predicting the brightness of the lunar surface under all conditions of viewing and illumination.

Photometric Model.- In the derivation of a photometric model (ref. 10) for the moon, the definition of albedo applicable to lunar studies may be used as the first step. Several definitions of albedo exist in scientific literature; but only one, normal albedo, is used for determinating the reflecting power of the lunar surface.

Normal albedo ρ is defined for the moon as the ratio between the luminance B of the lunar surface when observed parallel to the illuminating rays at full moon to the luminance, B_o, that a Lambert (a theoretical surface whose luminance is independent of the angle of emittance) surface or unit reflectivity will exhibit at zero angle of incidence and a illumination level equal to the solar luminous constant.

Thus,

$$\rho = \frac{B}{B_o} \tag{8}$$

It can be shown that the luminance B_o of a Lambert surface is related to the illumination E in lumens/unit area by the formula

$$B_o = \frac{E}{\pi} \tag{9}$$

By combining equations (8) and (9) the luminance of the lunar surface at full moon will be given by

$$B = \frac{E}{\pi} \rho \tag{10}$$

The luminance of the lunar surface under all conditions of illumination and viewing can be expressed in terms of full moon luminance by introducing the factor Φ.

$$B = \frac{E}{\pi} \rho \Phi \tag{11}$$

The variable Φ is termed the photometric function and depends on the value of the photometric angles i, ϵ, and α that define the viewing and illumination geometry. The variable i is the angle of incidence of the source measured from the normal of the reflecting plane, ϵ the angle of viewing again measured from the normal and α is the phase angle measured between the direction incidence and the direction of viewing (fig. 14). Since it has been observed that the isophotes (lines of equal brightness) for the lunar surface follow the meridians (if the effects of albedo differences are eliminated) the lunar photometric function can be expressed in terms of only two variables τ and α. The variable α is again the phase angle and τ is the angle measured in the phase plane containing α from the direction of viewing to the projection of the normal on the phase plane. The angle τ can be thought of as the projection of the angle of viewing, ϵ, onto the phase plane containing α.

The photometric function, therefore, is expressed as a function of the two variables α and τ and is shown in figure 15. Unlike α, the angle τ may be either positive or negative depending on the position of the sun relative to the observer. To uniquely define the function, Φ, the angle τ is arbitrarily considered positive only when the viewing line lies between the normal and the line of illumination as illustrated in sketch C of figure 16 and negative in all other cases.

The unusual photometric properties of the moon are believed to be due to the characteristics of the surface structure. If features exist on the moon with surface texture differing from the areas that the data was obtained from for the development of the model (fig. 15), it is highly probable that the model will not be applicable. The function given in figure 15 was obtained by normalizing the relative surface brightness of the moon to unity at 1.5° phase angle with the fundamental assumption that the surface features to which the model will be applied would attain their maximum brightness at full moon. Features such as Tycho, Copernicus and Aristarchus and some rays associated with them are examples of formations to which the model will not be applicable. They generally achieve maximum brightness when the sun is nearly vertical over the formation.

Natural Light Sources and Intensity.- The primary source of illumination for all solar bodies including the moon is that radiated by the sun. At the moon's mean distance from the sun, the solar luminous constant is 13.4 lumens/cm^2, but due to the eccentricity of the earth-moon system in its orbit about the sun it will vary from 12.9 lumens/cm^2 at aphelion to 13.9 lumens/cm^2 at the perihelion point.

The intensity of the earth reflected light (earthshine) upon the moon depends primarily upon the phase of the earth and to a lesser extent the earth albedo. For a mean earth albedo of 40 percent, figure 17 shows the variation of earthshine intensity as a function of earth phase (ref. 11).

The intensity at full earth is 1.35 x $(10)^{-3}$ lumens/cm^2, but due to the variation of earth albedo it may vary from 1.08 x $(10)^{-3}$ to 1.75 x $(10)^{-3}$ lumens/cm^2. The reflectance of the earth may take on values from 32 percent to 52 percent, depending on the amount of cloud cover present. For comparison purposes the intensity of earthshine on the moon at full earth and a 40 percent albedo is 60 times greater than the magnitude of the light striking the earth's surface from a full moon located at the zenith with an intensity of 2.26 x $(10)^{-5}$ lumens/cm^2 including 30 percent attenuation by the earth atmosphere.

In addition to sunlight and earthshine, the stars and the planets will illuminate the moon. Starlight on the moon will be 43 percent greater than here on earth and will have an intensity of 2.2 x $(10)^{-7}$ lumens/cm^2.

Surface Brightness.- The luminance of the lunar surface depends primarily upon the intensity of the illumination and secondarily upon albedo and the photometric angles, i, e, and α. The value for the albedo of

several prominent features of the lunar surface is given in table I. Figure 18 illustrates the change in surface brightness for a mare area at 0° λ, 0° β throughout a lunation. The large change in surface brightness between new moon and full moon is due primarily to the variation in illumination level. At full moon the illumination from the sun is 13.4 lumens/cm^2 and at new moon the intensity of earthshine is 1.35 × $(10)^{-3}$ lumens/cm^2 or a factor difference of 10,000.

The luminance values illustrated in figure 18 are for normal viewing and will not be applicable if the angle of viewing is other than normal. Figure 19 illustrates the dependency of observed brightness upon phase angle. An area will appear brightest when viewed parallel to the incident rays and dimmest when the observer is facing the direction of the source. One unusual characteristic of the lunar surface is that an area will have the same brightness regardless of its orientation to the illumination when viewed parallel to the illuminating rays.

To give a visual conception of the brightness of the lunar surface under earthshine conditions one may compare it to the luminance of the earth's surface under moonlight. A mare area of 6.5 percent albedo at the subearth point on the moon illuminated by a full earth with a 40 percent albedo will have a brightness of 2.8 × 10^{-5} candles/cm^2; on earth a sandy loam soil with an albedo of 25 percent illuminated by a full moon at the zenith has a brightness of 0.18 × $(10)^{-5}$ candles/cm^2 or a factor difference of 15. It should be noted that the condition described, that is, full earth and normal viewing, represents the most favorable earthshine lighting of the lunar surface.

Due to the unusual reflection properties of the moon the periphery of the surface surrounding the astronaut will appear dimmer than the surface immediately beneath him for normal incident illumination (fig. 20).

This effect is referred to as limb darkening. As the astronaut glances around, the angle of viewing varies and as a result the observed surface brightness will change. At a distance of five feet out, the luminance will have decreased to one half that observed at his feet; at fourteen feet, one third, and at his horizon at a distance of one and one-half miles, the surface luminance will have decreased to two-tenths that observed at his feet. For angles of illumination other than normal, the disk of light will be elongated in the direction away from the source and will appear the brightest at the tip of the astronaut's shadow (around his head shadow).

Visual Detection of LEM Hazards.- The range within which an astronaut will be able to detect possible protuberance hazards, while hovering in the LEM, depends to a great extent on the intensity and the angle of

illumination. In order to determine the range under earthshine conditions the lunar surface has been assumed to be covered with two protuberance shapes that represent the extremes of detection difficulty (ref. 12). The conservative model is that of right circular cones with slopes of 15° and heights of 50 cm, which constitute possible Apollo LEM hazards. The liberal model is represented by spherical shaped protuberances 50 cm in diameter.

The luminance that the conical shaped model will have can be determined by applying the photometric model. By subjecting the resulting luminance data to photovisual threshhold criteria it can be determined if the protuberance model exhibits sufficient contrast against the background to be detected. The results are illustrated in figure 21. The contours are the limits of the range to which the assumed cones will be detected from a hover altitude of 1,000 feet.

It is readily apparent that for a landing near the subearth point the astronaut will not be able to detect possible Apollo LEM hazards. But if the area should be illuminated at an angle of 70° (equivalent to E or W lunar equatorial longitude) the astronaut will be able to detect the conical hazards to a range of 2,000 feet, when looking in a direction away from the light source.

The spherical shaped protuberances cast a shadow that increases the ease of detecting its presence over that of conical shaped hazards. Figure 22 illustrates for different angles of illumination the limits of the range that spherical shaped hazards 50 cm in diameter will be detectable.

Since protuberance shapes that represent the extremes of detection difficulty have been analyzed, the actual limits will probably lie somewhere between the two extremes. Until reconnaissance missions are performed, so that protuberance shapes more representative of the actual surface can be studied, one would probably favor the results of the conservative conical model.

It is apparent that under earthshine conditions, even at "full earth", the lunar lighting environment is at best marginal due to the amount of light available. If a landing were to be attempted in earthshine, the best (relative) lunar phase would be near new moon ($\theta = 0°$) for maximum earthshine intensity. Also the landing site selected should be beyond ±60° longitude from the subearth point, in order to take advantage of maximum contrast afforded by the lunar photometric properties. However, all presently considered landing sites are well inside ±60° longitude. On the basis of light intensity and operational flexibility, a landing in earthshine does not appear to be feasible on early missions.

Under sunlight conditions, the lighting environment might be considered optimum; however, preliminary studies indicate that landing sites should be restricted to areas located between 45° and 75° from the subsolar point. At sites less than 45° longitude from the subsolar point, contrast will be low and shadows that could increase the detectability of an object may not be visible to the LEM crew. Landing areas beyond 75° from the subsolar point are not desirable, since shadows cast by large features may obscure surface texture that represents possible LEM landing hazards.

Maximum contrast between 8° slopes and surrounding level terrain will occur when the sun is behind and below the pilot's line of vision. At a 1,000 ft hover altitude, with a 1,000 ft translational capability the pilot's look angle will always be less than 45° from the vertical while the sunlight will be coming in at between 45° and 75° from the vertical. For maximum effectiveness, the pilot should keep the sun behind him whenever possible during the final approach.

To interpret this lighting requirement into phases of the lunar month, the following numbers will be useful. If the landing zone lies between 40° W and 40° E and the sun angle is between 45° and 75° to the local vertical, then somewhere in the east zone ($0 \leq \lambda \leq 40°$ E), the proper lighting conditions will exist whenever the lunar phase is between

$65° \leq \theta \leq 135°$ First and Second Quarter

$185° \leq \theta \leq 255°$ Third Quarter

Somewhere in the west zone ($0 \leq \lambda \leq 40°$ W) the proper lighting conditions will exist whenever the lunar phase is between

$105° \leq \theta \leq 175°$ Second Quarter

$225° \leq \theta \leq 295°$ Third Quarter

If the entire zone is considered, then somewhere within ±40° of the sub-earth point will have the proper lighting conditions whenever the lunar phase is between

$65° \leq \theta \leq 175°$ First and Second Quarter

$185° \leq \theta \leq 295°$ Third Quarter

EARTH LIGHTING CONDITIONS

Another environmental factor to be considered is the variation in earth lighting conditions during a lunar mission. If the time spent during the lunar mission from translunar injection to earth entry is known, the changes in lighting conditions at the earth may be approximately computed. Knowing the lighting condition at translunar injection, the lighting conditions at entry and at landing may be computed; or by specifying the entry lighting conditions, the process may be reversed. The resulting equations are relatively simple although the process for arriving at these equations involves many considerations.

First, several basic numbers must be established. The moon requires 27.32 days to make a complete 360° rotation of the earth. However, during that time the earth is rotating about the sun at about one degree per day (360°/365 days). Therefore, it requires about 29.5 days for the moon to go from full moon to full moon or to complete one full lunar cycle. In computing the lighting conditions these figures must be taken into account.

The parameters necessary for the calculation are illustrated in figure 23. In figure 23a, the lead angle θ_1 of the injection position ahead of the earth-moon line (taken at lunar arrival) is shown. For a nominal 78 hour mission θ_1 is 10 degrees. As an example, the case where the earth is approaching full earthshine has been chosen in figure 23 to illustrate the calculations involved. Since the earth rotates 360° every 24 hours, every 15 degrees of longitude on earth corresponds to a one hour variation in local time. For the case shown in figure 23a, the subsolar point is 5° off the earth-moon line so that injection occurs 15° past midnight or 1:00 a.m. local time.

Let θ_2 represent the angular rotation of the moon about the earth during the mission from translunar injection to earth entry. For a 14 day mission this rotation would correspond to $\theta_2 = 185°$. For the example of figures 23 a 12 day mission will be used involving a $\theta_2 = 158°$. During this 12 day period the earth-moon system will have moved (360)(12)/365 or 11.83° about the sun and hence the earth's terminator will have shifted (counterclockwise) the same amount. From translunar injection to earth entry this 12 day mission time corresponds to a change of 47 minutes in the local time of any position on the earth measured with respect to inertial space.

In figure 23b, the relative orientation of the earth-moon-sun at entry and landing are illustrated. The angle between the earth-moon

line taken at transearth injection and the entry position is denoted θ_3 and is shown in figure 23b in its negative sense. For average return trajectories (90 hours) vacuum perigee occurs at about -8° from the earth-moon line. Since the entry conditions are taken at 400,000 feet altitude, this condition occurs prior to vacuum perigee at a position which is generally twice the entry angle. Using an entry angle of -6°, entry will occur at -12° prior to vacuum perigee at a position which is generally twice the entry angle. Using an entry angle of -6°, entry will occur at -12° prior to vacuum perigee or -20° prior to the earth-moon line. In general θ_3 varies between -15° and -25°. For a 90 hour return time a $\theta_3 = -20°$ will be used and this condition is shown in figure 23b. The distance traveled around the earth from entry to landing is denoted θ_4. This distance will vary from 1,200 to 5,000 nautical miles (NM) which corresponds to a great circle distance of 20° to 83.3°. However, the great circle entry trajectory will not in general lie along the equator but will be inclined between 15° to 40° to the equator. Therefore, for these extremes the equatorial distance (in degrees longitude) will be as follows:

Inclination/Range	5,000 NM	1,200 NM
15°	80.4°	19.3°
40°	63.8°	15.3°

As an example case the maximum range for the 40° inclination case will be used. Therefore $\theta_4 = 63.8°$.

A composite of the (a) and (b) portions of figure 23 are shown in (c). During the 12 day mission the earth-sun line has rotated $\theta_5 = 11.83°$. The subscript "i" denotes the earth-sun line at injection; the subscript "e" denotes this line at entry. The angle between the injection position and the entry position, $\Delta\theta$, may be computed directly since:

$$\Delta\theta = \theta_3 - \theta_1 + \theta_{LO} \tag{12}$$

where

$$\theta_{LO} = T_{LO} \frac{360 \text{ degrees}}{27.32 \text{ days/degrees}} = \theta_2 - (T_{TL} + T_{TE}) \frac{360}{27.32}$$

where

T_{LO} = time in lunar orbit

T_{TL} = time in translunar trajectory

T_{TE} = time in transearth trajectory

Thus for the example case where

$$\theta_1 = 10^\circ$$

$$\theta_2 = (12 \text{ days}) \frac{360^\circ}{27.32 \text{ days}} = 158^\circ$$

$$\theta_3 = -20^\circ$$

$$\theta_4 = 63.8^\circ$$

$$\theta_5 = 11.83^\circ$$

$$\theta_{LO} = 65.88^\circ$$

$$T_{TL} = 78 \text{ hours} = 3.25 \text{ days}$$

$$T_{TE} = 90 \text{ hours} - 3.75 \text{ days}$$

$$T_{LO} = 5 \text{ days}$$

it can be seen that $\Delta\theta = 35.88^\circ$. Since the maximum distance (inclination of 40°) to landing will occur 63.8° further down range from the entry position, this gives an earth landing at 99.68° down range from the translunar injection position.

To convert this to local lighting conditions we must take the rotation of the earth-sun line into account. If translunar injection occurred at 1:00 a.m. then entry occurred at ΔT later where

$$\Delta T = \frac{\Delta\theta}{15^\circ/\text{hour}} - \frac{\theta_5}{15^\circ/\text{hour}} \qquad (13)$$

$$= \frac{35.88 - 11.83}{15} = 1.6 \text{ hours}$$

Thus entry will occur at 2:36 a.m. local sun time.

If the range from entry to landing covers 63.8° this corresponds to a change in local sun time of 4 hours and 15 minutes which would put the landing at a local sun time of 6:51 a.m. This landing time would provide almost a full day for recovery operations. A plot of earth local time for translunar injection, earth entry and landing as a function of moon phase at arrival in lunar orbit for T_{LO} of 5 days is shown in figure 24a. By selecting the moon phase desired for arrival in lunar orbit one can determine the earth local time for earth entry and landing based on an orbitrarily selected translunar injection time. A similar plot for a T_{LO} of 1.5 days is shown in figure 24b. Other factors such as the restrictions placed on the lighting conditions at translunar injection, transposition docking on the lunar surface and earth entry as well as stay time at the moon must be considered in the ultimate choice. As an example of this, MIT has stated that navigational sighting on the earth or moon during midcourse phases of flight cannot be made if the sun is within 15° of the planet. If this becomes a firm requirement, then certain phases of the moon (and earth) may be precluded for translunar or transearth transfers. Since the lunar plane makes an angle of 5° 09' to the ecliptic, this may or may not pose an undue restriction on the injection date.

A plot of the variation in $\Delta\theta$ (the change in the anomaly from injection to entry) and ΔT (the change in local sun time from injection to entry) as a function of lunar stay time is shown in figure 25. Positive values denote that entry occurs down range or later in local sun time from injection. Translunar and transearth times of 78 and 90 hours respectively were used for the calculation. It should be remembered that both $\Delta\theta$ and θ_5 are variables which depend on T_{LO}. An interesting situation arises where the parameters $\Delta\theta$ and ΔT pass through zero. In the case of $\Delta\theta = 0$, entry will occur at the same inertial orientation position as injection (not to be confused with the same position over the earth, since the earth is rotating beneath this inertial orientation position). In the case of $\Delta T = 0$, entry will occur at the same local sun time (same lighting conditions) as injection. It may be seen that for a 3 day mission at the moon, translunar injection and earth entry (400,000 ft.) occur at the same local sun time, but the two conditions occur about 12 degrees apart in longitude, the difference being due to the earth's motion about the sun during the mission. In every case (in this example) landing will occur at a position down range where the local sun time is 4 hours and 15 minutes (corresponding to an inclination of 40° and a maximum range of 5,000 NM) later. For smaller inclinations and shorter ranges following entry, the local time at landing will be different, but can be easily computed.

OPERATIONAL FACTORS

Free Return Trajectories.- For the first few lunar missions, the Apollo spacecraft is to be restricted to translunar trajectories which will return the spacecraft to earth after a lunar fly-by provided that no further propulsion is applied (or required) after injection into the translunar trajectory (provision for small injection errors is allowed if they can be overcome by small midcourse velocity corrections). As long as the Apollo lunar operations are restricted to these so-called "free return" translunar trajectories and as long as the spacecraft ΔV budget limits the orbital plane change that can be made at lunar orbit injection, the Apollo spacecraft will be restricted to lunar orbits of low inclination with respect to the lunar equator. The precise range of maximum latitudes (or orbital inclinations) that can be obtained from free return trajectories varies from day to day. In order to achieve the maximum reasonable launch window for any given launch date, only landing sites within $\pm 5^\circ$ latitude of the lunar equator should be chosen for these early missions.

Therefore, for the purposes of mission planning, landing sites within $\pm 5^\circ$ of the lunar equator should be chosen due to the operational requirement of "free return" translunar trajectories.

Navigation and Guidance Considerations.- One of the more critical factors which will affect the accuracy of the Apollo navigation system, and hence the LEM guidance to the lunar surface, will be the updating of the MIT navigation system with accurate sightings on established lunar landmarks. The MIT program for the LEM guidance to the lunar surface indicates the desirability of sightings on at least five lunar landmarks in the equatorial region and, whenever possible, a sighting on a landmark just prior to the injection of the LEM into the equal-period transfer orbit. This transfer orbit will place the LEM in a position to perform the final braking maneuver to the lunar surface after traveling about 90° around the moon. This means that it would be desirable to have at least one navigational landmark established at 100° to 105° east of the proposed landing site. This requirement is not compatible with the other criteria for lunar landing site selection.

Recognizing this restriction, MIT has reverted to the use of "Star-Horizon" (SH) measurements on the backside of the moon by noting the time and elevation angle of known stars above the lunar horizon. Also multiple orbits have been studied to improve the orbit determination technique (by passing over the five landmarks twice) but neither technique satisfactorily corrects for the navigation (primarily, orbital position) errors at the critical time of LEM transfer. The best way found to date to correct for navigational inaccuracies is to make a landmark sighting

within a few minutes of each major thrusting maneuver required to perform the lunar landing. Since the ability of the LEM to land with one-half mile CEP (Circular Probable Error) of a predesignated landing site is so strongly dependent on accurate navigational information and proper alignment of the IMU (Inertial Measurement Unit) at the time of LEM transfer to an equal-period orbit. Serious consideration should be given to accurately mapping lunar landmarks wherever then are needed on the lunar surface.

At the present time, the choice of landmarks is restricted to those features on the lunar surface which are visible from earth. Although we may "see" in longitude about 195° of the lunar surface (180° plus 15° due to the longitudinal librations), the oblique views of the areas near the east and west limbs seriously limit our ability to identify and establish prominent landmarks there. At present, there are some differences of opinion as to what constitutes a "landmark" (what appears to be a landmark from 240,000 miles away may not be a landmark from 80 - 100 miles away) and the mapping accuracy to which these landmarks may be located. The USAF Aeronautical Chart and Information Center has prepared a Preliminary Analysis of Horizontal and Vertical Control Accuracies on the lunar surface as they are estimated at the present time. (See table II.)

It should be noted that ACIC currently estimates absolute horizontal accuracies of features near 0° latitude and longitude as 1,740 meters CEP. This accuracy rapidly degrades toward the limb regions. If only earth-based photography is available, the best accuracies they expect to achieve by 1968 will be about ±800 meters CEP in absolute horizontal position, and ±150 meters (P.E.) in absolute elevation near the mean libration point. The accuracy will again degrade rapidly toward the limb regions.

Although no firm accuracy requirement has been established, MIT is currently allowing 1,500 feet for landmark location uncertainty in error studies to determine the LEM landing CEP. In view of the ACIC estimates, this value is barely credible as the very best accuracy we can expect to achieve by 1968 for landmarks within a few hundred miles of the mean libration point, and is completely unrealistic for landmarks near the limb regions. If more accurate control data, such as may be provided by a manned lunar reconnaisance mission, is not available before operational mission planning for the first landing mission, accessory landing aids or other guidance techniques may be required.

If, on the other hand, a lunar reconnaissance mission is performed prior to the lunar landing mission this situation will change. If, for instance, a reconnaissance spacecraft spends seven days in equatorial or near equatorial orbit during the period $\theta = 90°$ (first quarter) until $\theta = 180°$ (full moon), a major part of the equatorial belt from 180° east

longitude to 90° west longitude can be mapped to a detail sufficiently accurate to provide landmarks. Schematic drawings illustrating this mission are shown in figure 26a and 26b. This type of mission could provide the proper lighting for detailed photography of the landing site areas based on a criteria for site selection and verification. Although near the terminator only very prominent proturberances will be distinguishable due to the very long shadows, this is a reasonable (and may be the optimum) condition for landmark selection. On the other hand, it appears that the photography requirements for selection and verification of the landing sites must be taken at higher sun angles, but not at the subsolar point. Areas between 20°-50° from the terminator will be sufficiently well-lighted for reconnaissance photography for landing site selection and verification. Therefore, the two requirements (landmark mapping and site verification) are not incompatible and the reconnaissance mission can be tailored to achieve both results with a lunar orbit stay time of 6 or 7 days.

If such a reconnaissance mission is performed prior to the landing mission, landmarks could be established in the eastern half of the equatorial belt (up to 180° east longitude) with proper photogrammetric procedures established, to more nearly provide the landmarks with the 1,500 feet relative positional accuracy which is felt to be desirable. Since, for the landing mission, MIT feels that sightings on landmarks can be made in either earthshine or sunshine conditions, it will then be possible to utilize for lunar landing sites the entire ±40° belt in longitude, by making one or more sightings on established landmarks at points 100° or greater east of the proposed landing zone. As a minimum goal, this would require at least one landmark in the vicinity of 140° east longitude (or greater) with a relative positional accuracy of 1,500 feet (or better) to the subsequent landmarks. The regions discussed are illustrated in figure 27.

For the purposes of mission planning, it is felt that knowledge of the lunar surface discussed in the preceding paragraph must be available at the time the first landing is attempted and that selection of landing sites at this time should not be restricted to the western hemisphere (0° - 90°W).

DSIF Communications.- Another factor which enters into the selection of lunar landing areas is that of earth-moon communication.

It is desirable that continuous communication by code, voice, and television with the Command Module in orbit and the Lunar Excursion Module on the lunar surface be maintained without moving the earth based antenna back and forth.

A brief study has been made by the Instrumentation and Electronics Systems Division with regard to the effects of ground based high gain

antenna patterns on the LEM and CM communications link capabilities, reference 13. In this study the antenna pattern of the 85 foot Goldstone antenna with a circularly polarized feed was considered.

Figure 28 shows the relative signal level from the earth based DSIF antenna seen by the orbiting Command Module when the DSIF antenna is (a) tracking the LEM sitting on the lunar surface, and (b) tracking the CM in lunar orbit.

The line "East Horizon" is the point in the pattern at which the CM comes into view of the ground station. "West Horizon" is the point at which the CM disappears. A (0,0) position of the LEM on the moon's surface is depicted in the top-center of the figure. The ordinate on the left of the figure represents the reduction in signal level as measured at the antenna terminal of the Command Module when the antenna is fixed on the LEM. The ordinate on the right is the relative signal strength at the LEM when the antenna is tracking the CM. In both bases the reference level is the signal strength measured at the Command Module when the CM is located at the center of the beam. It may be noted that when the position of the LEM and CM coincide, the signal strengtn of the LEM antenna has a 7 db gain over that of the Command Module; thus, it may appear to be more desirable to track the CM and allow the additional LEM signal strength to absorbe the loss. This is the best tracking situation for signal strength purposes but requires constant moving of the DSIF antenna which may not be desirable.

Figure 28 may also be used to calculate the relative signal strengths of the CM and LEM when the LEM is at any other location on the moon. If for instance, the LEM is located 0.2 lunar radii toward the east of center, the "path of the Command Module" will be shifted to the west (left) such that the abscissa should be read from 1.3 to the west (left) to 0.9 to the east (right).

One particular tracking procedure is of special interest. If the DSIF antenna is pointed at a position somewhere in between the CM and the LEM (rather than tracking either module), the signal strength from both the CM and LEM can be kept equal. This procedure will allow both systems to see a minimum signal of -3 db provided the LEM is located on the lunar surface within ±37° of zero longitude or within an area with a radius which is 0.6 that of the moon's radius, R_m, as shown in the shaded area of figure 29. If the "equal signal" tracking technique is used and the worst possible case existed where the LEM is on one limb of the moon and CM is on the other, then the maximum loss would amount to only -6.5 db.

Based on the foregoing considerations, it is the opinion of the Instrumentation and Electronics Systems Division that there will be no

restriction necessary on lunar landing sites on the visible side of the moon due to the earth-moon communications network.

Lunar Surface Communications.- In the present framework of the Apollo communication network, the astronaut on the lunar surface - external to the LEM - will have the capability of communicating directly with both the astronaut remaining in the LEM and the CM, if wearing the space suit personal communication system. Direct communication with the CM or earth by the astronaut on the lunar surface will not add any additional constraints on landing site selection or the date of landing.

As the astronaut leaves the vicinity of the LEM landing site to carry out the scientific portion of the mission, that is, in search of geological samples and the placement of scientific packages upon the surface, the communication link with the LEM will be terminated by either of two physical obstructions - protuberances or curvature screening. If the area in the immediate vicinity of the landing should be relatively smooth with no major protuberances that may obstruct the line-of-sight or depressions that the astronaut may enter, the large curvature rate of the moon will rapidly depress the astronaut below the LEM's horizon as he ventures across the surface, cutting off the communication tie. The distance at which the screening will occur depends upon the antenna height of both the LEM and the astronaut. Table III lists the horizon distance for various object heights on the moon assuming a perfectly smooth spherical surface. The range cut-off point will be the sum of the horizon distances for the astronaut and the LEM based upon antenna height above the surface. Figure 30 illustrates the configuration of the problem.

The range of the astronaut-LEM communication link could be extended by increasing the height of the LEM's antenna. The range will be 4.3 statute miles if an antenna is not extended above the 20 foot high LEM; however, by the addition of a 30 foot antenna the line-of-sight communication link could be increased to 6 statute miles.

The range determined by the summation of horizon distances is quite optimistic. The presence of protuberance such as pressure ridges and large boulders between the LEM and the astronaut will obstruct the line-of-sight contact link decreasing the communication range. Contact will also be terminated if the astronaut in his exploration over the surface should enter a crater or rille whose sides or walls obstruct the LEM from view. Such small scale topography at the landing site cannot be predicted or verified at this time. However, this factor should be considered in landing site selection and astronaut activities on the lunar surface.

LUNAR GEOLOGICAL FACTORS AFFECTING LANDING AREA SELECTION

All lunar surface models that have been proposed to this date are hypothetical, and their verification is dependent upon the procurement of better data. Visually, our direct telescope observations are limited to those lunar surface features which are larger than 500 meters.

Until direct measurements can be made on the lunar surface by manned or unmanned probes or vehicles, it will not be possible to state quantitatively the physical structure of the lunar surface materials. Knowledge of the structure of these materials may be hypothesized on the basis of physical measurements such as: photometric, infrared, radio emission, radar reflection, polarization, albedo, and color from earth based observations, or may be predicted by examination of the effects of possible physical processes such as: meteorite impact, radiation, seismic shock, volcanism, vacuum welding, and thermal fracture assumed to be active on the lunar surface. Of these processes only volcanism, vacuum welding, and meteorite impact are considered significant. Both volcanic and impact processes produce debris which covers most of the lunar surface. High velocity impact studies show that the ejecta from an impact crater has a mass that is 10^3 to 10^5 times the mass of the impacting particle. Variations of the size, mass, and velocity of the impacting particle and the physical properties of the target rock, will vary the size and amount of debris produced and the distances the particles are ejected from the impact area.

Volcanic processes on earth produce wide variations in surface topography, with most of the surfaces being extremely rough on a scale of a few meters.

The average size of particles ejected either by impact or volcanic processes will decrease away from the area of injection.

Current information indicates that loose "dust" is not present on the lunar surface. Small particles generated on the lunar surface probably are bonded into a cohesive, porous aggregate. (Salisbury, and others, 1963, ref. 14).

There is general agreement among the scientific community that on the millimeter scale the lunar surface will be rough and complex. However, on the centimeter and meter scale there is a difference of opinion. Based on the radar data one research group states that the surface will be smooth. The other group, using the same data, but interpreted differently, states that the surface will be extremely rough.

It is possible to measure the regional slopes near craters and mountain ranges. However, an extrapolation to the scale required for a landing site cannot be justified as a result of these measurements. An area which appears smooth on a scale of 500 meters could be extremely rough when viewed in reference to a few meters.

If the most pessimistic views on the nature of the lunar surface are taken as design criteria, then the task of designing a vehicle to land on this "worst-case moon" becomes extremely difficult. The only approach that may be taken at this time is to determine what type of surface may be within reasonable design capabilities; in the light of present knowledge of the lunar surface, determine if this surface is probable; and then, when better data becomes available, confirm landing sites with a surface equal to or better than the assumed surface.

A surface within reasonable design capability is one with static bearing strength of 1 psi at 10 cm, dynamic bearing strength of 12 psi at 60 cm, and 95 percent of the effective slopes less than 15° after possible modification by landing dynamics, reference 15.

The heterogeneous size distribution of the ejecta in any area will result in bearing strength equal to or greater than that specified above.

Infall of micrometeoroids tends to erode the surface and the ejecta will fill in the spaces between larger pieces of debris with smaller particles. The infall of larger meteoroids tends to roughen the surface, but there is no data available on the flux of large meteoroids. Attempts have been made to extrapolate crater size frequency below the limits of direct visual observation (ref. 16 - Hackman, Shoemaker and Eggleton). In this study it was found by extrapolation that the lunar surface would be completely saturated with small impact craters (on the order of 10 meters and smaller).

The steepest slopes observable on the lunar surface are found on inside crater walls in certain mare craters. These slopes can exceed 40°. Slopes along the outside crater rims are approximately 3-4° and slopes on the mare surfaces are generally under 1°. Therefore many local areas with average slopes considerably less than 15° must exist which may be suitable landing sites.

More precise information on the nature of the moon's surface will not be obtained until vehicles have been landed on its surface or have been placed into orbit about it. Ranger probes will be able to obtain television photographs of limited sections of the moon at a resolution somewhat better than earth based telescope photographs. The soft-landed Surveyor will take close-up television pictures of a very limited area

in its immediate vicinity. Detailed information on landmarks and on large specific areas of the lunar surface will be obtained only from orbiting reconnaissance vehicles. MSC studies indicate that the maximum amount of information would be obtained by a manned orbital reconnaissance mission. This mission could obtain high resolution photography of the entire area of interest on the lunar surface, returning the film to earth for processing and analysis. The reconnaissance module would also be equipped to land probes on the surface to obtain precise soil mechanics measurements of specific sites which visually appear to be favorable locations.

LUNAR LANDING AREAS

Criteria for Lunar Landing Area Selection.- At the present time, there is no detailed knowledge of the small scale topography of the lunar surface. The precise location of desirable or even acceptable landing sites at this time is unjustified. However, we can stipulate general areas where acceptable landing sites are most likely to be found, based on information such as contained in this paper and on observable lunar features. The smallest lunar feature which can now be distinguished visually from earth under the best "seeing" conditions is about 500 meters.

For simplicity we may analyze the lunar surface in terms of three types of terrain listed below:

1. Continental Terrain: Is a very complex but composed predominantly of rough and moderately bright upland areas. These areas are mostly covered with overlapping craters ranging in size from 180 miles in diameter to craters which are smaller than the limit of optical resolution. Mountains, valleys, ridges, rilles, and fault scarps add to the general roughness of the continental terrain. Small but relatively smooth areas may exist in limited isolated locations.

2. Mare Terrain: This is dark, low-lying, and is smooth relative to the continental areas. It is most likely composed of volcanic materials with impact ejecta superimposed and intermixed. This terrain is not featureless but the features that are present are fewer in number and smaller in size than those in the continental terrain. Many of these features are at the extreme limits of optical resolution and can be seen only at low angle illumination.

3. Younger Crater Terrain: This terrain consists of volcanic and impact craters and ejecta that are younger than the mare surfaces. This relationship is established either by the craters being in the mare surface or by the ejecta from a crater in the continental terrain spreading over a mare surfaces. Because most of the ejecta is deposited

near the point of origin, suitable landing sites will not be found within a distance of two or three diameters from the rims of larger craters.

In order to choose areas possessing the greatest potential for containing suitable landing sites, the following factors will be considered:

1. Regional Slopes: Regional slopes are defined by elevation differences over distances greater than one kilometer and can be measured from the LAC charts (lunar charts produced by the USAF-ACIC) with accuracy limitations as listed in table II. Regional slopes cannot be extrapolated to local (less than 1 kilometer) slopes.

   a. The mare terrain is favorable in most areas.

   b. The continental terrain and the younger crater terrain are less favorable due to the improbability of finding an extensive area of similar slope characteristics.

2. Surface Texture: Local slopes and local relief due to protuberances and depressions are defined by elevation differences over distances of less than one kilometer. Even though extensive areas of the lunar surface appear smooth on the LAC charts, the small scale relief that is visible during the periods of excellent seeing is not listed. Some of these apparently "smooth" areas will exceed the LEM landing capability.

   a. Mare terrain is generally favorable except in areas of younger crater terrain, fault scarps, and rough lava flows.

   b. Continental terrain is generally unfavorable because of the probability of local slopes exceeding the LEM landing capability.

   c. Younger crater terrain is unfavorable because of steep local slopes and coarse ejecta.

3. Structural Strength: The surface bearing strength and the supporting strata must be competent in the landing area. Current information indicates that loose "dust" is not present on the lunar surface. However, dust clouds may be generated by meteoroid impact and erosion of the surface by retrorockets. Small particles generated on the lunar surface will be bonded into a cohesive porous aggregate upon contact by vacuum welding. On the basis of present knowledge, no choice exists between the structural strength and probable bearing strength of the continental terrain, the mare terrain and in the younger crater terrain.

4. Landmarks: It is considered desirable to have a series of landmarks lying along the probable approach (landing) corridor, at least one prominent landmark which is visible from the landing site after the landing.

a. Mare surface is generally less favorable except along eastern margins.

b. Based on a necessity for using major land form features to locate position after landing on lunar surface, continental terrain or younger crater terrain are favored due to greater relief character of the topography.

c. Based on earth based observatory telescopic photography, the current best precision measuring techniques, and current data reduction techniques, only regions of ±40° longitude can be considered favorable due to uncertainty of regions outside these longitudes meeting the landmark positional accuracy requirements of the MIT guidance and navigation equipment.

d. Due to necessity for locating landing site accurately and for locating landmarks within the accuracy requirement, the only region favored for both is within ±10° longitude.

5. Isolated Features: It is not required that a landing area be totally acceptable everywhere within a defined landing area. Isolated craters (between 0.5 - 5.0 km in diameter) and protuberances are permitted in the landing area provided they do not exceed 5 percent of the area. (It should be noted that this corresponds to the landing site requirement which allows 5 percent unacceptable texture).

6. Size and Shape: No rigid restriction is placed on the size or shape of an area of interest; however, as a rule of thumb, the size should be about 900 km^2 (equivalent to a square area of 1° by 1° at the lunar equator). This landing area corresponds in size to the "landing zone" defined in section 9.1.3 of reference 16.

7. Position: For the first few missions (due to launch date flexibility for free return trajectories) areas as close as possible to the lunar equator should be chosen. Areas inside of ±3° (latitude) are desired, inside ±5° are acceptable and areas from 5° to 10° may be selected only if a sufficient number of areas do not exist closer to the equator. The longitude of the landing area should be kept to within ±40°. The choice here is a compromise between the desire to keep the areas as close as possible to 0° (mapping accuracies) but the necessity of having a number of areas spread out as far as possible over the

visible face (launch date flexibility for achieving the desired lighting and heating conditions at one of the chosen areas).

Recommended Lunar Landing Areas.- In the past, a number of possible lunar landing areas have been considered by the Space Environment Division. Based on selection criteria that existed at the time, groups of potential sites were compiled and published in two documents. Four sites were compiled by Space Environment Division in May 1963 and subsequently published in the "Natural Environment and Physical Standards for Project Apollo" (ref. 15). These four sites were picked from those suggested by the various scientists in the country and were chosen as a compromise between geological interest and basic mission planning acceptability.

Five sites were chosen by Space Environment Division in September 1963 at the request of Flight Operations Division based on an FOD criteria for sites located within 3° latitude of the lunar equator and lying at the center of a circle 20 statute miles in diameter with no apparent obstructions within that circle (area). These sites were published in the minutes of the 4th meeting of the Apollo Spacecraft Trajectory Subpanel (ref. 17) and have been used for mission trajectory studies.

Each of the areas surrounding these sites plus several other sites have been listed and evaluated in table IV on the basis of the area criteria given in the preceding section. Since degrees between the two suggest knowledge which does not exist, only two ratings were used: favorable (F) and unfavorable (U). It may be seen that several of these sites are though to be undesirable based on the present criteria.

After careful study of the areas surrounding each of the sites listed in table IV and based entirely upon the present criteria, ten recommended lunar landing areas have been chosen subject to reconnaissance verification. These recommended lunar landing areas, indicated with an asterisk in table IV, are listed as follows:

I.	36°55'	E.	1°45'	N.
II.	31°	E.	0°	N.
III.	28°22'	E.	1°10'	N.
IV.	24°10'	E.	0°10'	N.
V.	12°50'	E.	0°20'	N.
VI.	1°28'	W.	0°30'	S.
VII.	13°15'	W.	2°45'	N.
VIII.	28°15'	W.	2°45'	N.
IX.	31°30'	W.	1°05'	S.
X.	41°30'	W.	1°10'	S.

Sections of LAC charts showing each of these areas are given in figure 31. Only centroids of landing areas are listed. However, it should be noted that some of the areas straddle the lunar equator.

Area V requires some qualification. Between 3° E and 20° E there is a large gap in mare regions where the Central Highlands rise above the mare floor. The Central Highlands are a continental region and in general, continental regions are not expected to provide favorable landing areas. However, it is operationally desirable to locate potential landing areas as evenly as possible across the visible lunar face. Therefore, an effort was made to find a potential landing area in this region. The area listed as V is considered worthy of reconnaissance because it is the only area in this continental region which appears to be reasonably devoid of large scale topographic features and may provide a landing site.

Until such time as our knowledge of the lunar surface is significantly improved, these areas are recommended as most likely to contain acceptable lunar landing sites and satisfy operational constraints.

CONCLUDING REMARKS

In the foregoing sections, a number of factors has been covered to various degrees of depth which may influence the choice of launch dates (by year, by month, by day, and by lunar phase). Surprisingly enough, most of these factors complement rather than oppose each other with two phases predominating: First Quarter ($\theta \approx 90°$) and Third Quarter ($\theta \approx 270°$). Very briefly, the conclusions from each consideration are given below for sites lying between ±40° longitude where at least one site will always be within the designated limits.

Meteroids.- The best months for the Apollo mission occur between the middle of January through April. For maximum meteoroid protection while on the lunar surface, the landing should occur on the selenocentric trailing face of the moon (that is, the trailing face of the moon as the earth-moon system moves around the sun).

$$150° < \theta < 30° \quad \text{(a 10° overlap allowed)}$$

Radiation.- Although a high certainty cannot be assigned at this time, the best months appear to be May, June, December and January. For maximum radiation protection while on the lunar surface, the landing should occur on the selenocentric trailing face of the moon displaced 50° to the west.

$$200° < \theta < 80° \quad \text{(a 10° overlap allowed)}$$

Lunar Temperatures.- Although we know with reasonable certainty the variation in the average lunar surface temperature, the actual equilibrium temperature of the LEM sitting at an elevated position above

the lunar surface produces uncertainties in the maximum temperature that may be reached. The same uncertainties exist for the man moving about on the lunar surface. Therefore, it is recommended that the subsolar point be avoided on early missions. Landing about 60° from the subsolar point appears to be best from equilibrium temperature considerations. The effects of space suit and spacecraft subsystems operations during a transition through the terminator into lunar night must be investigated before more definitive restrictions can be specified.

$$65° < \theta < 175°$$
$$185° < \theta < 295°$$

Lunar Lighting.- The albedo, contrast and probable surface roughness should influence the choice of lighting conditions for at least the first few missions. The mare landing areas which appear best at this time are basically a very low albedo (dark), low contrast material apparently of volcanic origin. Superimposed on this surface will be a roughness due to four billion years of meteoroid and micrometeoroid impacts. The probable homogeneous roughness, contrast and albedo will make the choice of a touchdown area difficult at best. Because of this a landing in earthshine is considered to be too marginal and is not recommended for the first few missions. Based on the present lunar photometric model, the best visual conditions will exist when the sun is between 45° and 75° from the lunar vertical (this corresponds to longitudes between 45° and 75° away from the subsolar point).

$$65° < \theta < 175°$$
$$185° < \theta < 295°$$

Earth Lighting.- For a 1.5 day stay time in lunar orbit, the local lighting conditions on earth at translunar injection and earth entry and landing will differ by only two to three hours. Therefore, for lunar missions when the moon is at First Quarter ($\theta = 90°$) translunar injection and earth landing will occur during the early morning hours (local earth time). Transposition will take place in daylight and the spacecraft will remain in daylight throughout the translunar phase of the mission. For lunar missions near $\theta = 270°$ (Third Quarter) translunar injection and earth landing will occur in the late evening hours (local earth time). Transposition in darkness will probably be required. Recovery will probably occur in darkness or twelve hours after landing.

$$70° < \theta < 110°$$

DSIF.- No restriction.

Free Return Trajectories.- Ten landing areas within 3° of the lunar equator have been chosen and should provide no restriction to launch windows.

Navigation and Guidance.- Accuracies of lunar mapping control points favor a landing as near 0° longitude as possible. Present knowledge of lunar landmarks for navigation favors an extreme west zone landing. Better mapping accuracies of landing sites and landmarks are necessary before reasonable navigation and guidance to a designated landing site can be expected. In order to utilize sun-lit landmarks between 90° and 135° east of the landing site, it will be necessary to land near the first quarter.

$$65° < \theta < 175°$$

Lunar Surface Communications.- No known restrictions other than surface curvature and local surface protuberances and depressions.

Landing Areas.- Ten areas most likely to contain landing sites have been recommended on the basis of present knowledge. Reconnaissance of these areas for small scale topographic features must be made before more definitive knowledge can be documented. The ten landing areas - five in the east and five in the west extend from 41° west to 38° east. The largest gap between areas is about 15°.

This paper is intended only to cover environmental factors and some operational considerations closely associated with environmental factors. Based only on these considerations, the months of January and May look best for the Apollo mission. The lunar lighting and heating considerations indicate that a sunlit landing near First or Third Quarter of the lunar phase would be optimum. Both meteoroid and radiation hazards are reduced if the landing is made more than 40° east of the subsolar point when the moon is near the Third Quarter phase ($200° < \theta < 295°$). On the other hand, the earth lighting conditions (for missions with lunar orbit stay times on the order of one or two days) are best when the moon is near First Quarter ($70° < \theta < 110°$). For operational planning studies, both phases of the moon should be considered. There are no environmental factors which indicate that new moon or full moon are desirable for lunar landing missions.

REFERENCES

1. Whipple, F. L.: "The Meteoritic Risk to Space Vehicles." Vienna, Springer, Verlag, 1958, Proc. of the VIIIth International Astronautical Cong. Barcelona, 195?, pp. 418-428.

2. Whipple, F. L.: "The Dust Cloud About the Earth." Nature, Vol. 169, (Jan. 14, 1961), pp. 127.

3. Alexander, W. M., McCracken, C. W., Secretan, L., and Berg, O. E.: "Review of Direct Measurements of Interplanetary Dust from Satellites and Probes." Presented at the COSPAR meeting, May 1962, NASA X-613-62-25.

4. Hawkins, Gerald S.: "A Radio Echo Survey of Sporadic Meteor Radiants." Monthly Notice, Rep. Astronomical Soc., Vol. 116 No. 1, 1956, pp. 92-104.

5. MSC Environment of August 23, 1963.

6. Gault, D. E., Shoemaker, E. M. and Moore, H. J.: "Spray Ejected from the Lunar Surface by Meteoroid Impact." NASA TN D-1767, 1963.

7. Bohn, J. L. and Fuchs, O. P.: "High Velocity Impact Studies Directed Towards the Determination of the Spatial Density, Mass and Velocity of Micrometeorites at High Altitudes." Contract AF 19 (604) - 1894 Scientific Report No. 1, ASTIA AD 243 106, Jan. 31, 1958.

8. Pettit, Edison and Nicholson, Seth B.: "Lunar Radiation and Temperatures." Astrophy J.; Vol. 71, 1930, pp. 102.

9. Murray, Bruce C. and Wildey, Robert L.: "Surface Temperature Variations During the Lunar Nighttime." (1963), Contr. No. 1173, Div. of Geol. Sci., Calif. Inst. of Tech. (Submitted to Astrophy J.)

10. Herriman, A. G., Washburn, H. W., and Willingham, D. E.: "Ranger Preflight Science Analysis and the Lunar Photometric Model." TR No. 32-384 (rev.) Jet Propulsion Laboratory, Calif. Inst. of Tech., Pasadena, Calif., Revised March 11, 1963.

11. Kuiper, G. P.: "The Earth as a Planet." The Univ. of Chicago Press, Chicago 1954, Chapter 15.

12. Breshears, R. R., Lewyn, L. L.: "Visual Detection of Protuberance Hazards on the Lunar Surface." Office of Systems, NASA, Washington, D. C., 1963.

13. Chicone, E. L.: Private Communication. Instrumentation and Electronic Systems Division.

14. Salisbury, J. W., Glaser, P. E., Stein, B. A., and Vonnegut, B.: "Adhesive Behavior of Silicate Powders in Ultra-High Vacuum." Presented at the 44th Annual Meeting of American Geophysical Union, April 17-20, 1963, Washington, D. C.

15. OMSF Program Directive, "Natural Environment and Physical Standards for Project Apollo." M-D E 8020.0C8 A, August 1963 (CONFIDENTIAL)

16. Shoemaker, Hackman, and Eggleton: "Correlation of Geologic Time Advances in the Astronautical Sciences." Vol. 8, 1962, pp. 70-89.

17. Minutes of 4th meeting of the Apollo Spacecraft Mission Trajectory Subpanel. August 12, 1963. OFO (THS/JPM:dpf) (CONFIDENTIAL)

18. Geoffrion, Korner, and Sinton: "Isothermal Contours of the Moon." Lowell Observatory Bulletin No. 106, May 1960.

TABLE I.- ALBEDOS OF TYPICAL LUNAR AREAS

	Albedos	
	Average	Range
Dark plains (maria)	0.065	0.05 - 0.08
Brighter plains (paludes)	.091	0.09 - 0.10
Mountain regions (terrae)	.105	0.03 - 0.12
Crater bottoms	.112	0.06 - 0.18
Bright rays	.131	0.10 - 0.16
Brightest spot (Aristarchus)	.176	-
Darkest spot (inside Oceanus Procellarum)	0.051	-

Table compiled from:

1. Kuiper, G. P., "Planets and Satellites." University of Chicago Press, Chicago, 1961, p. 236.

2. Markov, A. V., "The Moon, A Russian View." University of Chicago Press, Chicago, 1962, p. 362.

TABLE II.- PRESENT ACCURACIES OF CONTROL POINTS ON THE LUNAR SURFACE*

DEPARTURE FROM 0° LAT, 0° LONG	PROBABLE ERROR IN METERS		
	ABSOLUTE HORIZONTAL	VERTICAL	
		ABSOLUTE	RELATIVE
0°	1740	950	90
10°	1760	1000	100
20°	1850	1065	120
30°	2000	1120	140
40°	2270	1180	170
50°	2700	1240	260
60°	3470	1300	440
70°	5070	1370	960

*USAF - ACIC

TABLE III.- HORIZON DISTANCE ON MOON'S SURFACE

Arc Length
Moon Diameter = 2,160 Statute Miles

HEIGHT FEET	STATUTE MILES	HEIGHT FEET	STATUTE MILES	HEIGHT FEET	STATUTE MILES	HEIGHT FEET	STATUTE MILES
1	0.6	50	4.5	440	13.4	2,800	33.8
	0.9	55	4.7	450	13.6	2,900	34.4
3	1.1	60	5.0	460	13.7	3,000	35.0
4	1.3	65	5.2	470	13.9	3,100	35.6
5	1.4	70	5.4	480	14.0	3,200	36.2
6	1.6	75	5.5	490	14.2	3,300	36.7
7	1.7	80	5.7	500	14.3	3,400	37.3
8	1.8	85	5.9	520	14.6	3,500	37.8
9	1.9	90	6.1	540	14.9	3,600	38.4
10	2.0	95	6.2	560	15.1	3,700	38.9
11	2.1	100	6.4	580	15.4	3,800	39.4
12	2.2	105	6.6	600	15.7	3,900	39.9
13	2.3	110	6.7	620	15.9	4,000	40.4
14	2.4	115	6.9	640	16.2	4,100	40.9
15	2.5	120	7.0	660	16.4	4,200	41.4
16	2.6	125	7.2	680	16.7	4,300	41.9
17	2.6	130	7.3	700	16.9	4,400	42.4
18	2.7	135	7.4	720	17.2	4,500	42.9
19	2.8	140	7.6	740	17.4	4,600	43.4
20	2.9	145	7.7	760	17.6	4,700	43.8
21	2.9	150	7.8	780	17.9	4,800	44.3
22	8.0	160	8.1	800	18.1	4,900	44.8
23	3.1	170	8.3	820	18.3	5,000	45.2
24	3.1	180	8.6	840	18.5	6,000	49.5
25	3.2	190	8.8	860	18.8	7,000	53.5
26	3.3	200	9.1	880	19.0	8,000	57.2
27	3.3	210	9.3	900	19.2	9,000	60.6
28	3.4	220	9.5	920	19.4	10,000	63.9
29	3.4	230	9.7	940	19.6	15,000	78.2
30	3.5	240	9.9	960	19.8	20,000	90.3
31	3.6	250	10.1	980	20.0	25,000	101.0
32	3.6	260	10.3	1,000	20.2	30,000	111.0
33	3.7	270	10.5	1,100	21.2	35,000	119.0
34	3.7	280	10.7	1,200	22.2	40,000	128.0
35	3.8	290	10.9	1,300	23.1	45,000	135.0
36	3.8	300	11.1	1,400	23.9	50,000	142.0
37	3.9	310	11.3	1,500	24.8	60,000	156.0
38	3.9	320	11.4	1,600	25.6	70,000	168.0
39	4.0	330	11.6	1,700	26.4	80,000	180.0
40	4.1	340	11.8	1,800	27.1	90,000	191.0
41	4.1	350	12.0	1,900	27.9	100,000	201.0
42	4.2	360	12.1	2,000	28.6	200,000	282.0
43	4.2	370	12.3	2,100	29.3	300,000	343.0
44	4.2	380	12.5	2,200	30.0	400,000	393.0
45	4.3	390	12.6	2,300	30.7	500,000	437.0
46	4.3	400	12.8	2,400	31.3	600,000	475.0
47	4.4	410	13.0	2,500	32.0	700,000	510.0
48	4.4	420	13.1	2,600	32.6	800,000	541.0
49	4.5	430	13.3	2,700	33.2	900,000	571.0

TABLE IV.- LUNAR LANDING AREAS

Previously Selected Landing Site Locations					Regional Slope	Surface Texture	Structural Strength	Landmarks	Position
3°40'	E	2°40'	N		F	U	F	F	F
36°	W	3°	S	**	F	U	F	U	F
14°12'	W	5°06'	N		F	U	F	F	F
44°	W	3°	S		F	F	F	F	U
36°55'	E*	1°45'	N		F	F	F	F	F
28°22'	E*	1°10'	N		F	F	F	U	F
1°28'	W*	0°30'	S	***	F	F	F	F	F
13°15'	W*	2°45'	N		F	F	F	F	F
31°30'	W*	1°05'	S		F	F	F	F	F
Other Sites Considered									
3°30'	W	2°50'	S		F	F	F	F	F
31°	E*	0°	N		F	F	F	F	F
28°15'	W*	2°45'	N		F	F	F	F	F
24°10'	E*	0°10'	N		F	F	F	F	F
12°50'	E*	0°20'	N		F	U	F	F	F
41°30'	W*	1°10'	S		F	F	F	U	F

*Ten Recommended Landing Areas Subject to Reconnaissance Verification
**Reference 15
***Reference 17
F = Favorable
U = Unfavorable

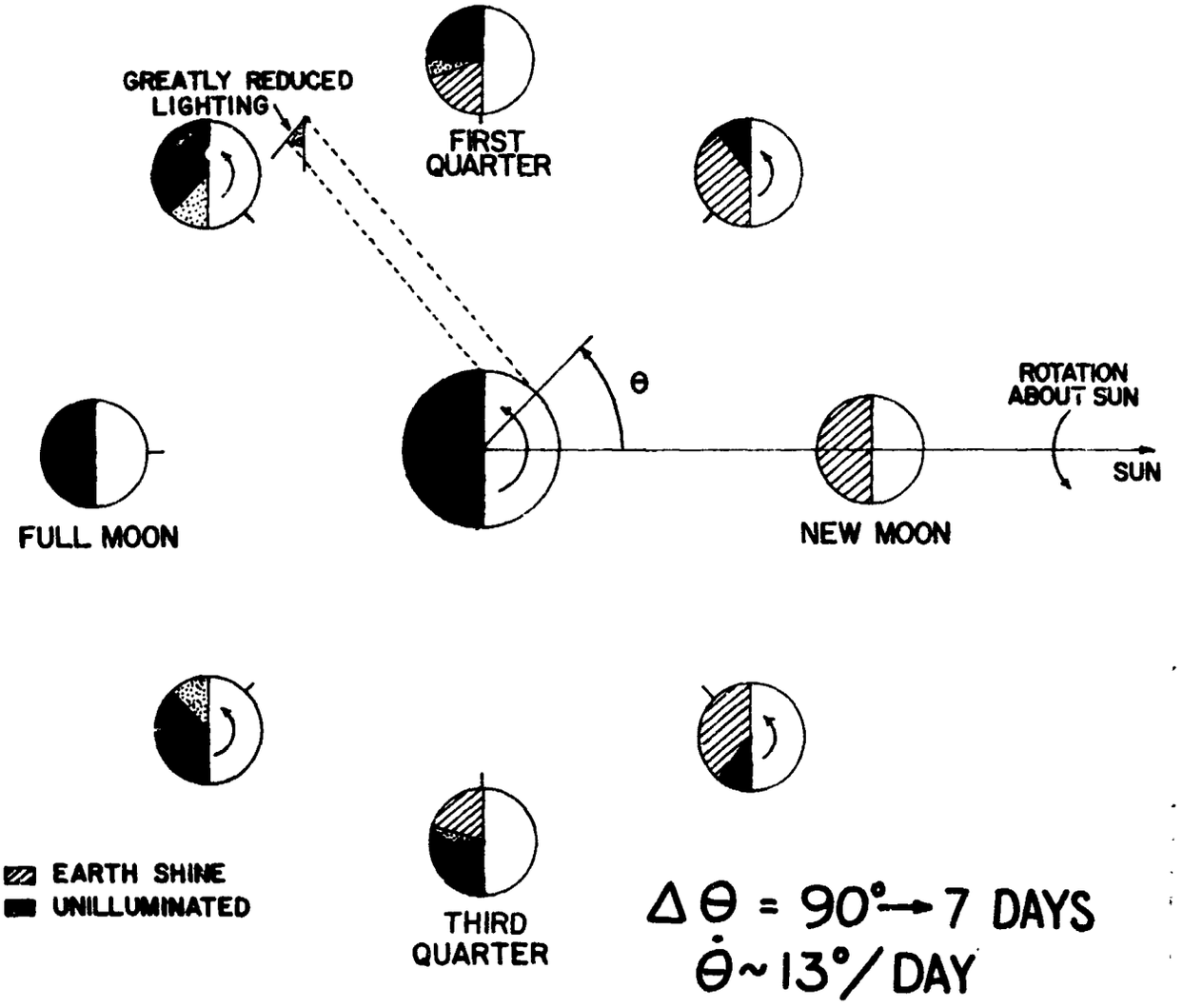

FACTORS

1 LIGHTING (LUNAR SURFACE)
2 HEATING (LUNAR SURFACE)
3 LAUNCH WINDOW (EARTH)
4 NAVIGATION (LUNAR ORBIT)
5 LANDING SITE SELECTION (LUNAR)
6 EARTH REENTRY LIGHTING
7 EARTH-MOON COMMUNICATIONS
8 METEOROIDS (LUNAR SURFACE)
9 RADIATION (LUNAR SURFACE)

Figure 1.- The geometry and factors involved in the choice of lunar operational dates and the choice of lunar landing sites.

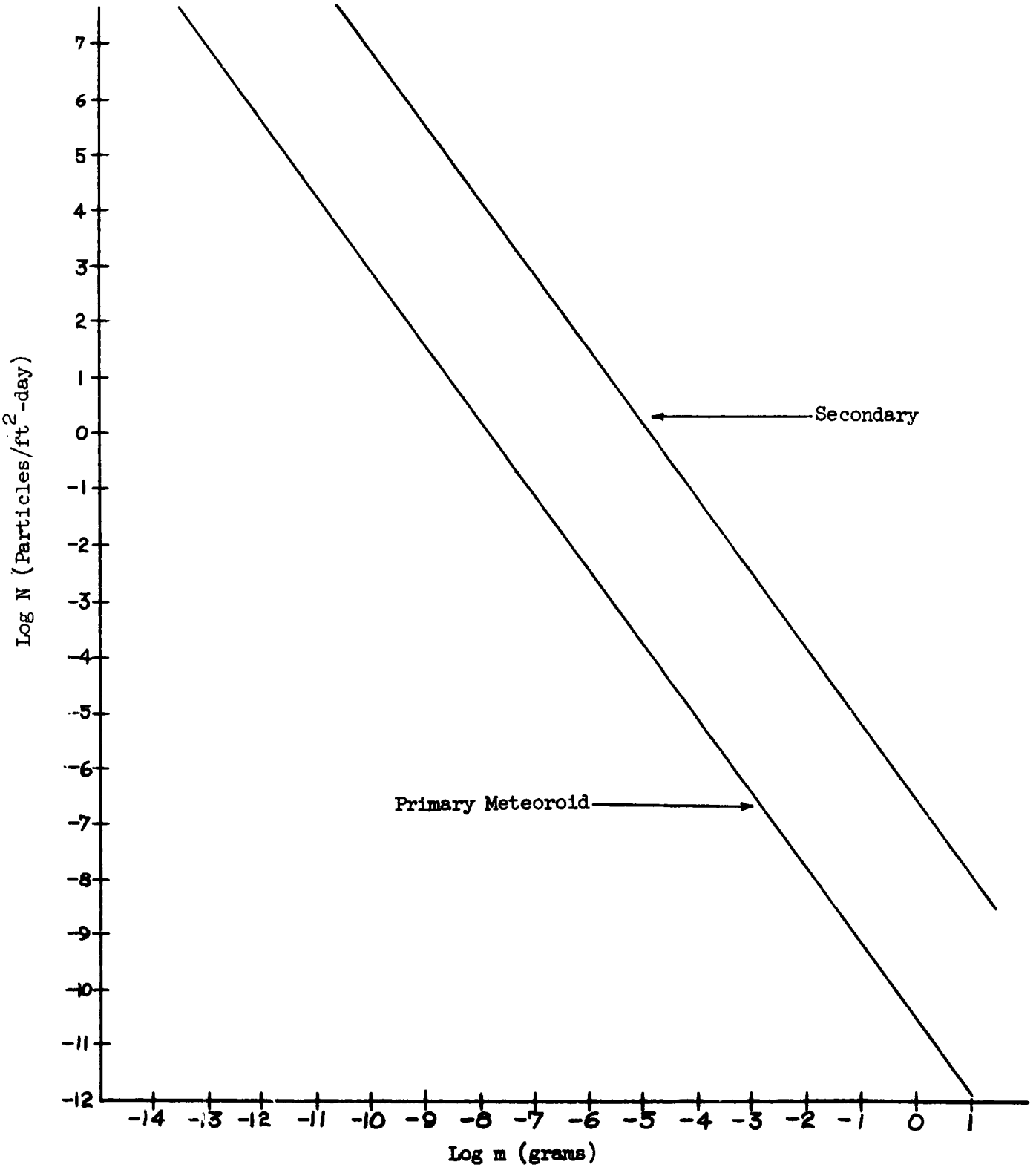

Figure 2.- MSC cislunar meteoroid environment with meteoroid flux as a function of meteoroid mass. Secondary flux produced by impinging primary meteoroid flux upon lunar surface.

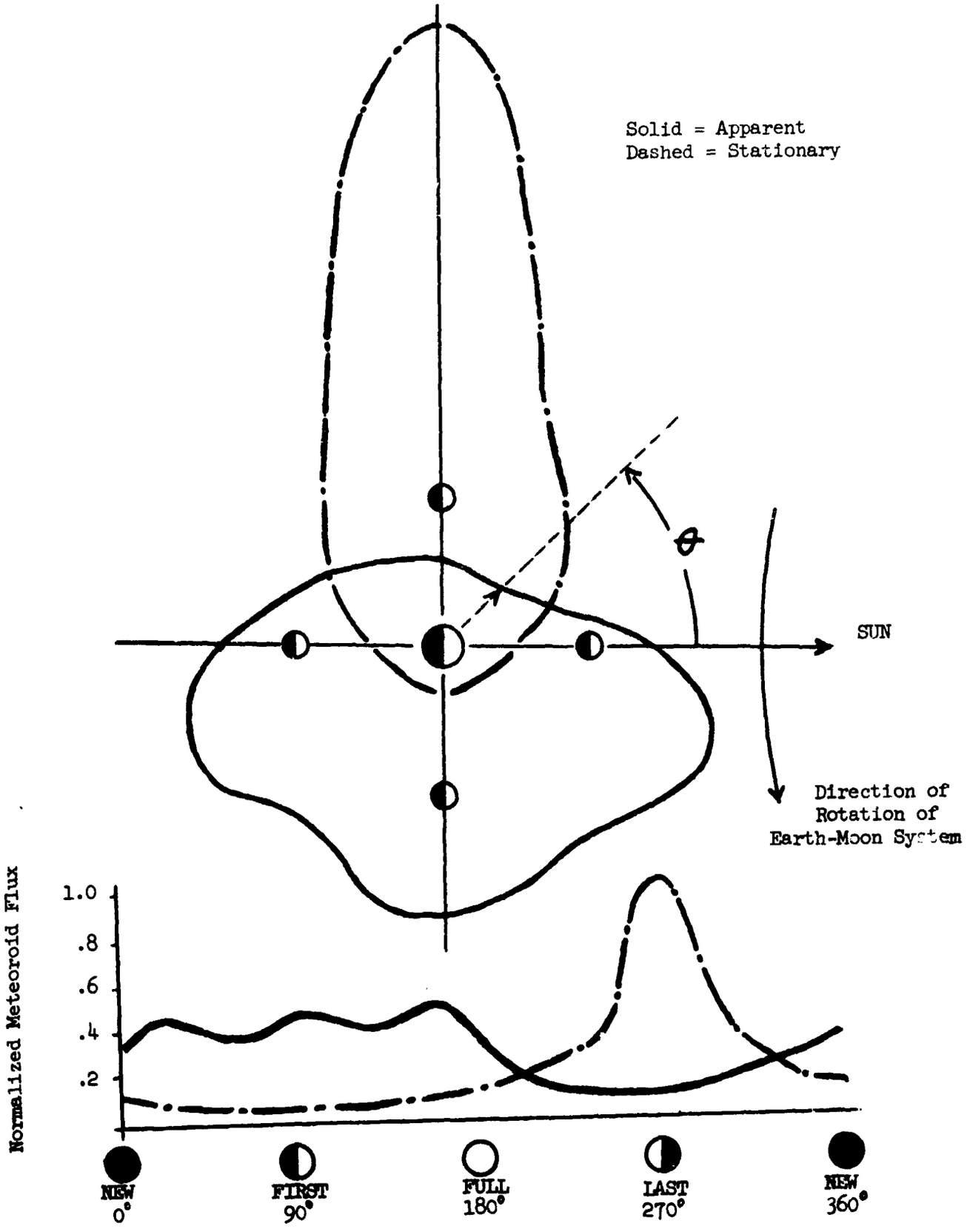

Figure 3.- Sporadic meteoroid distribution in the ecliptic plane for the earth-moon system.

Clear = Sporadic
Shaded = Stream

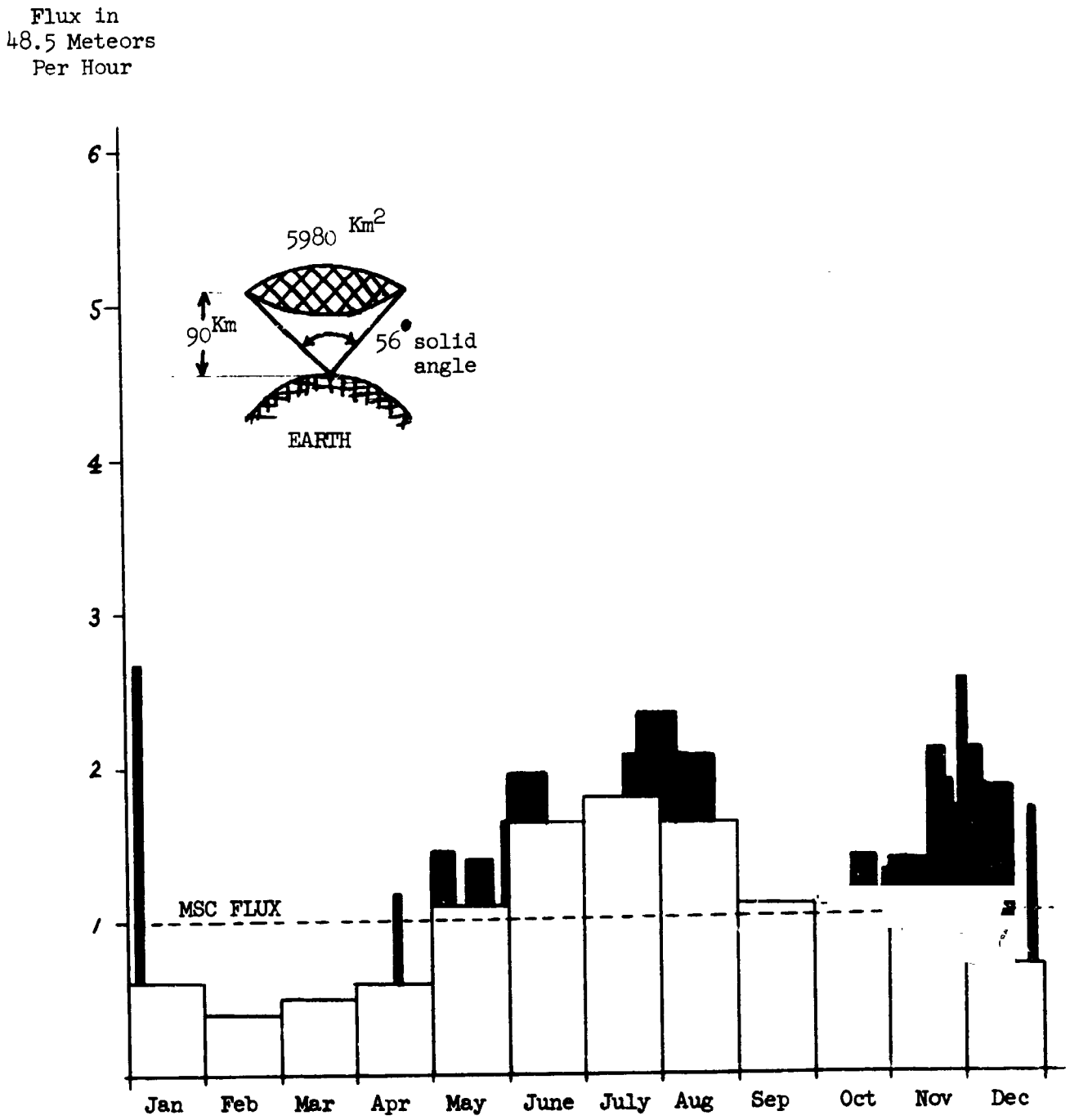

Figure 4.- Yearly sporadic and stream meteor flux at visual magnitude 5.

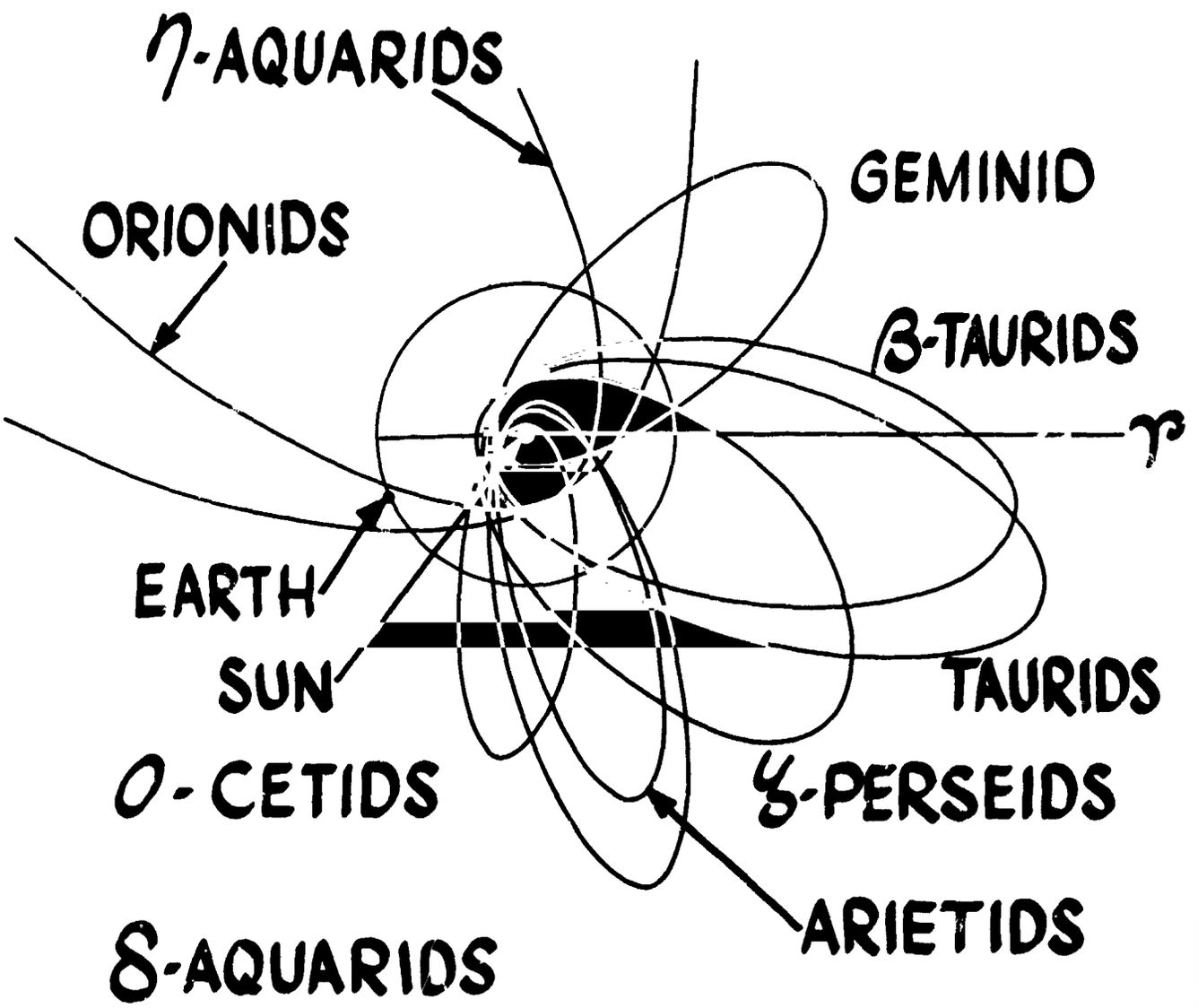

Figure 5.- Orbits of meteor streams intersecting the ecliptic plane.

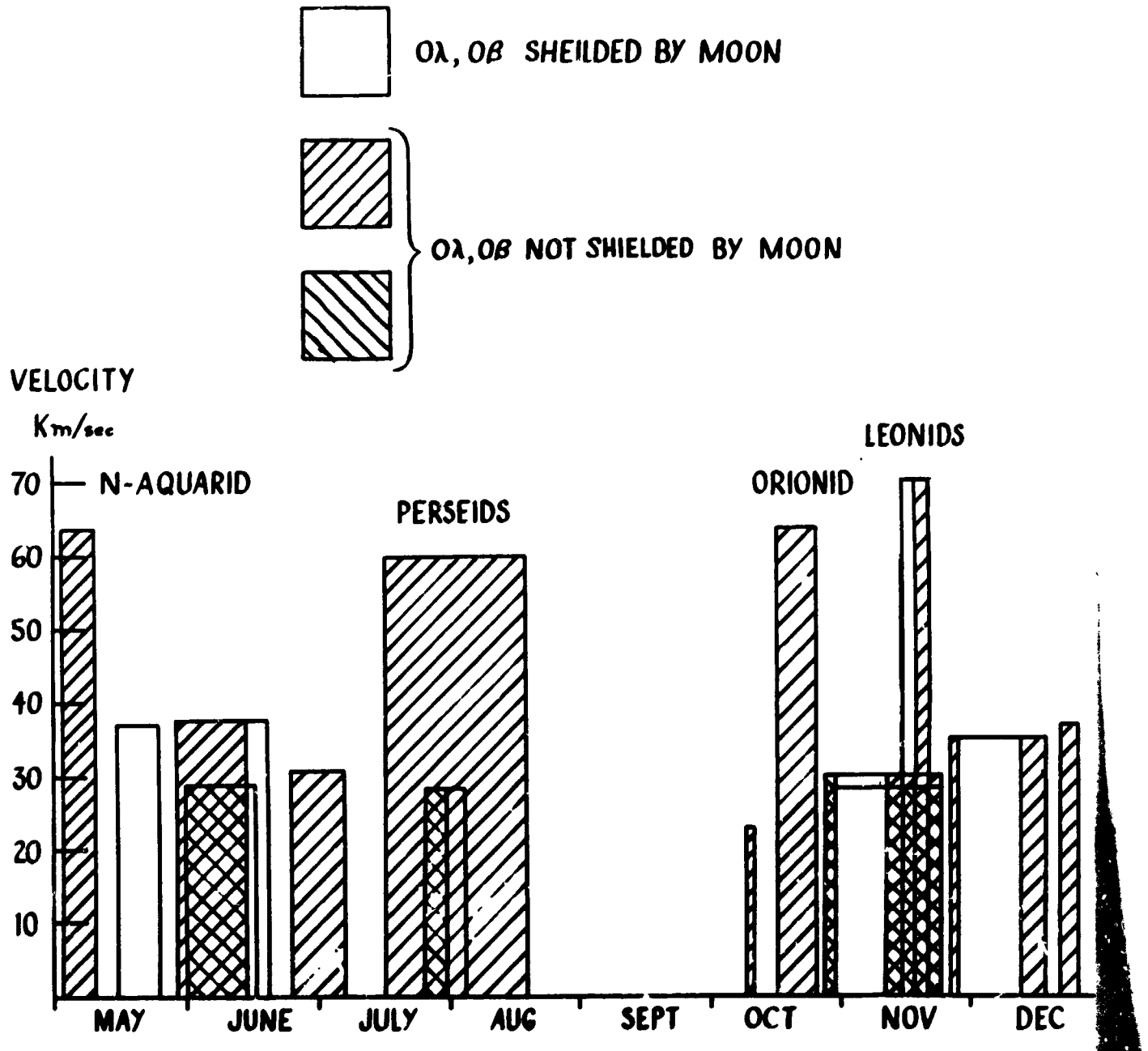

Figure 6.- Meteor stream velocity and annual distribution.

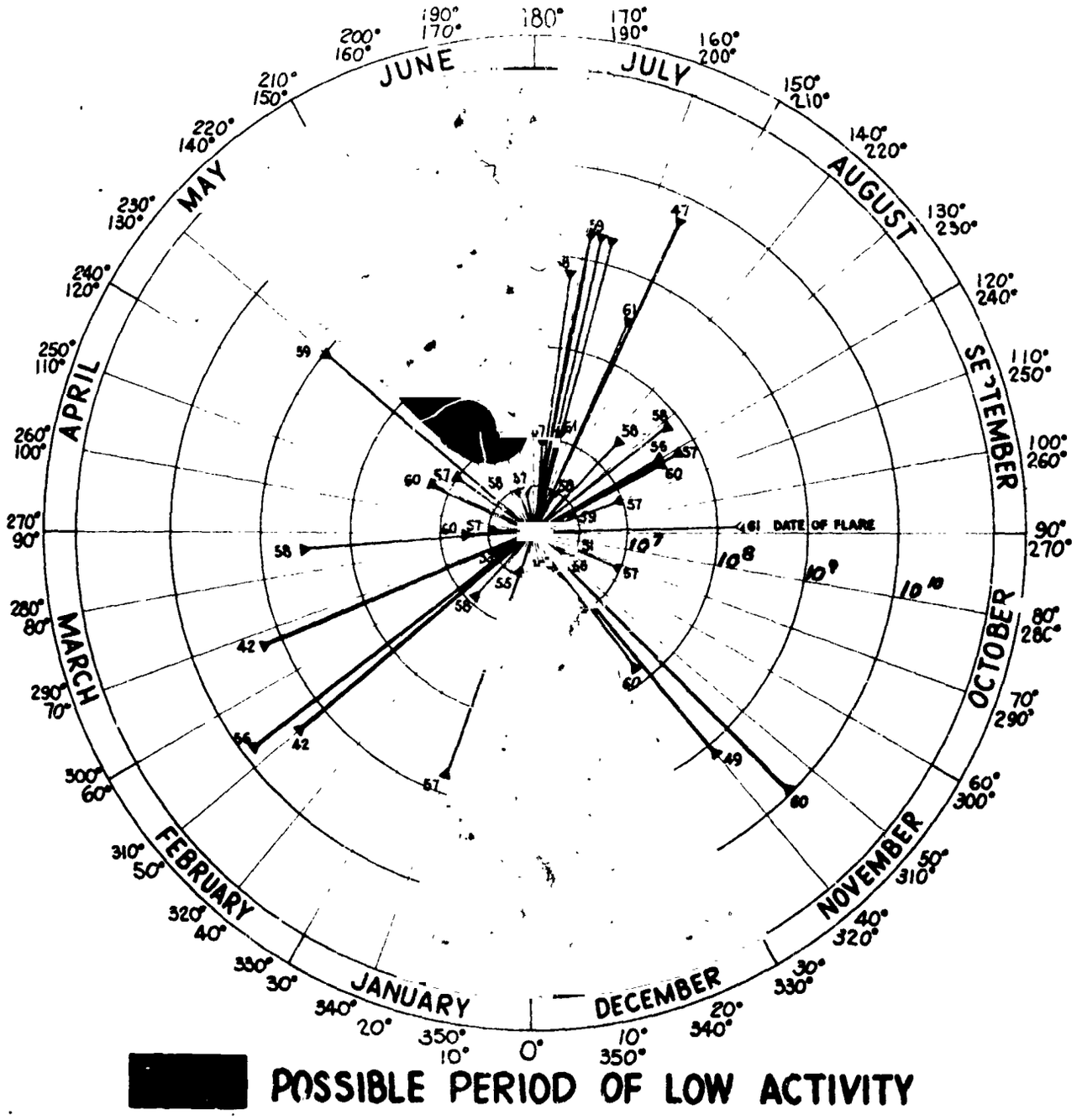

Figure 7.- A polar plot of the number of protons per square centimeter having energy greater than 30 Mev for every event during solar cycle 19.

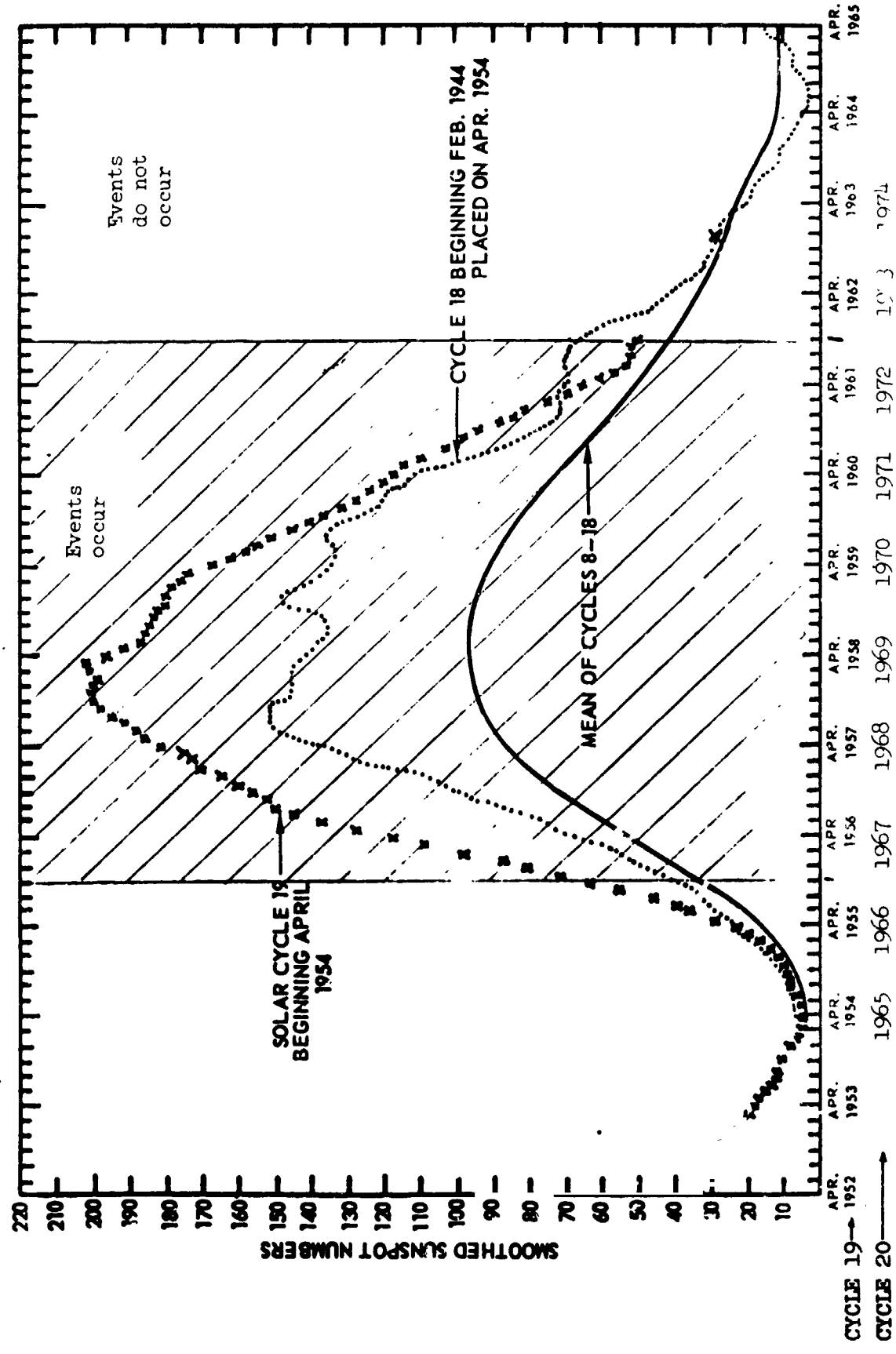

Figure 8.- Occurrence of sclar flare proton events in 11 year sunspot cycles.

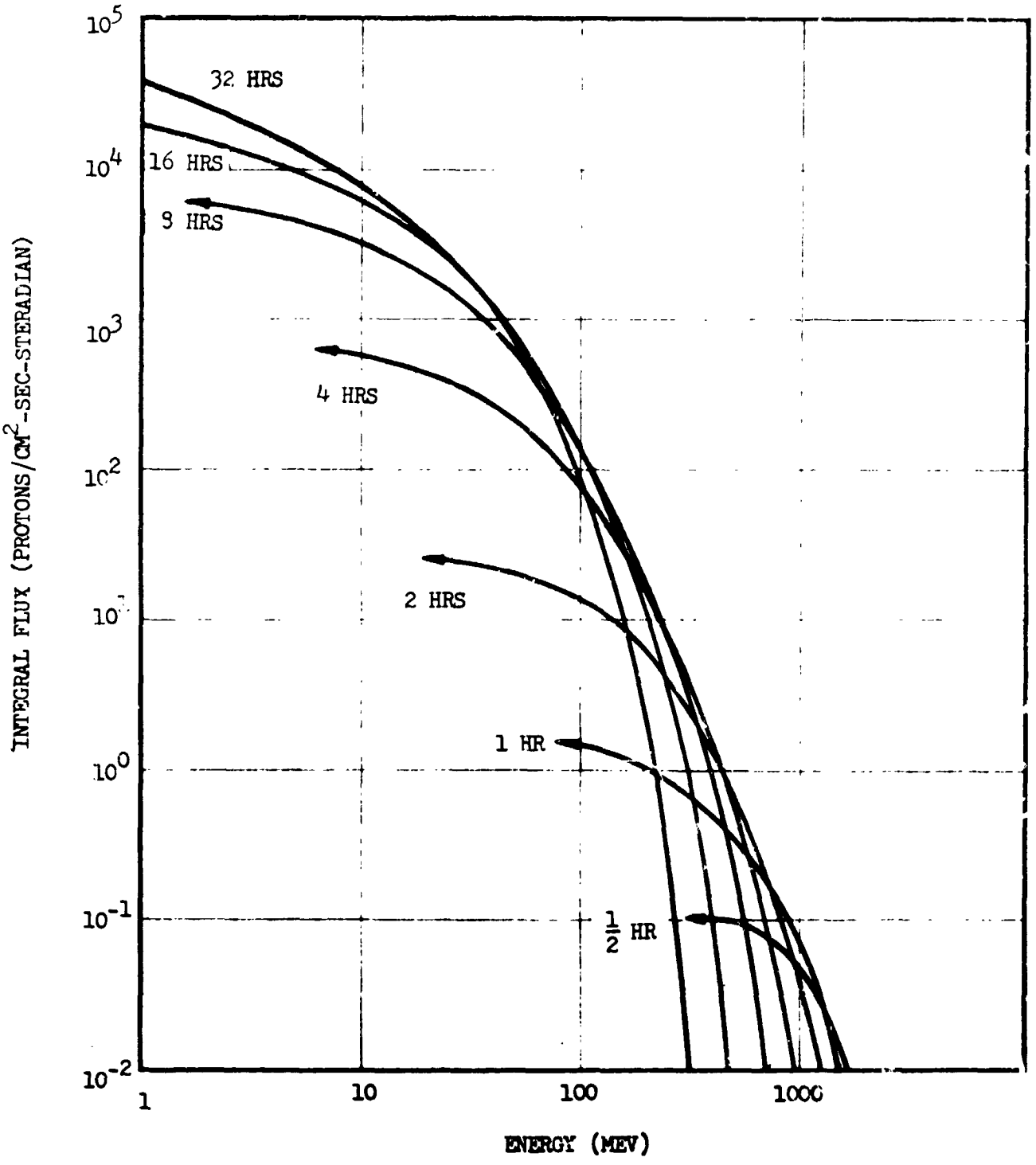

Figure 9a.- Variation of Solar Proton Energy Spectra with Time. (Bailey Model)

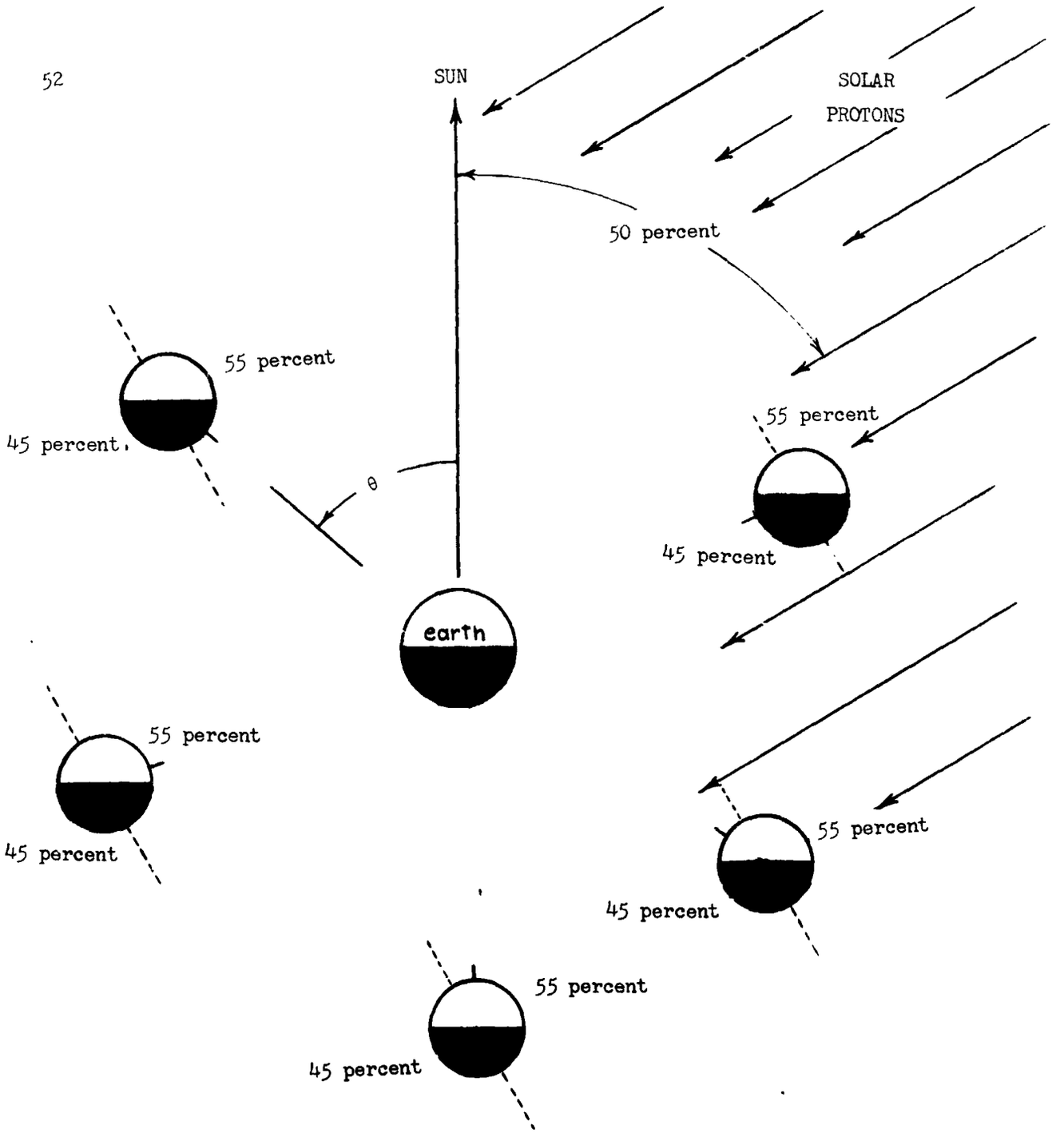

Figure 9b.- Dose reduction by lunar shielding from solar flare proton events.

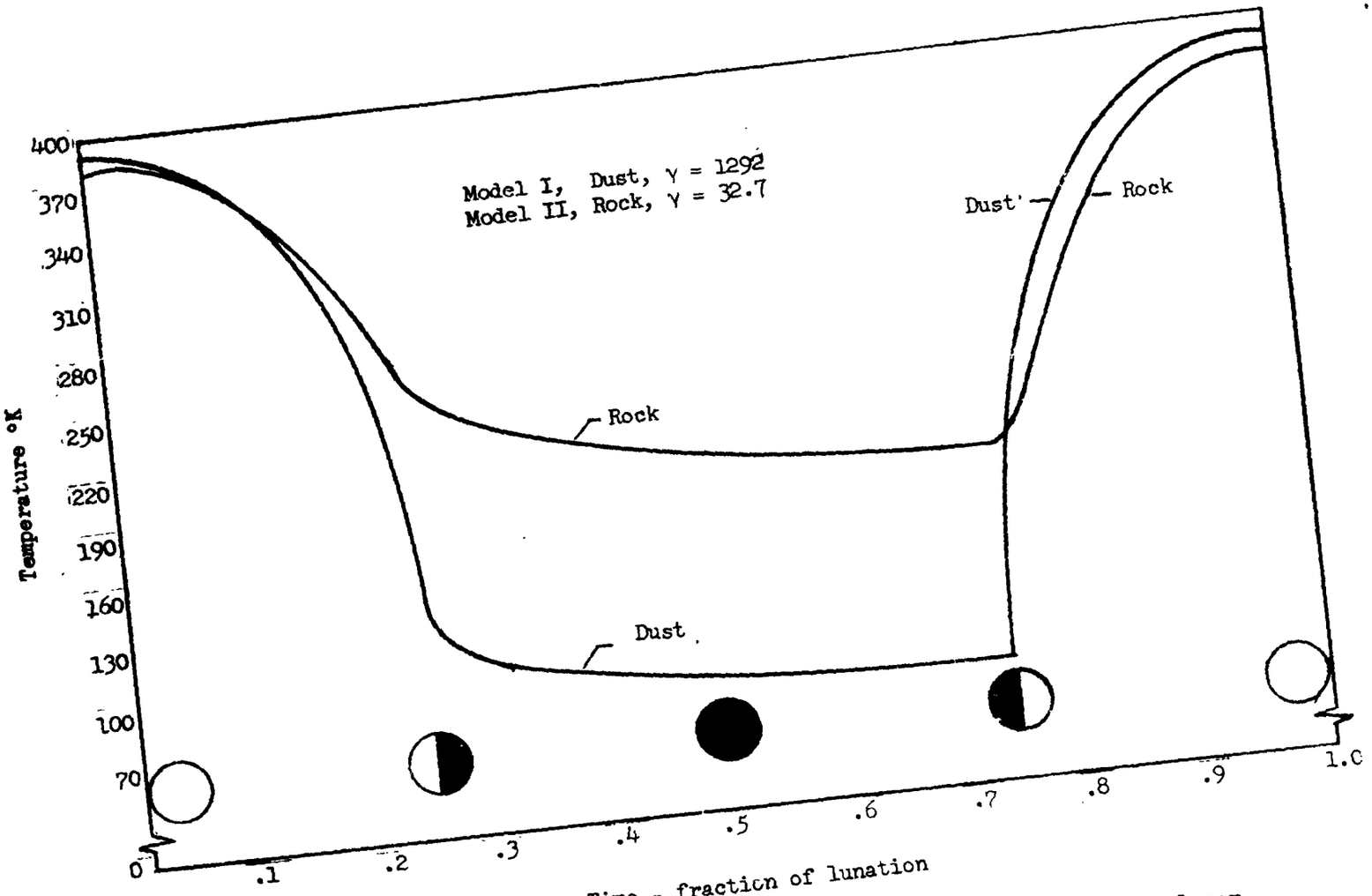

Figure 10.- Surface temperature during a lunation for two extreme lunar surface models at the lunar equator.

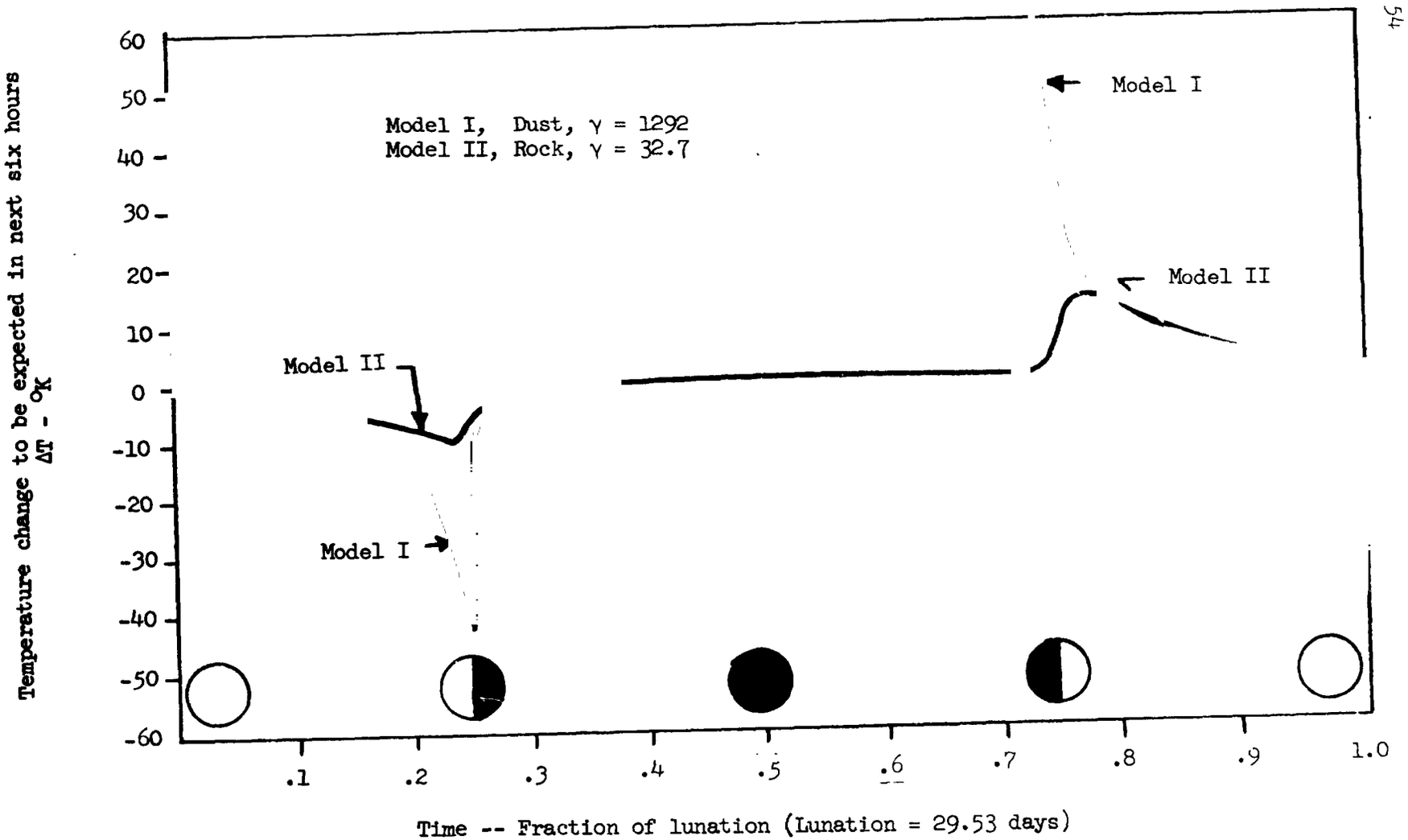

Figure 11.- Rate of change of surface temperature every six hours.

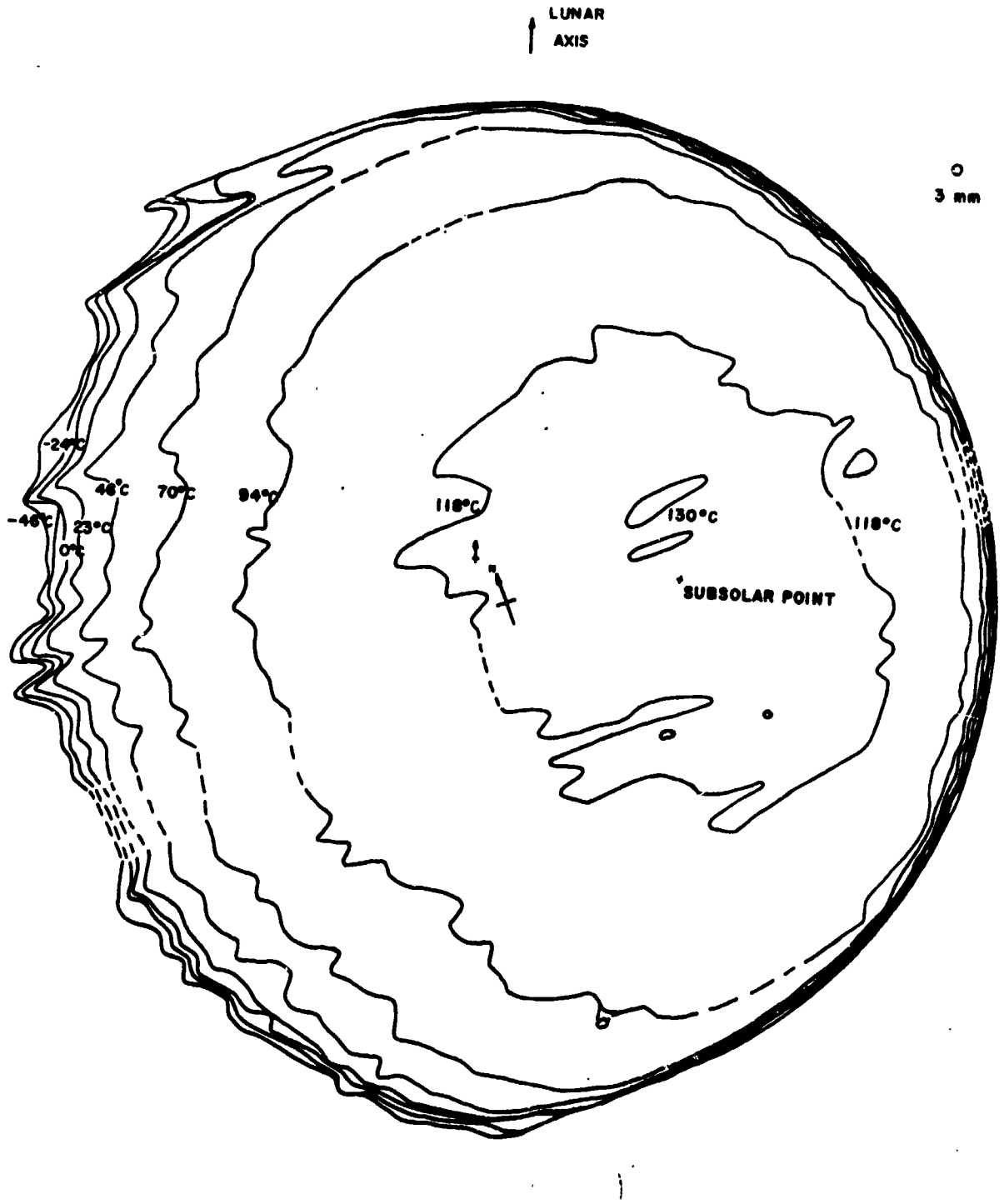

Figure 12.- Isothermal contours in degrees Centigrade for a 0.98 illuminated moon (near full moon). The small circle represents the size of the 3 mm. sensor aperture relative to this figure. (Reference 18)

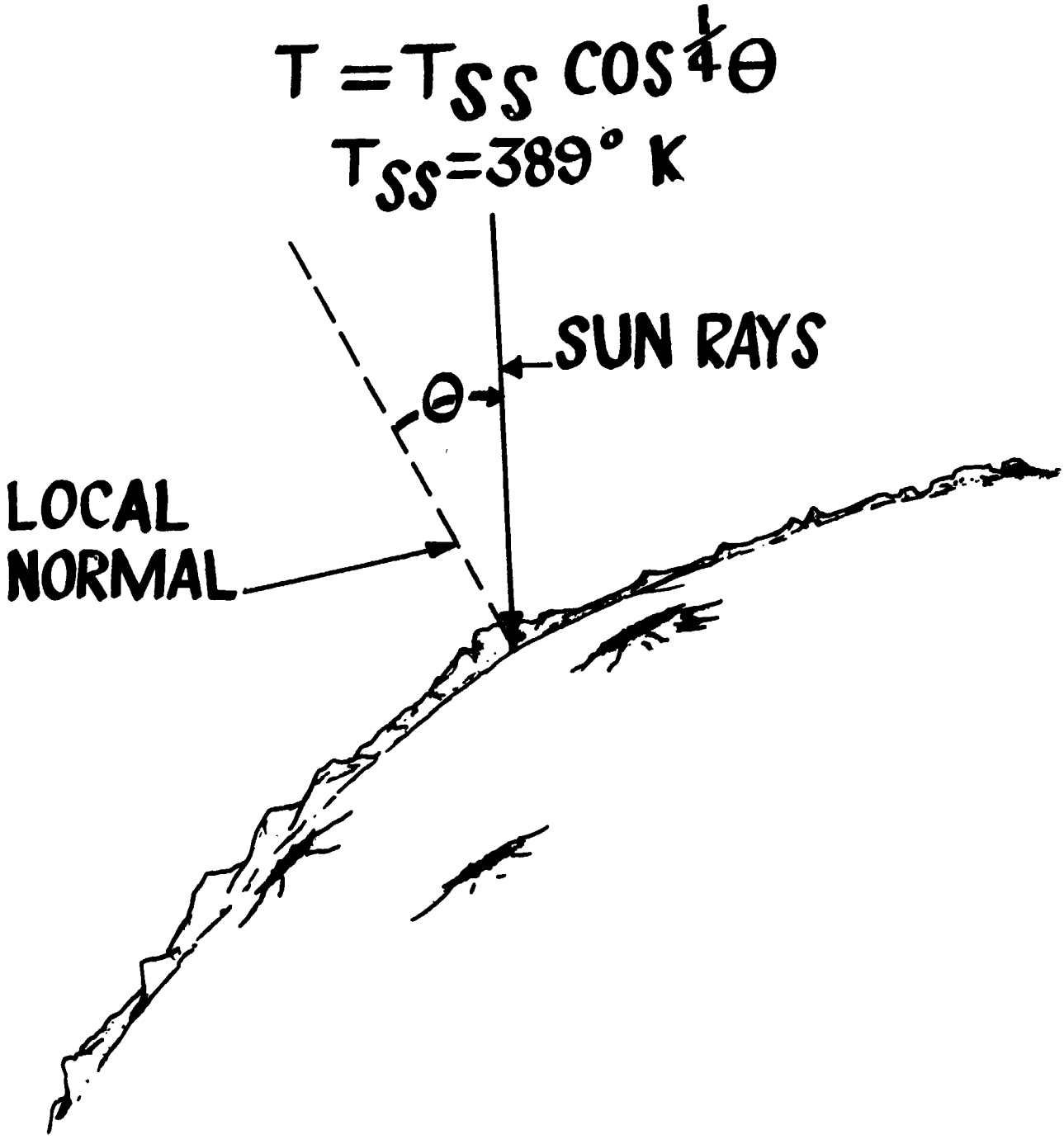

Figure 13.- Local temperature variation due to oblique incident sun rays on the lunar surface.

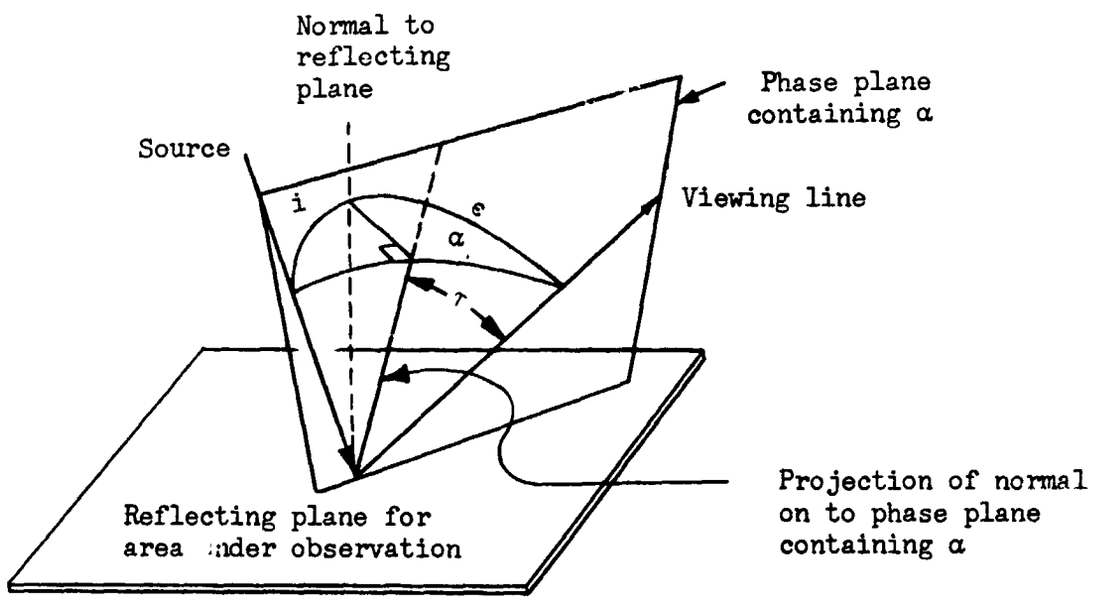

Figure 14.- Diagram of the three photometric angles i, ε, and α. Angle τ is the projection of angle ε onto phase plane containing α.

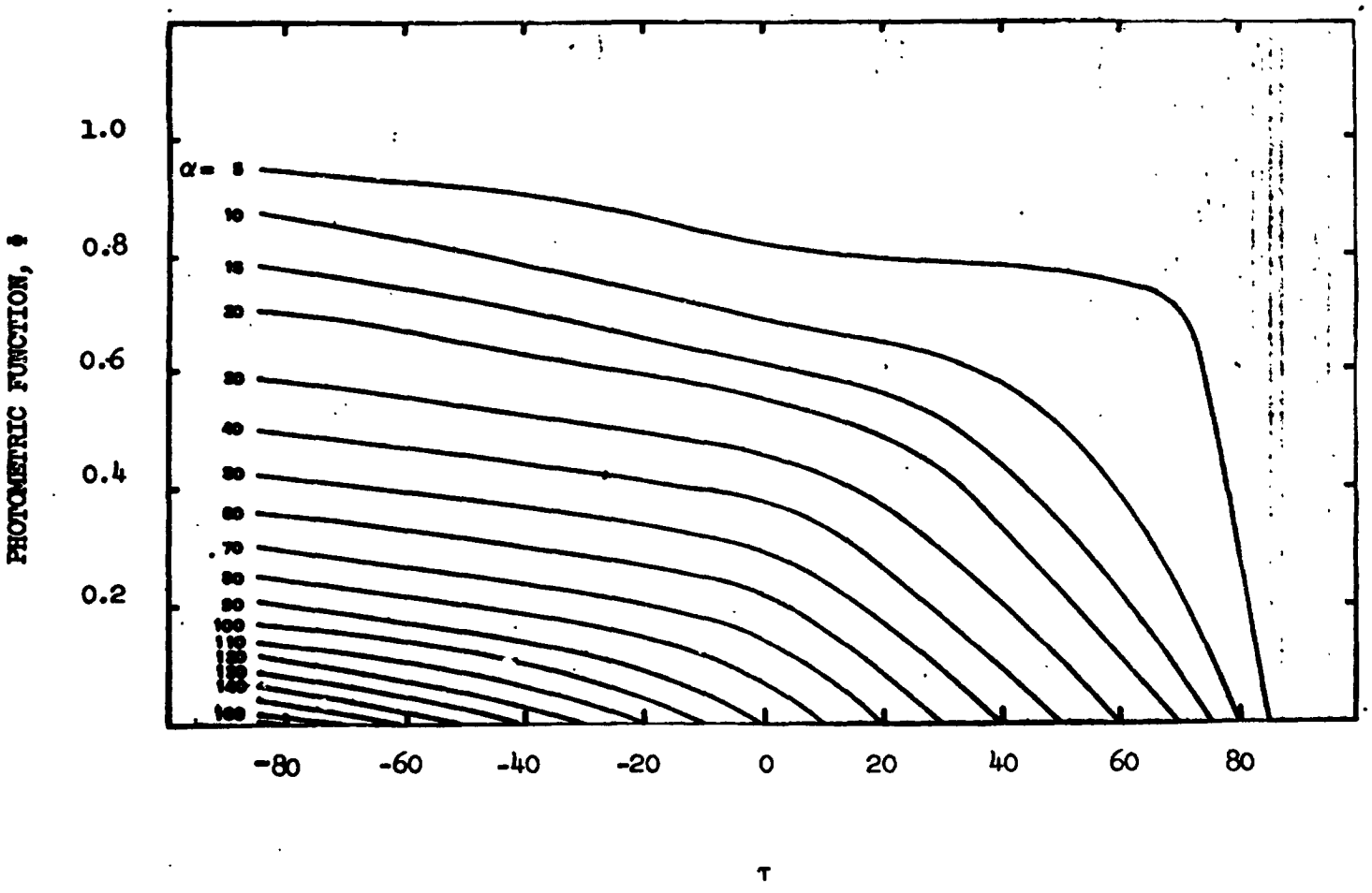

Figure 15.- Variation in photometric function Φ as a function of photometric angle τ for different phase angles.

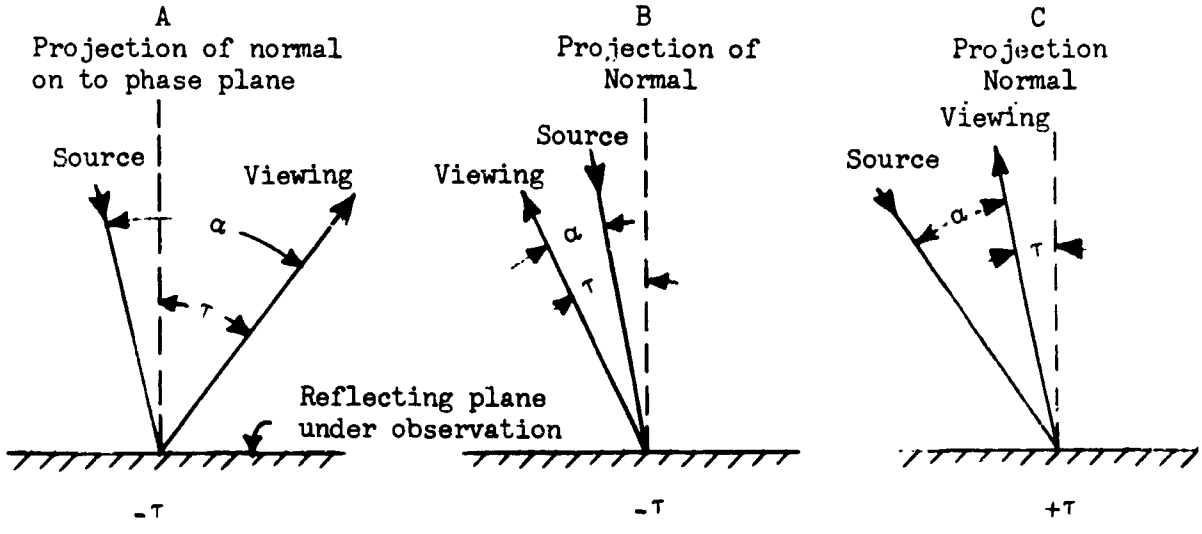

Figure 16.- Sketches defining angle τ. Angle τ is considered to have positive values when viewing line lies between source line and the normal to reflecting plane under observation as illustrated in sketch (c).

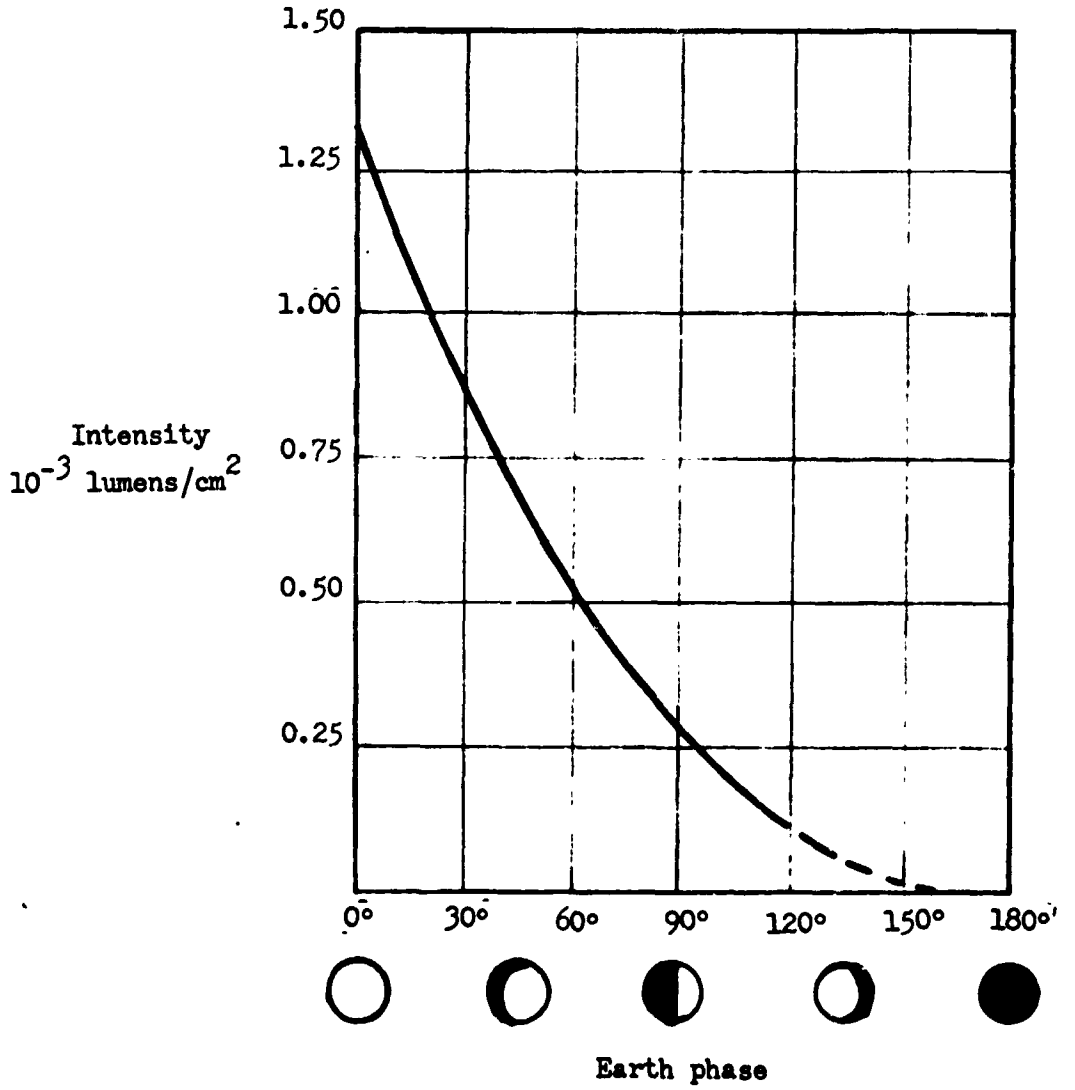

Figure 17.- Earthshine intensity upon the moon as a function of earth phase. Values are for mean earth albedo of 40 percent corrected to mean distance between earth-moon and earth-sun.

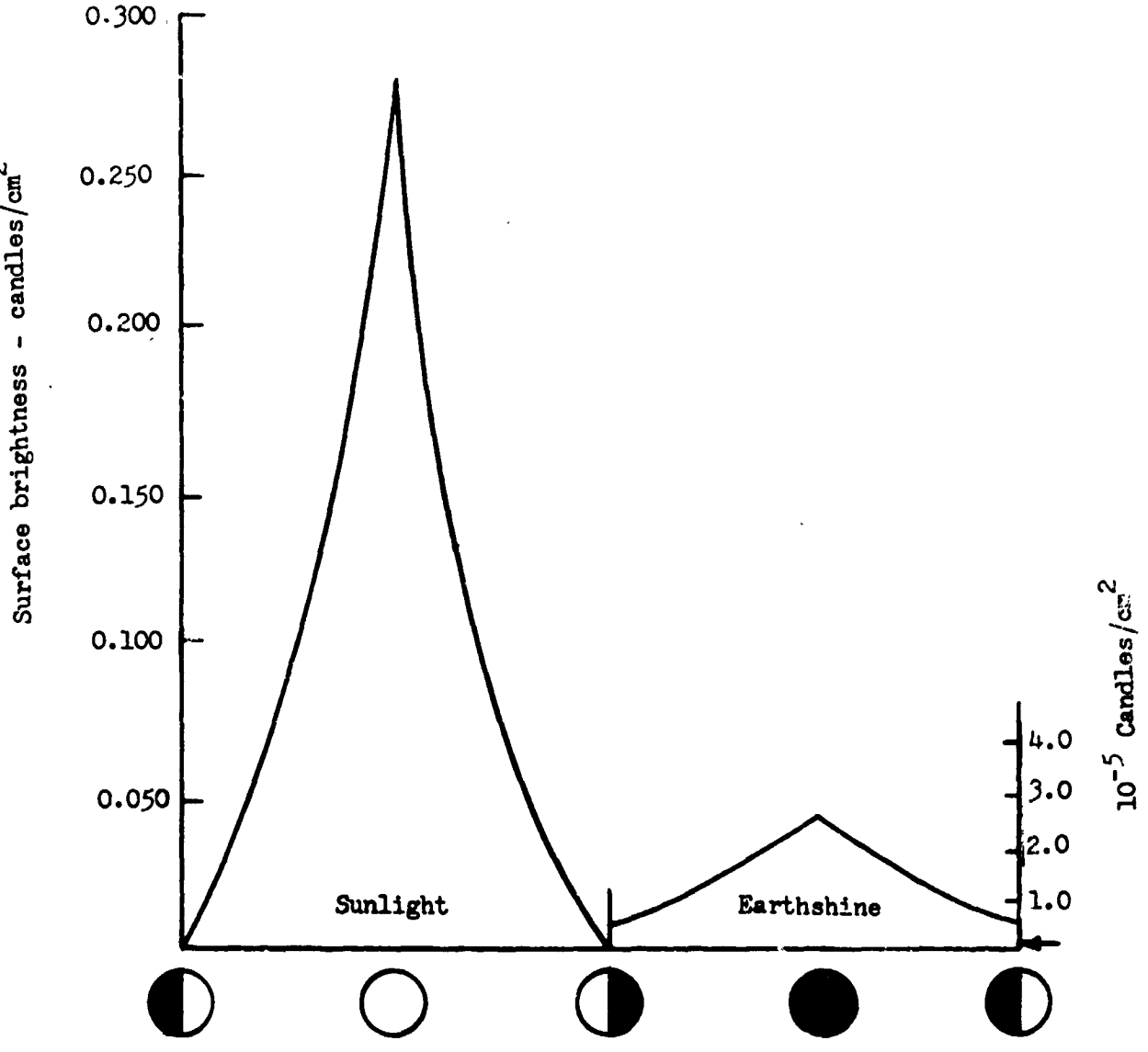

Figure 18.- Variation in surface brightness for normal viewing throughout a complete lunation for a mare area. Albedo of 0.065 at 0° λ, 0° β. For comparison purposes, the brightness of sandy loam soil on Earth with an albedo of 25 percent under full moon is indicated by an arrow on the earthshine ordinate.

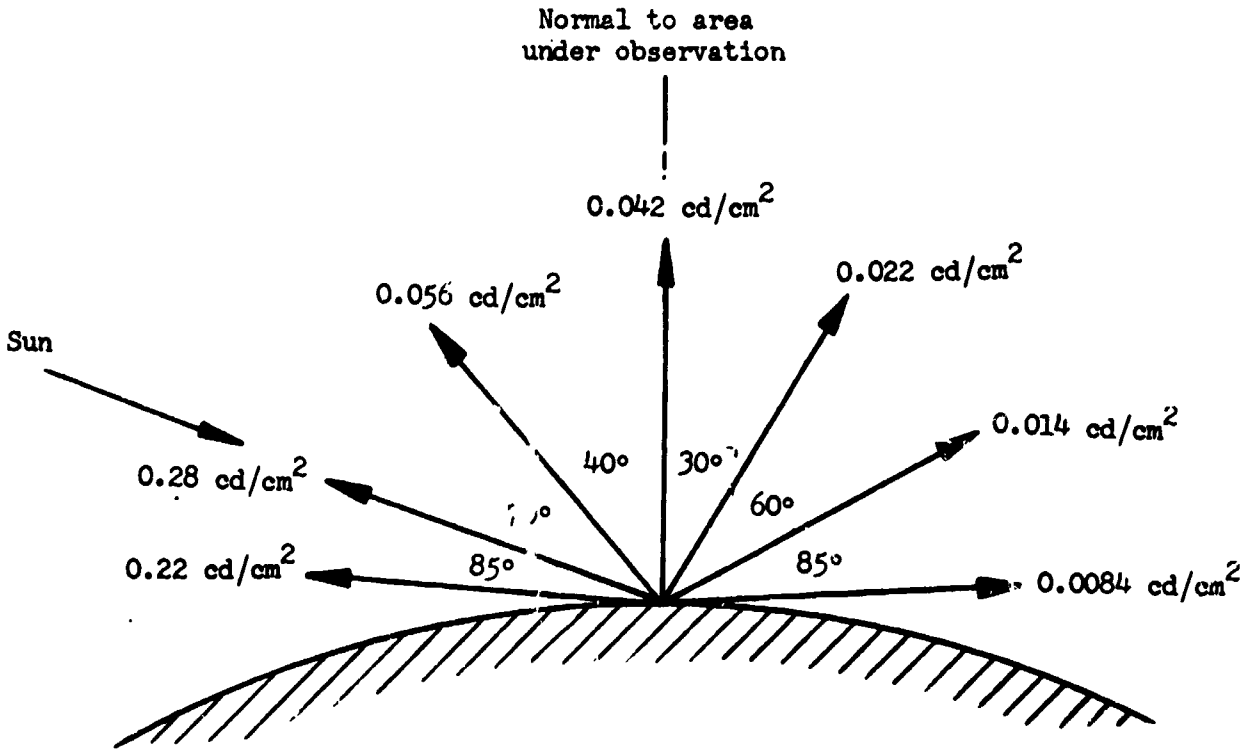

Figure 19.- Lunar surface brightness for various viewing angles from the normal with sun at 70° from normal. Values for maria area albedo of 0.065.

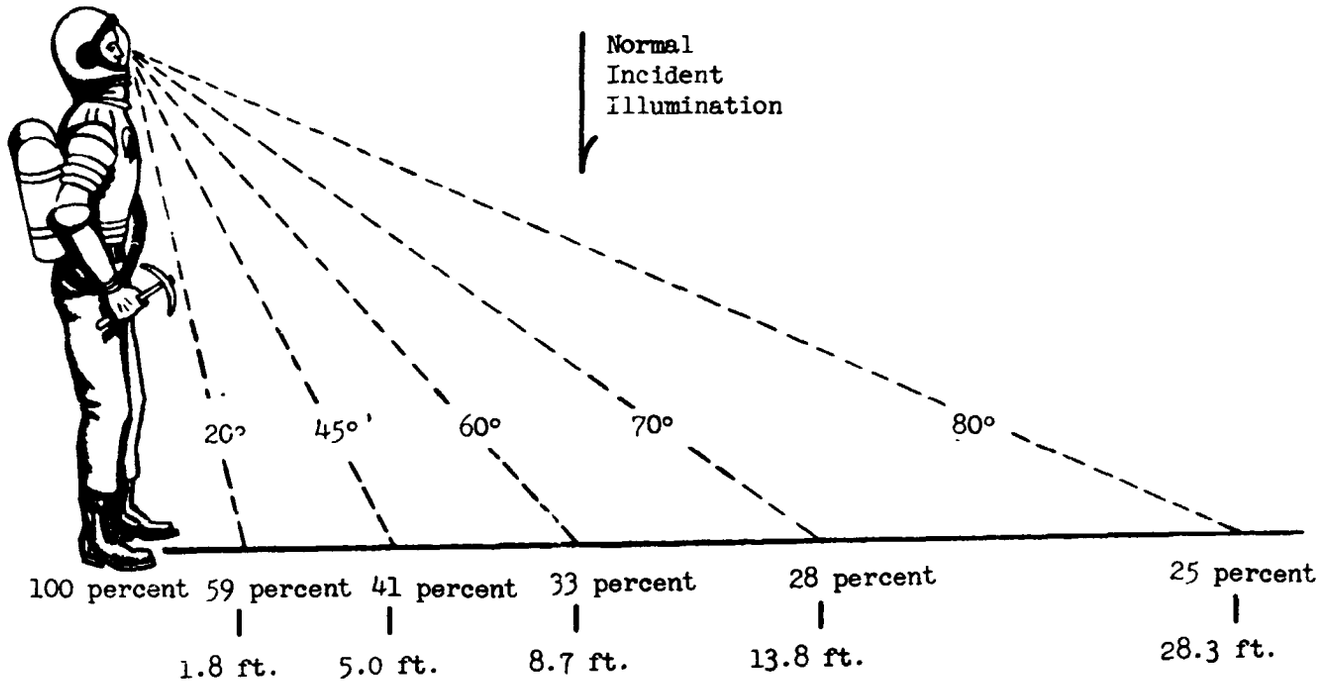

Figure 20.- Fall-off of surface luminance that an astronaut will observe for normal incident light on the lunar surface.

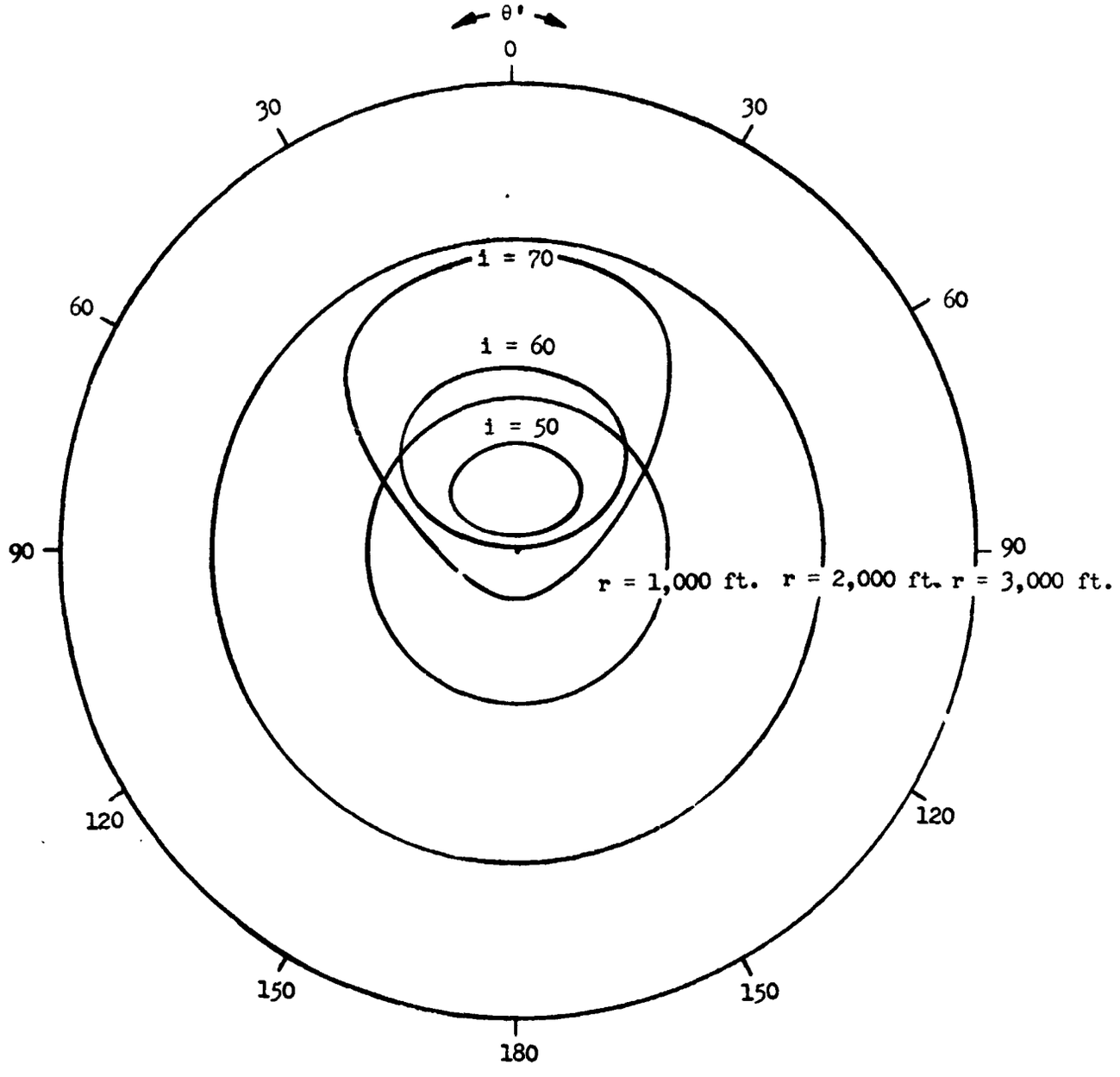

Figure 21.- Visual range limits to which conical protuberances 50 cm high may be detected from a hover altitude of 1,000 feet over maria with albedo of 0.065 illuminated by full earthshine.

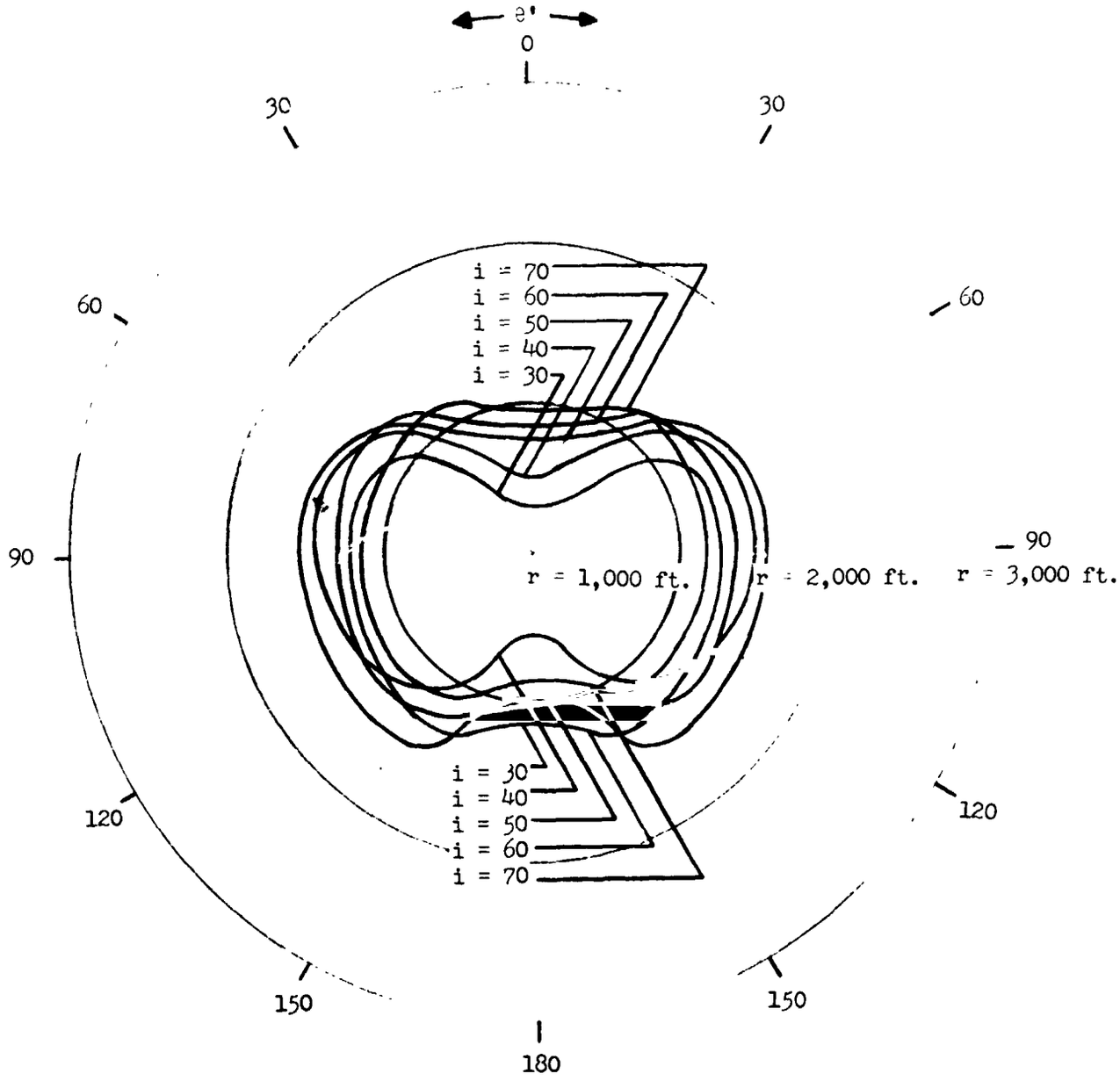

Figure 22.- Visual range limits to which spherical shaped protuberances 50 cm in diameter may be detected from a hover altitude of 1,000 feet over maria area with albedo of 0.065 illuminated by full earthshine.

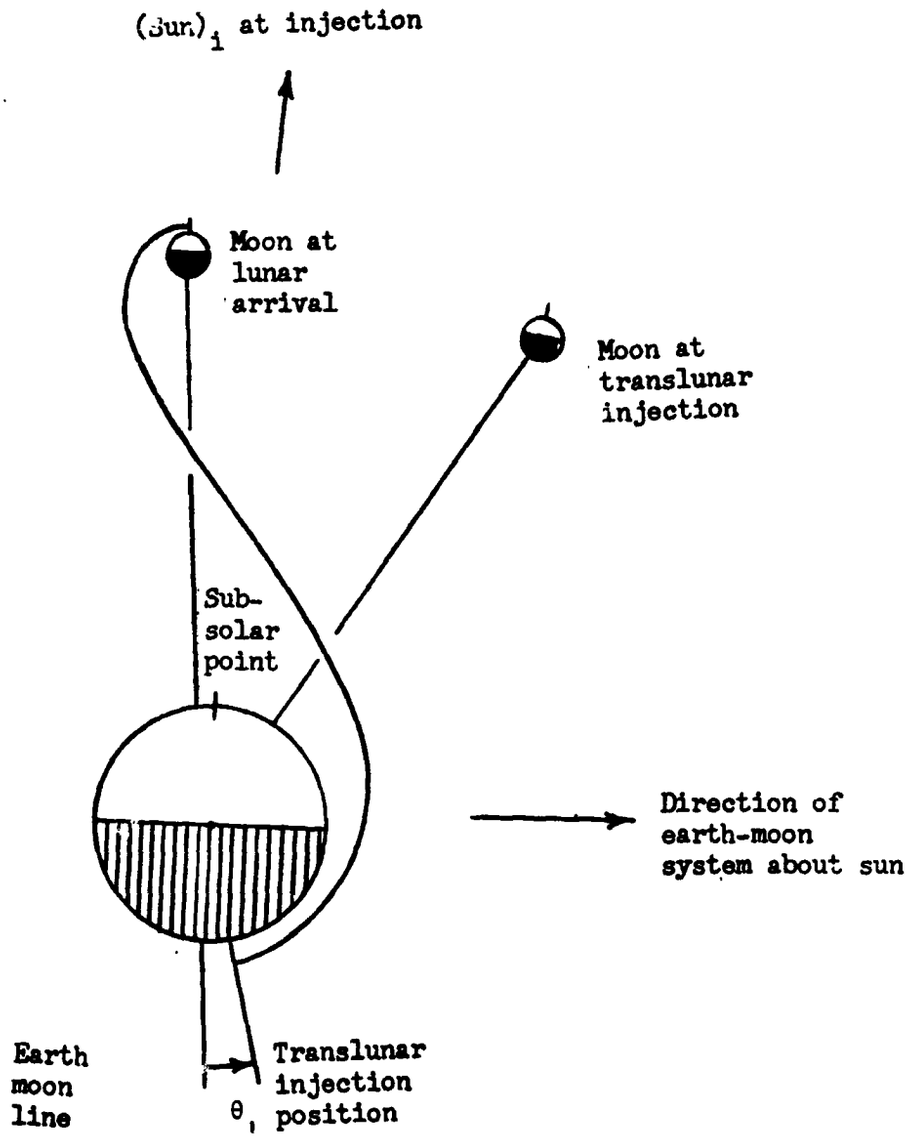

(a) Relative orientation of translunar injection position to the position of the moon at injection and at arrival at the moon.

Figure 23.- Variation in earth-lighting conditions during a lunar mission. Earth position held fixed in space.

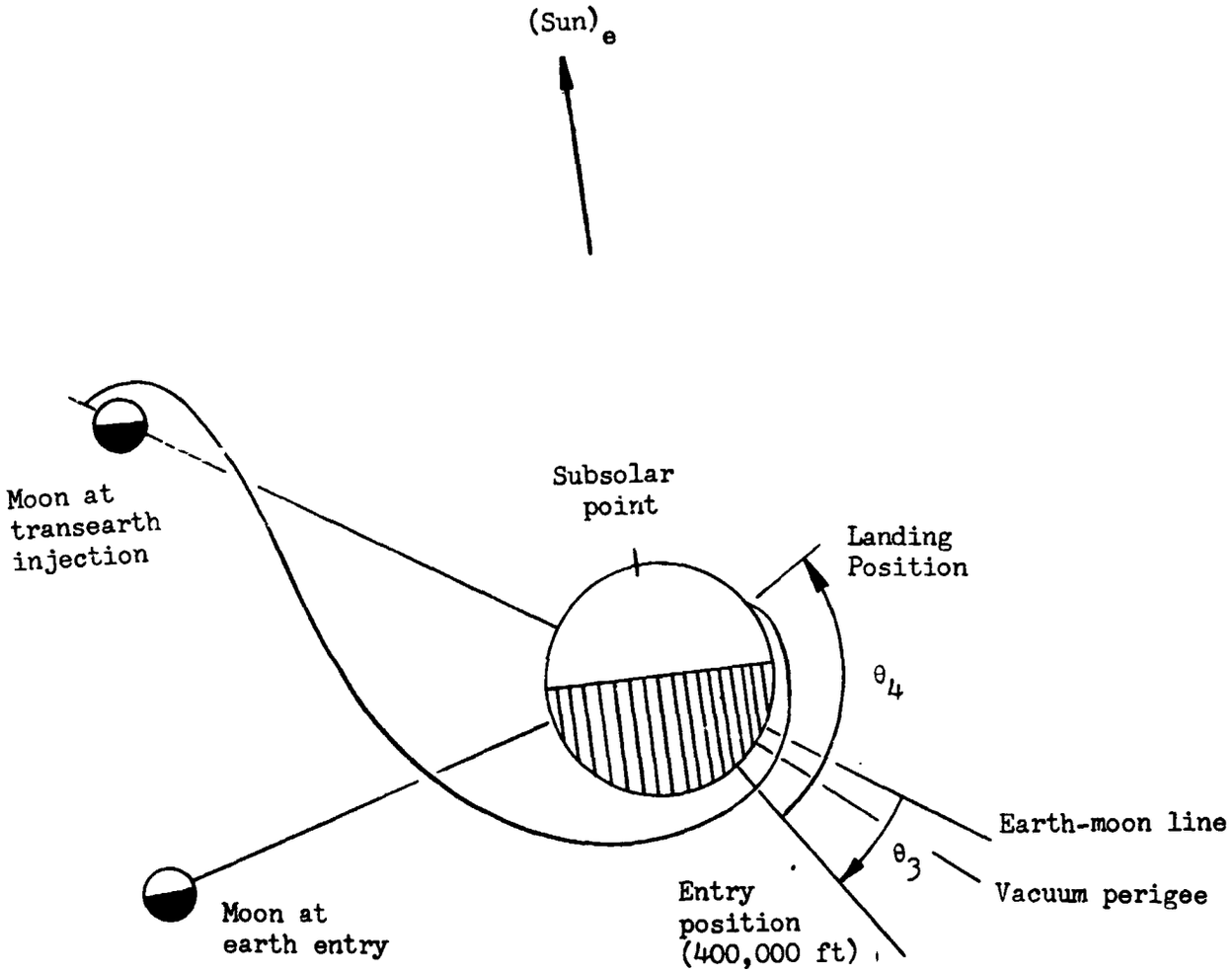

(b) Relative orientation of entry and landing position to the position of the moon at transearth injection and at the time of entry.

Figure 23.- Variation in earth-lighting conditions during a lunar mission. Earth position held fixed in space - Continued.

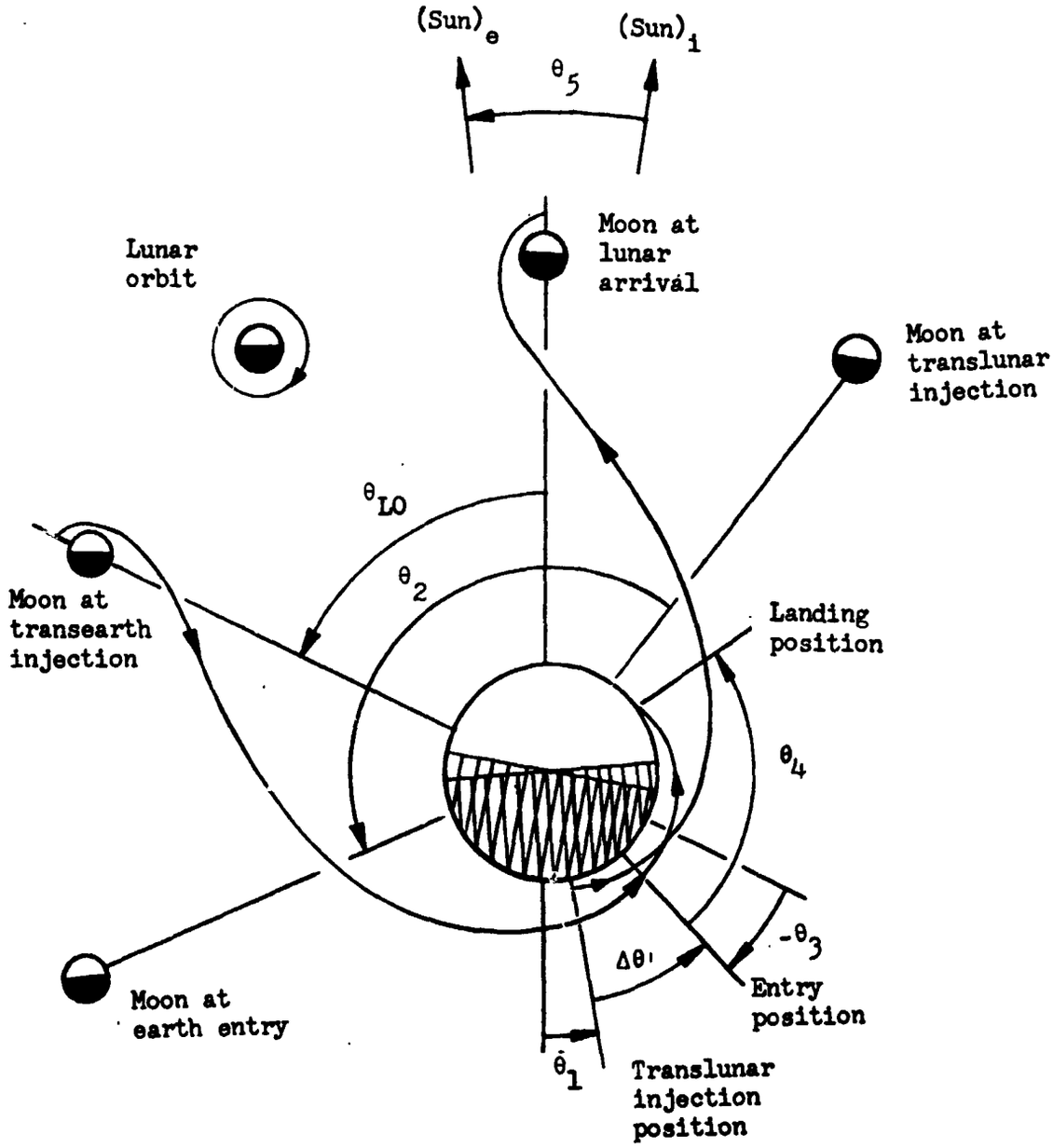

(c) Composite of position of earth-moon system during entire lunar mission.

Figure 23.- Variation in earth-lighting conditions during a lunar mission. Earth position held fixed in space - Concluded.

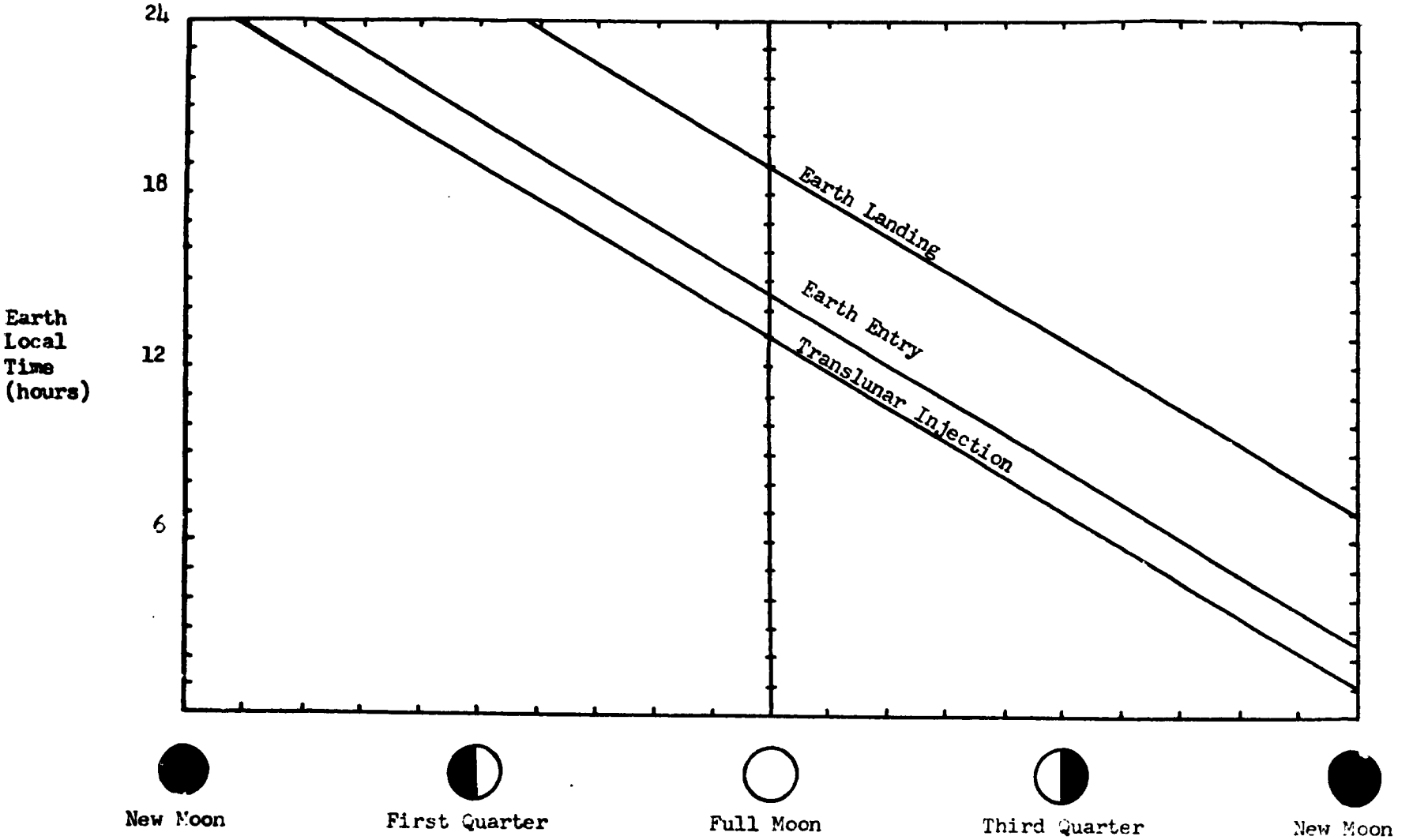

(a) 5 day lunar orbit

Figure 24.- Variation in the earth local time at translunar injection, earth entry, and earth landing as a function of the moon phase at lunar arrival.

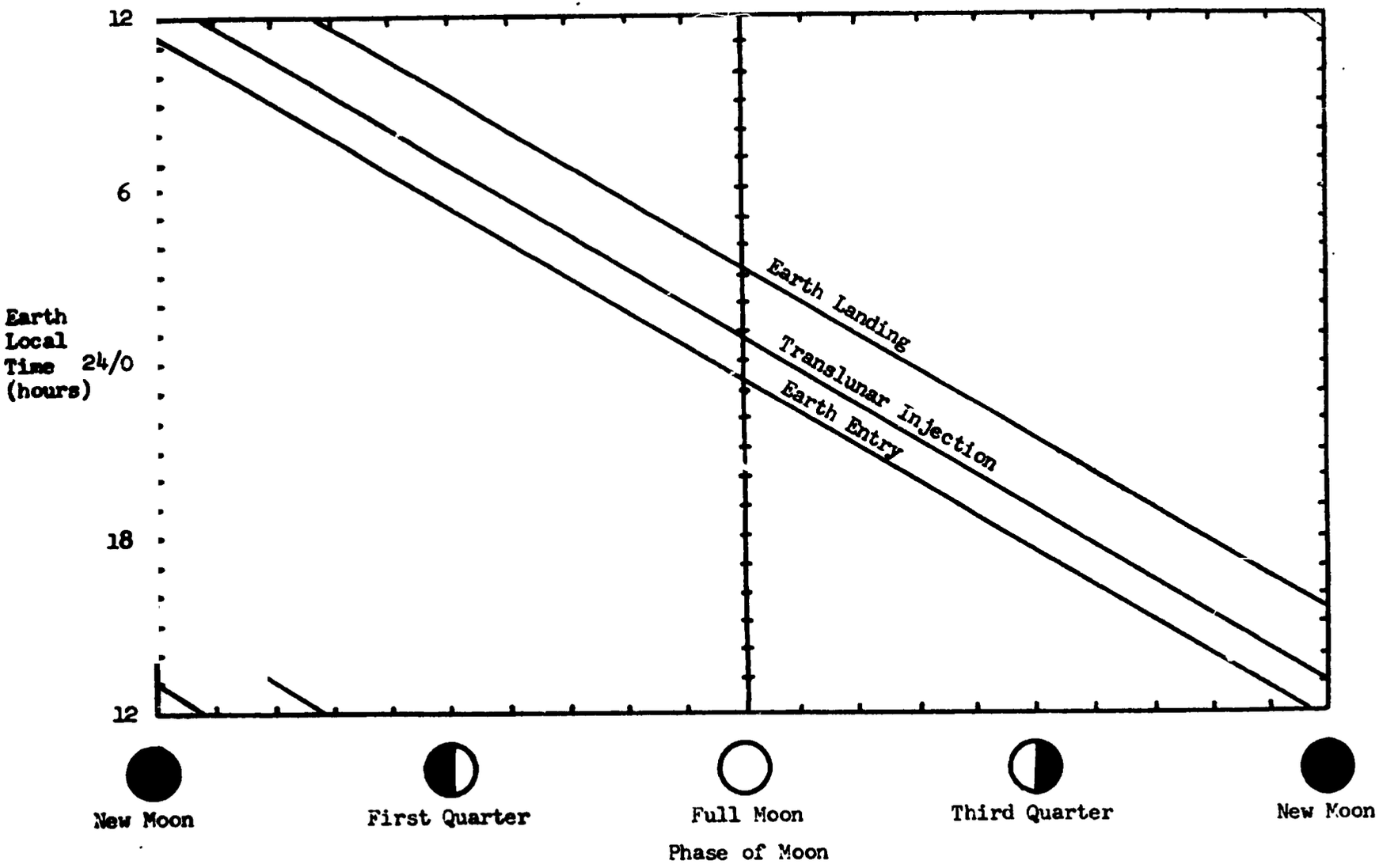

(b) 1.5 day lunar orbit

Figure 24.- Variation in the earth local time at translunar injection, earth entry, and earth landing as a function of the moon phase at lunar arrival - Concluded.

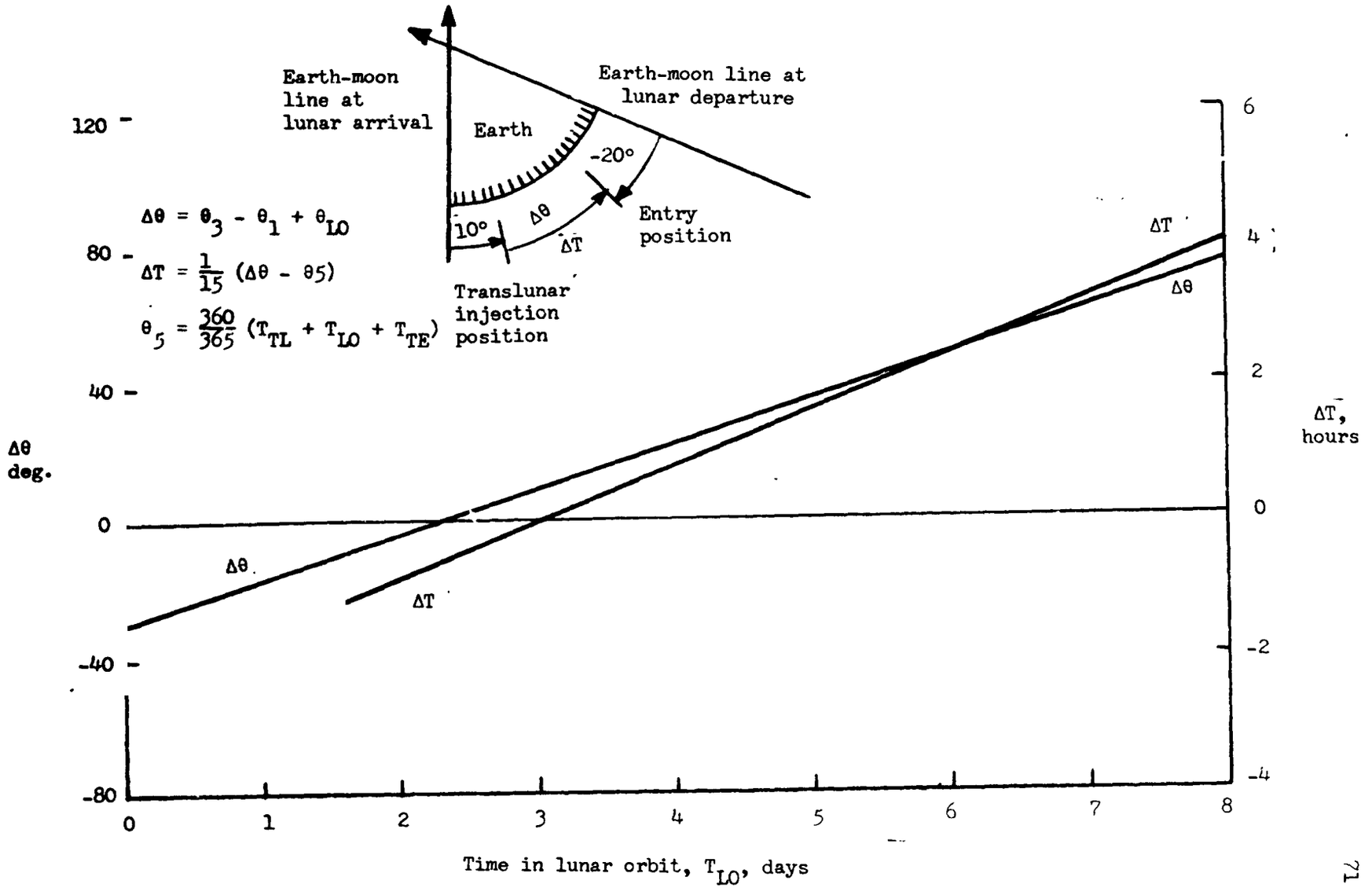

Figure 25.- Variation in inertial position (Δθ) and local solar time (ΔT) between the ejection and entry (400,000 feet) conditions as a function of lunar stay time (ΔT). A translunar time of 78 hours and a trans-earth time of 90 hours assumed.

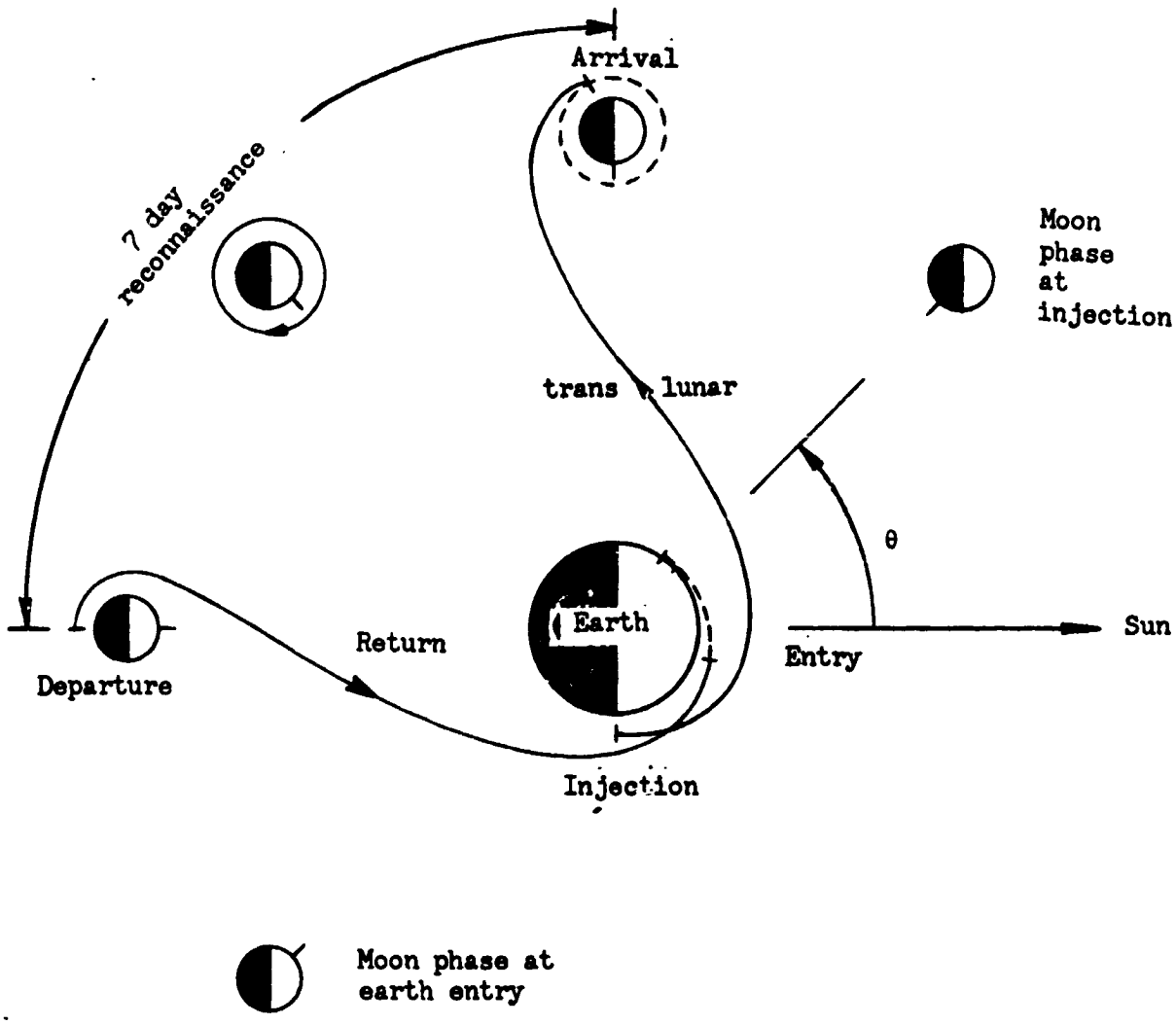

(a) General earth-moon configuration

Figure 26.- Configuration of earth and moon during a 14 day (7 day lunar stay time) Apollo reconnaissance mission. Ticks on moon denote 0° longitude, 0° latitude.

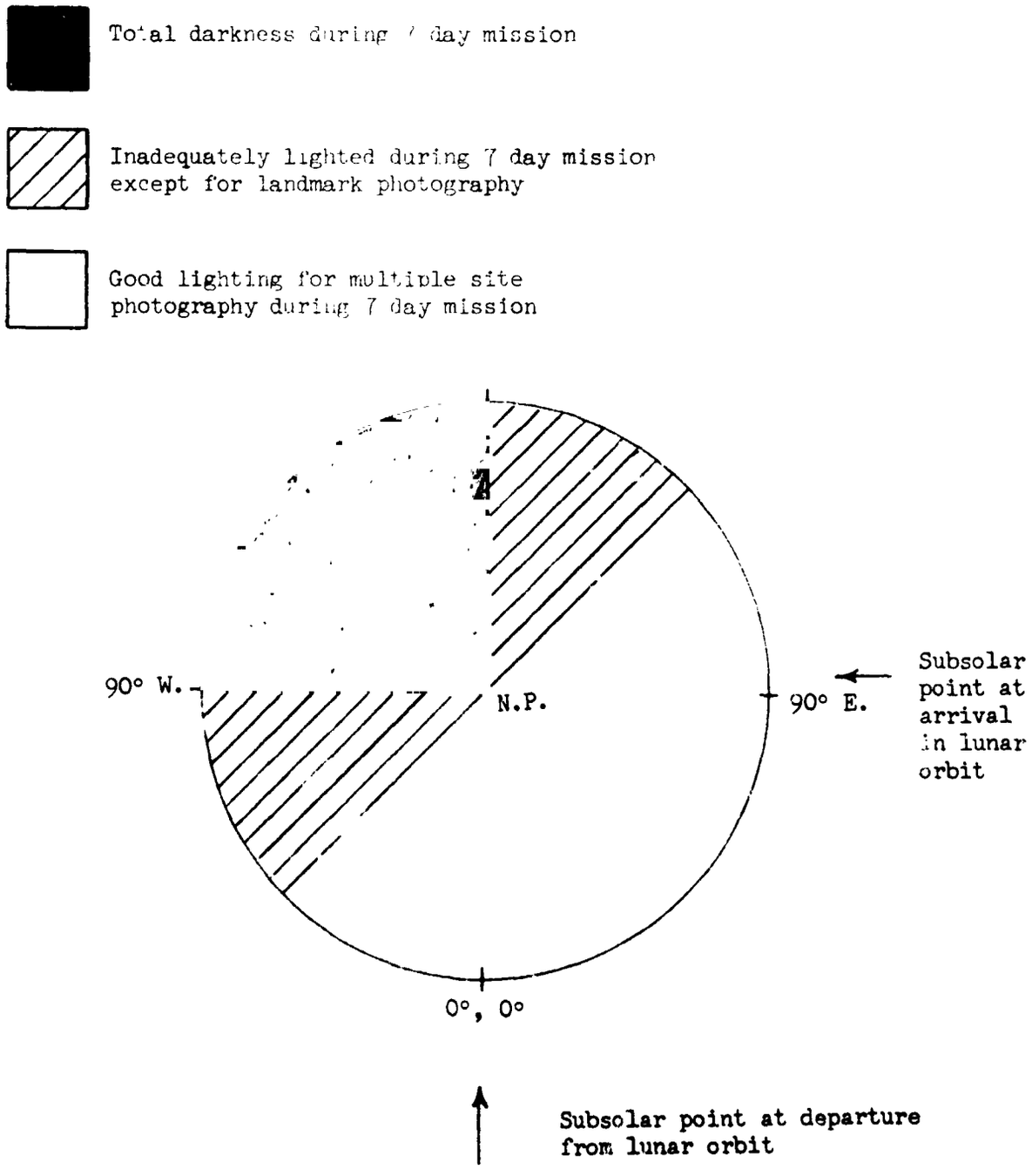

(b) Lighting conditions on moon during 7 day lunar stay time

Figure 26.- Configuration of earth and moon during a 14 day (7 day lunar stay time) Apollo reconnaissance mission. Ticks on moon denote 0° longitude, 0° latitude - Concluded.

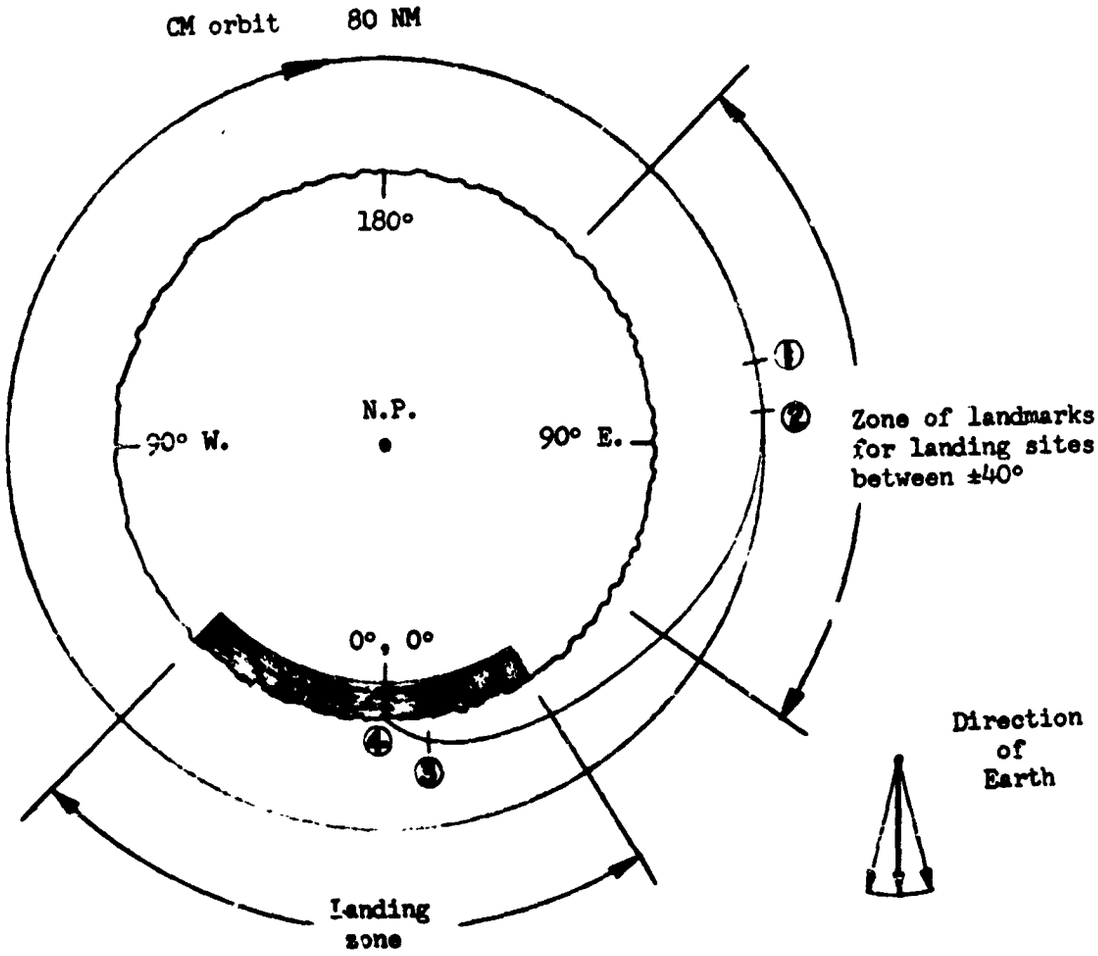

1. Position of CM and LEM at last landmark sighting prior to LEM descent for landing site at (4)
2. LEM transfer to equal period orbit
3. Initiate final braking maneuver to lunar surface
4. Landing site

Figure 27.- Relationship between landing zone and zone of landmarks for final invigational sighting prior to LEM descent. Example: Landing site at 0°, 0°.

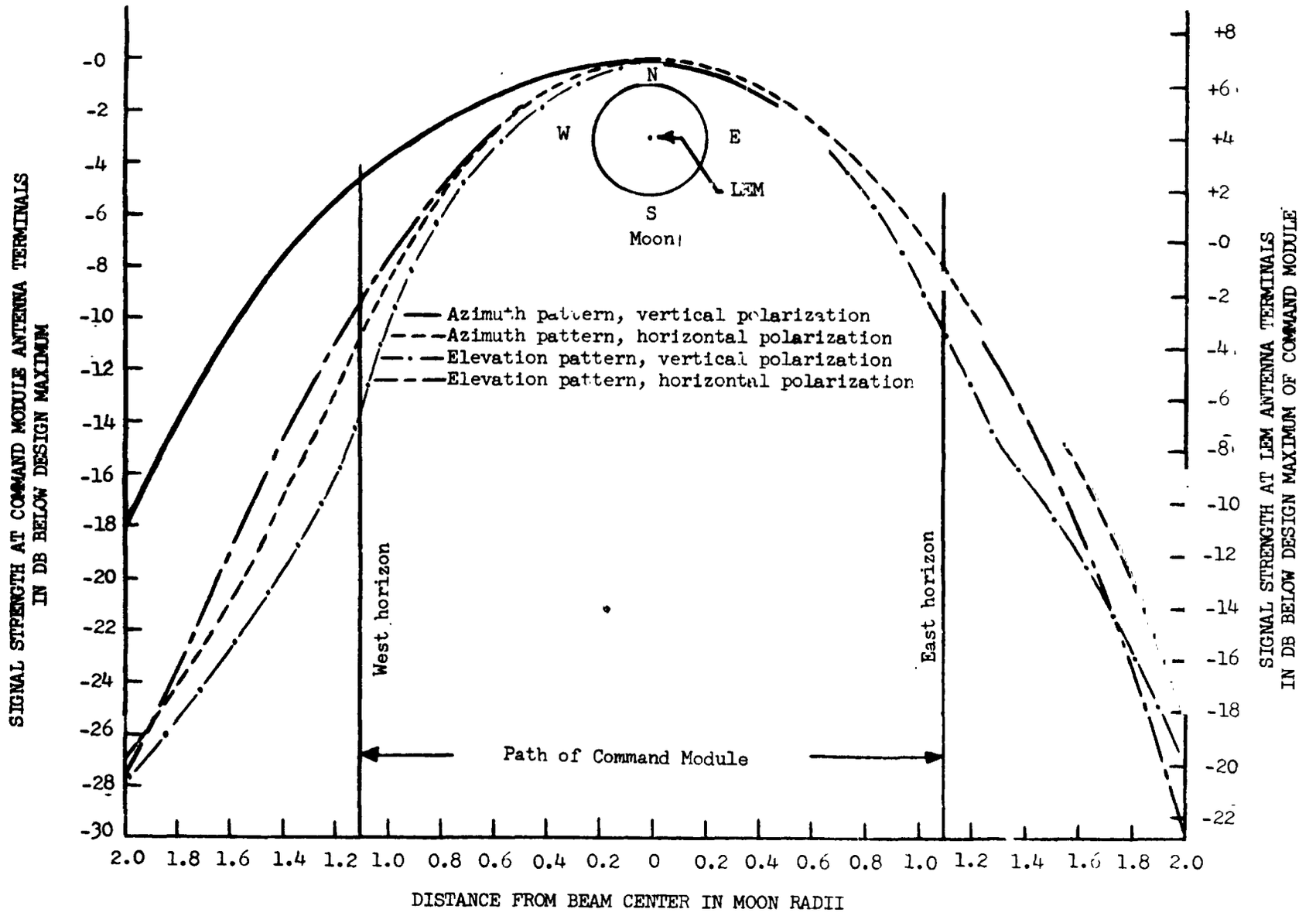

Figure 28.- Relative signal level seen by orbiting Command Module and LEM.

Moon's Surface as seen by Ground Station

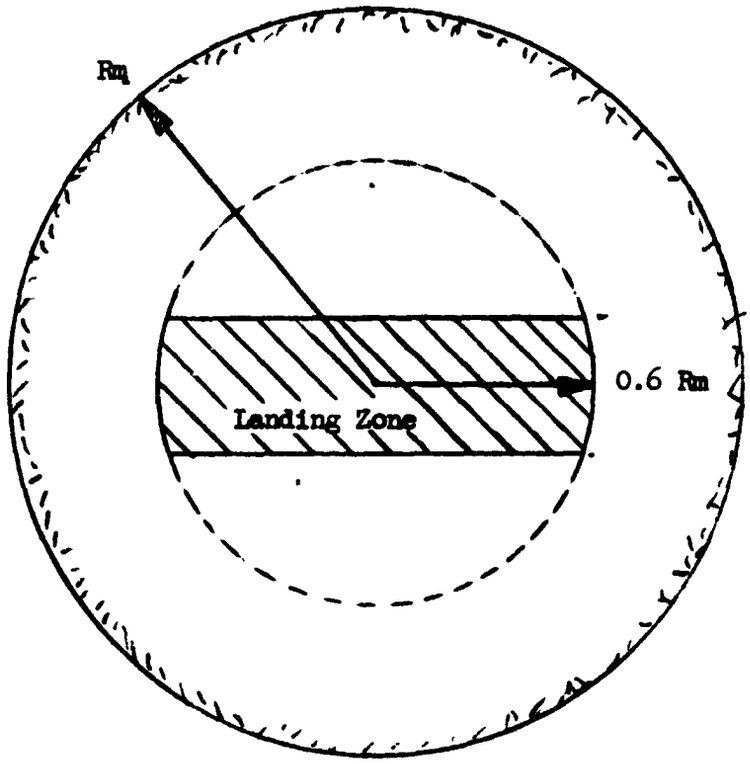

Figure 29.- Minimum relative signal level of -3 db may be maintained at both Command Module and LEM when the LEM is located within shaded area.

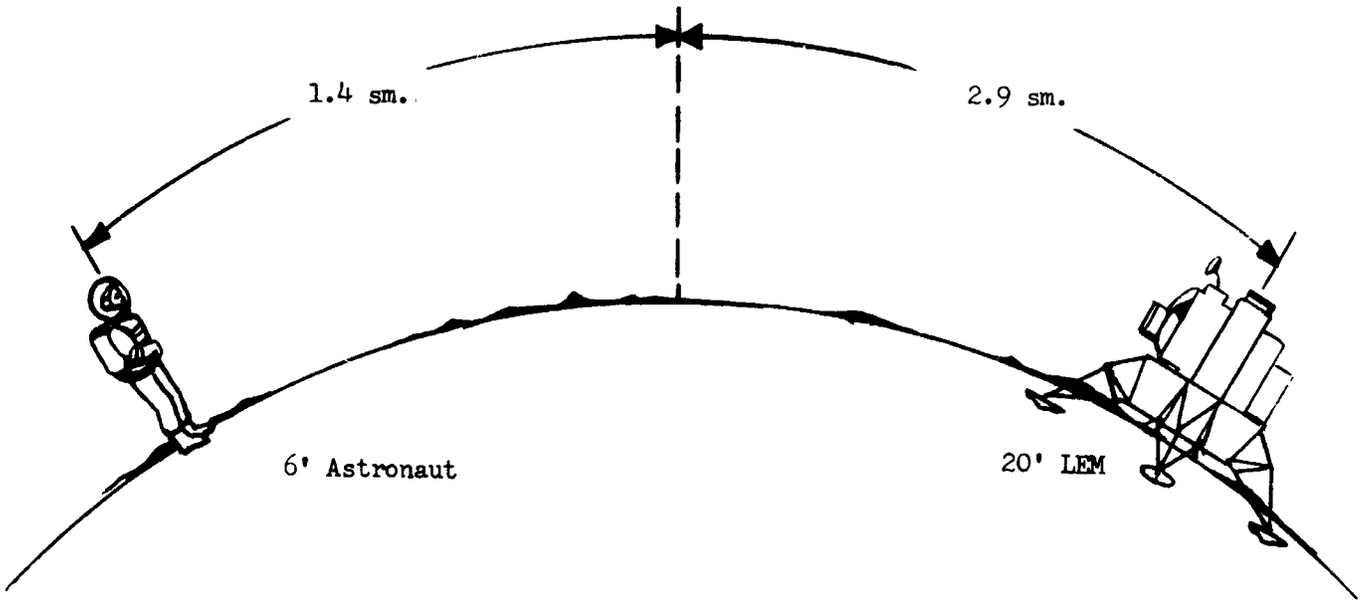

Range = 1.4 + 2.9 = 4.3 statute miles

Figure 30.- The range cut-off point due to curvature of lunar surface. Range is equal to the sum of the horizon distances for the astronaut and the LEM.

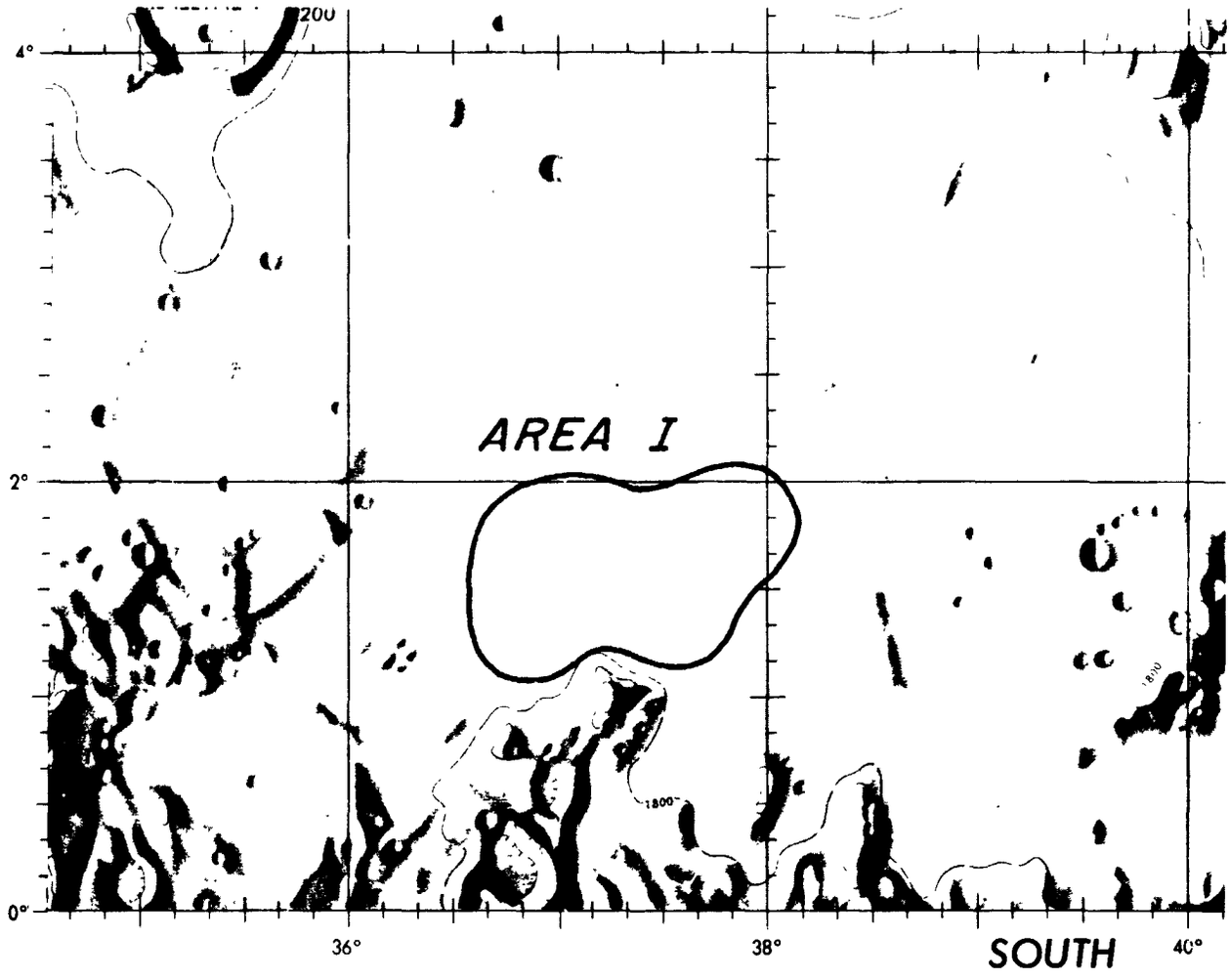

LUNAR CHART

SCALE 1:1,000,000

Published for
UNITED STATES AIR FORCE
and
NATIONAL AERONAUTICS AND SPACE ADMINISTRATION
by
AERONAUTICAL CHART AND INFORMATION CENTER
UNITED STATES AIR FORCE
ST. LOUIS 18, MISSOURI

TARUNTIUS

LAC 61

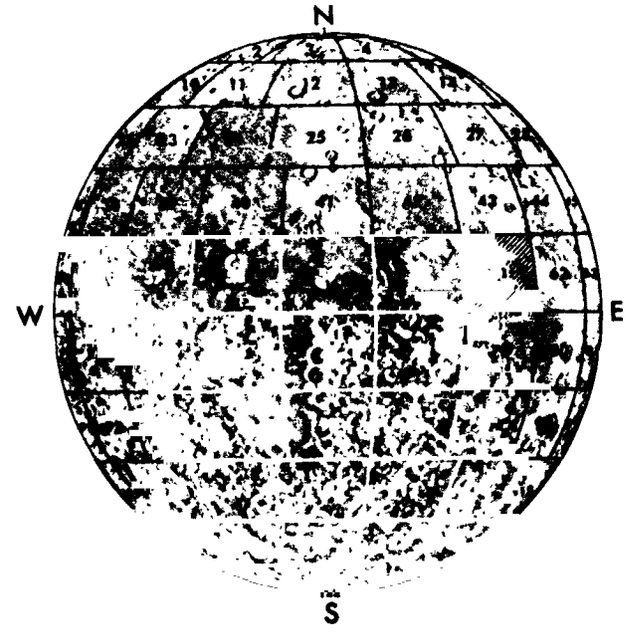

(a) Area I 36°55' E. 1°45' N.

Figure 31.- Recommended lunar landing areas.

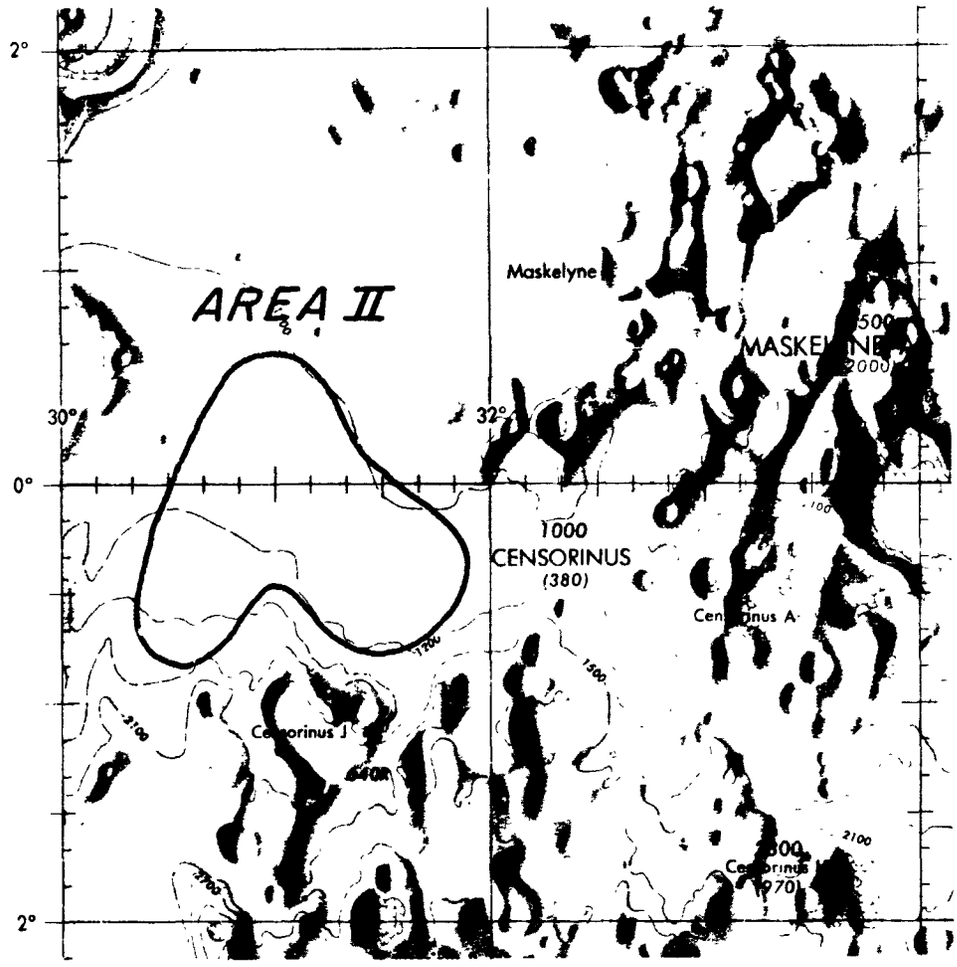

LUNAR CHART

SCALE 1:1,000,000

Published for
UNITED STATES AIR FORCE
and
NATIONAL AERONAUTICS AND SPACE ADMINISTRATION
by
AERONAUTICAL CHART AND INFORMATION CENTER
UNITED STATES AIR FORCE
ST. LOUIS 18, MISSOURI

COLOMBO

LAC 79

Mercator Projection
Scale 1:1,000,000 at 11°00'45"

1ST EDITION APRIL 1963

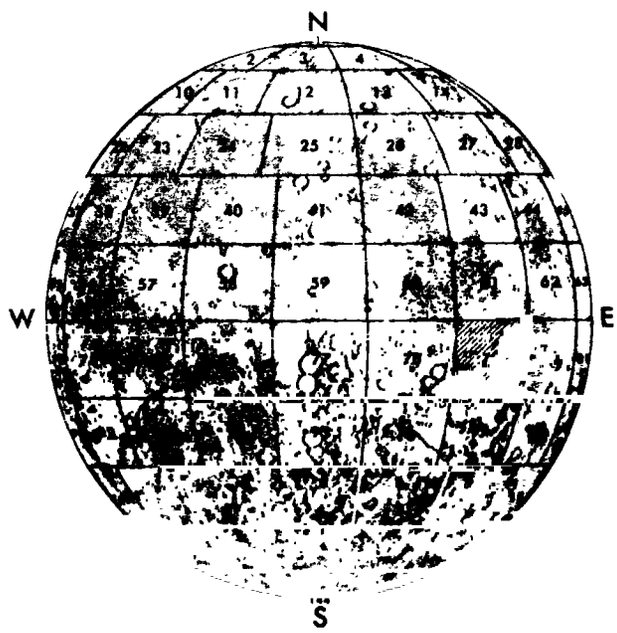

(b) Area II 31° E. 0° N.

Figure 31.- Recommended lunar landing areas - Continued.

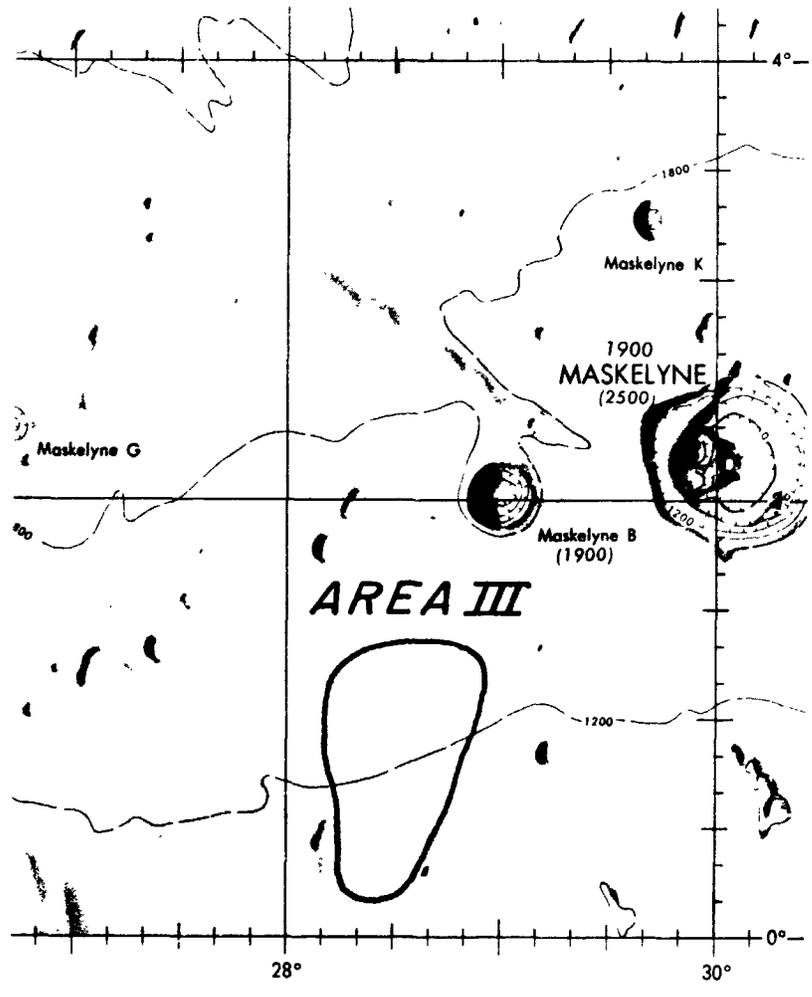

LUNAR CHART

SCALE 1:1,000,000

Published for
UNITED STATES AIR FORCE
and
NATIONAL AERONAUTICS AND SPACE ADMINISTRATION
by
AERONAUTICAL CHART AND INFORMATION CENTER
UNITED STATES AIR FORCE
ST. LOUIS 18, MISSOURI

JULIUS CAESAR

LAC 60

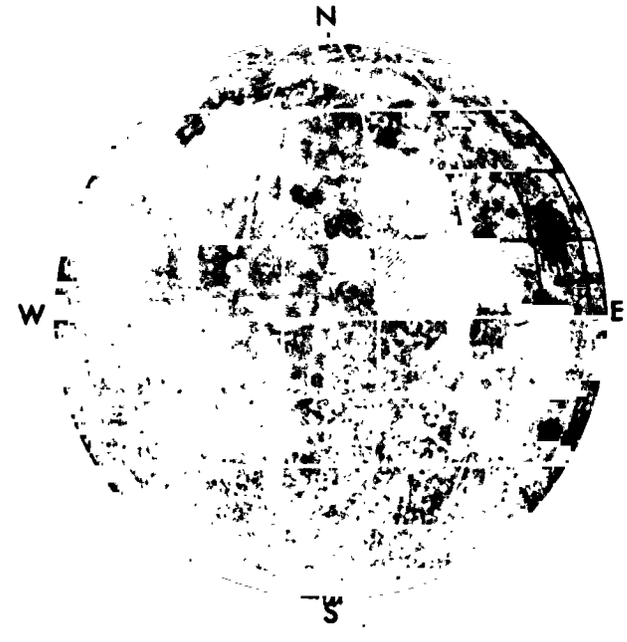

(c) Area III 28°22' E. 1°10' N.

Figure 31.- Recommended lunar landing areas - Continued.

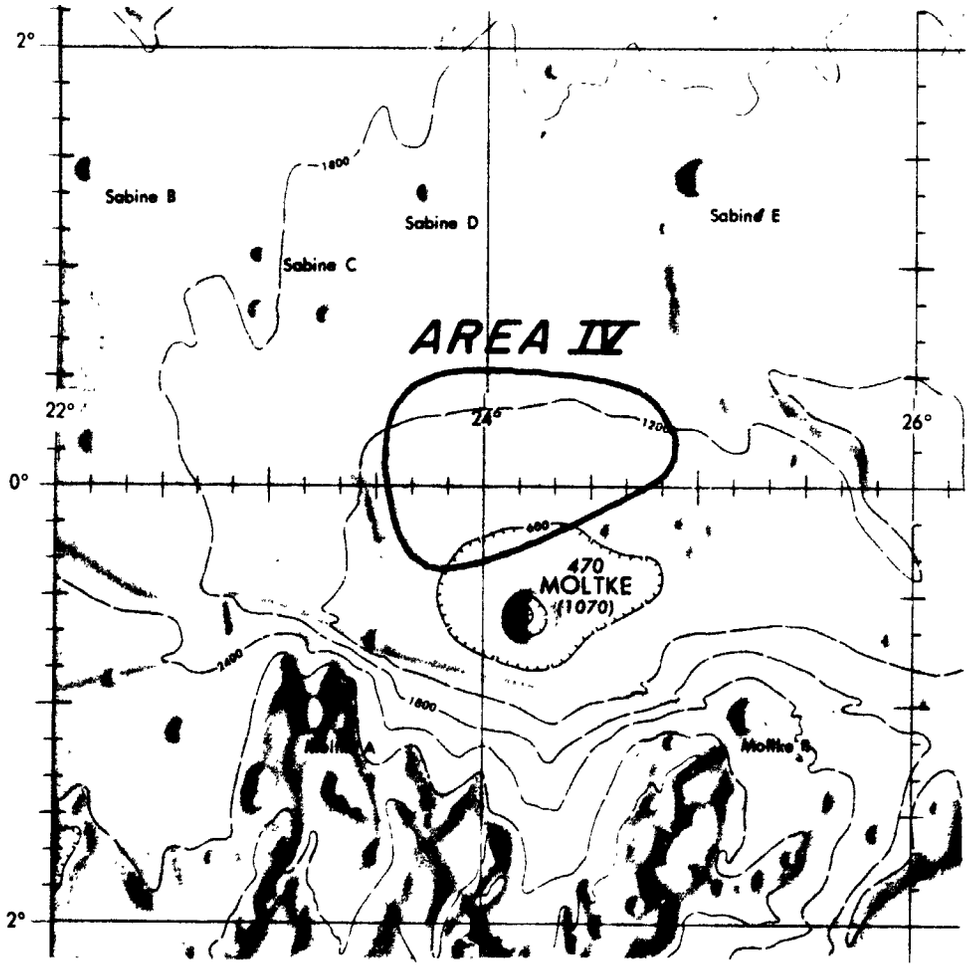

LUNAR CHART

SCALE 1:1,000,000

Published for
UNITED STATES AIR FORCE
and
NATIONAL AERONAUTICS AND SPACE ADMINISTRATION
by
AERONAUTICAL CHART AND INFORMATION CENTER
UNITED STATES AIR FORCE
ST. LOUIS 18, MISSOURI

THEOPHILUS

LAC 78

Mercator Projection
Scale 1:1,000,000 at 11°00'45"

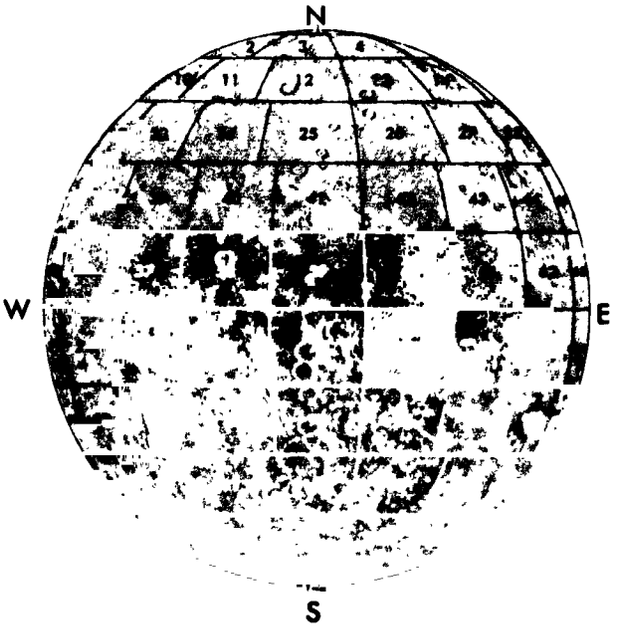

(d) Area IV 24°10' E. 0°10' N.

Figure 31.- Recommended lunar landing areas - Continued.

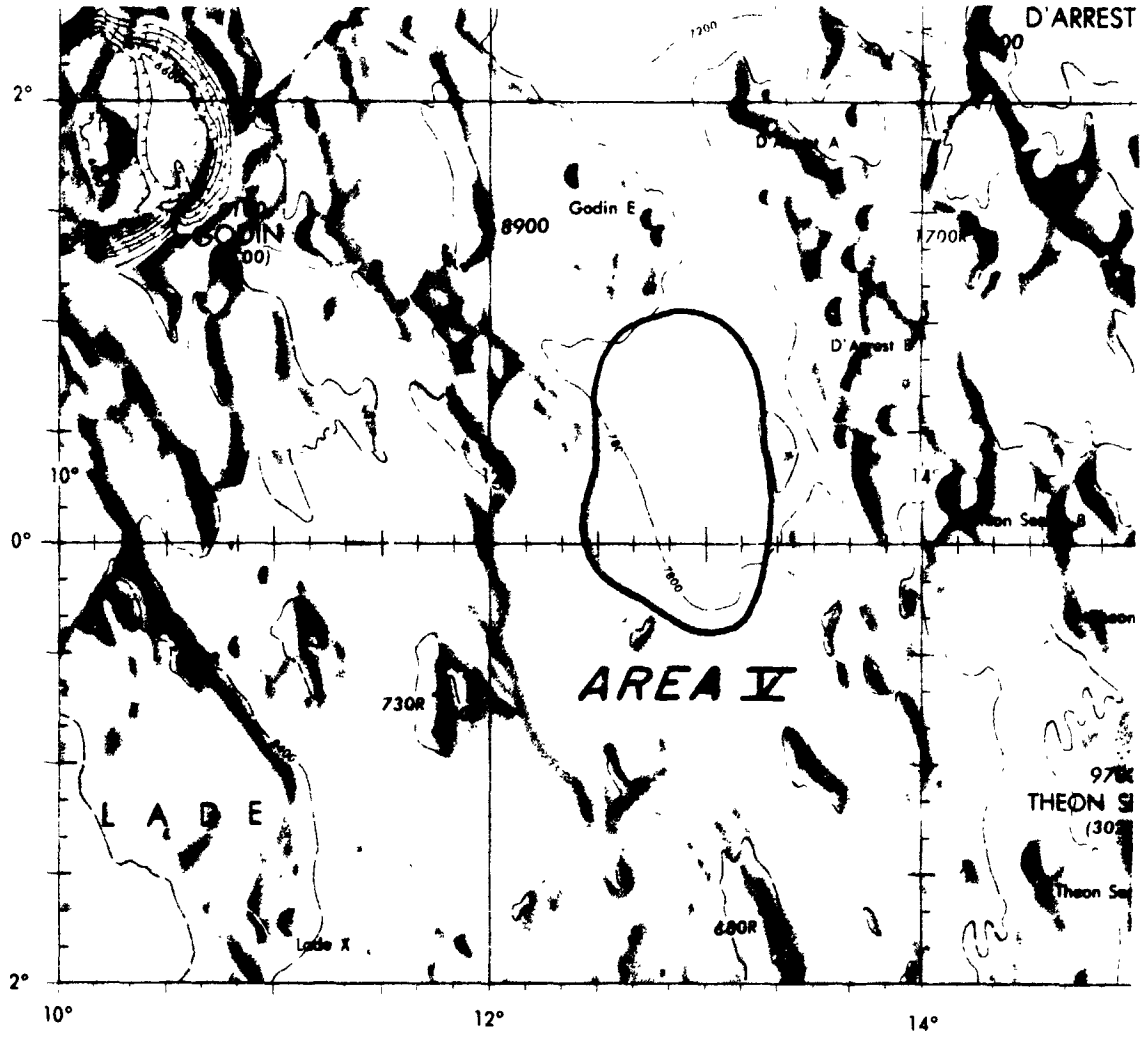

LUNAR CHART

SCALE 1:1,000,000

Published for
UNITED STATES AIR FORCE
and
NATIONAL AERONAUTICS AND SPACE ADMINISTRATION
by
AERONAUTICAL CHART AND INFORMATION CENTER
UNITED STATES AIR FORCE
ST. LOUIS 18, MISSOURI

JULIUS CAESAR

LAC 60

(e) Area V 12°50' E. 0°20' N.

Figure 31.- Recommended lunar landing areas - Continued.

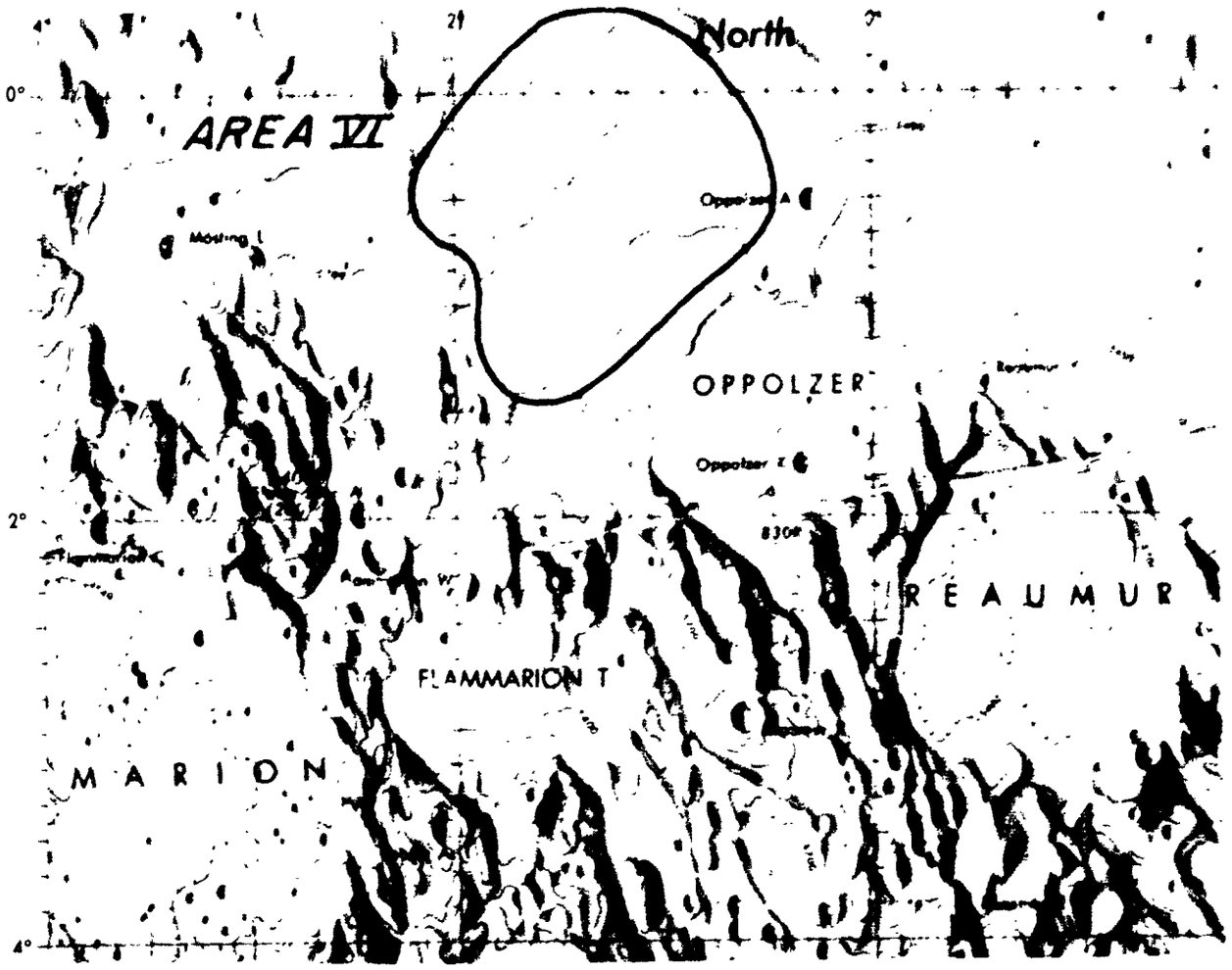

LUNAR CHART

SCALE 1:1,000,000

Published for
UNITED STATES AIR FORCE
and
NATIONAL AERONAUTICS AND SPACE ADMINISTRATION
by
AERONAUTICAL CHART AND INFORMATION CENTER
UNITED STATES AIR FORCE
ST. LOUIS 18, MISSOURI

PTOLEMAEUS

LAC 77

Mercator Projection
Scale 1:1,000,000 at 11°00'45"

1ST EDITION MAY 1963

LOCATION OF CHART AREA

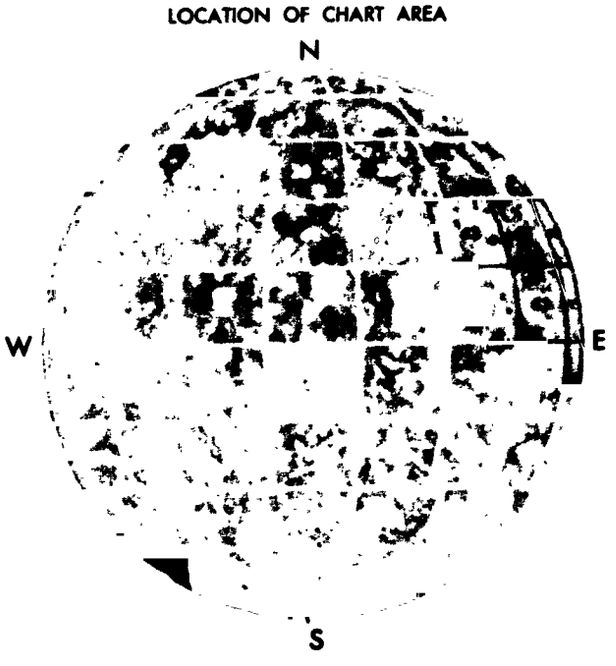

(f) Area VI 1°28' W. 0°30' S.

Figure 31.- Recommended lunar landing areas - Continued.

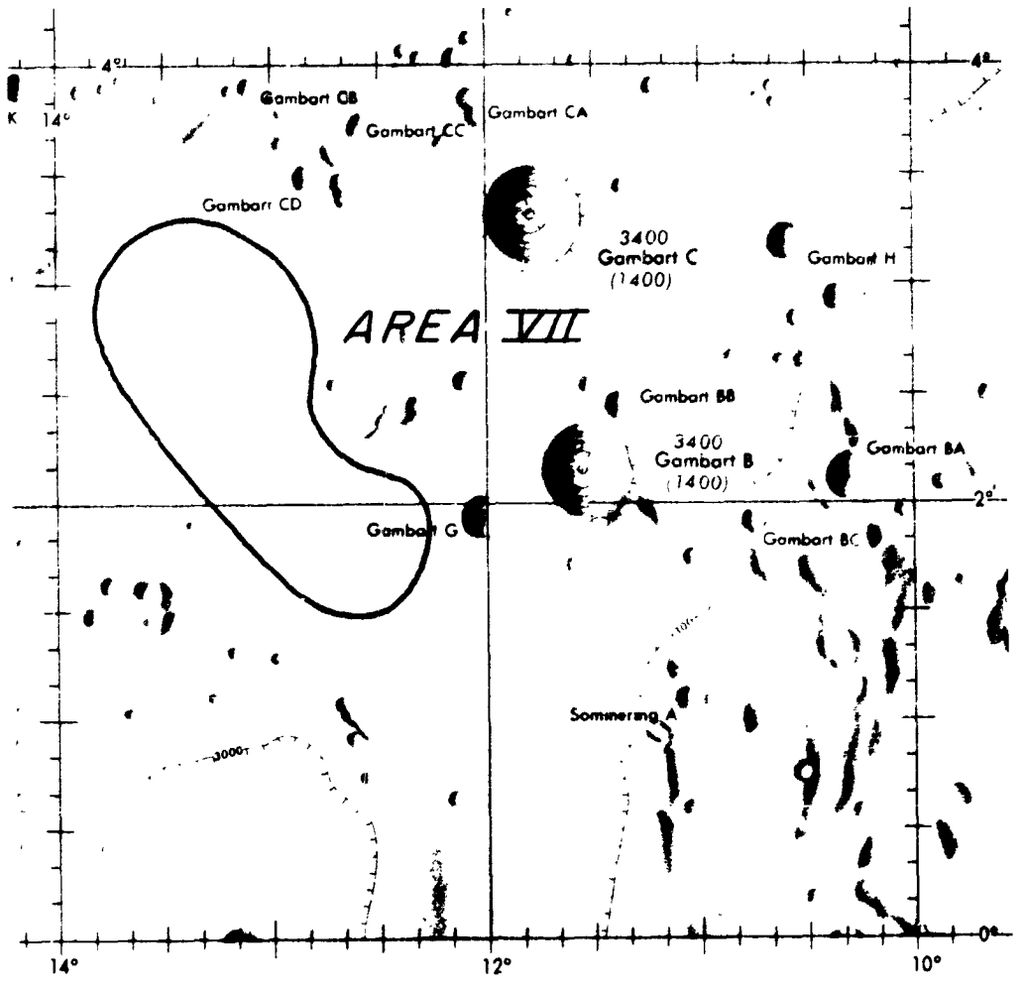

LUNAR CHART

SCALE 1:1,000,000

Published for
UNITED STATES AIR FORCE
and
NATIONAL AERONAUTICS AND SPACE ADMINISTRATION
by
AERONAUTICAL CHART AND INFORMATION CENTER
UNITED STATES AIR FORCE
ST LOUIS 18, MISSOURI

COPERNICUS

LAC 58

Mercator Projection
Scale 1:1,000 000 at 11°00'45"

1ST EDITION JULY 1961

INDEX TO ADJOINING SHEETS

(g) Area VII 13°15' W. 2°45' N.

Figure 31.- Recommended lunar landing areas - Continued.

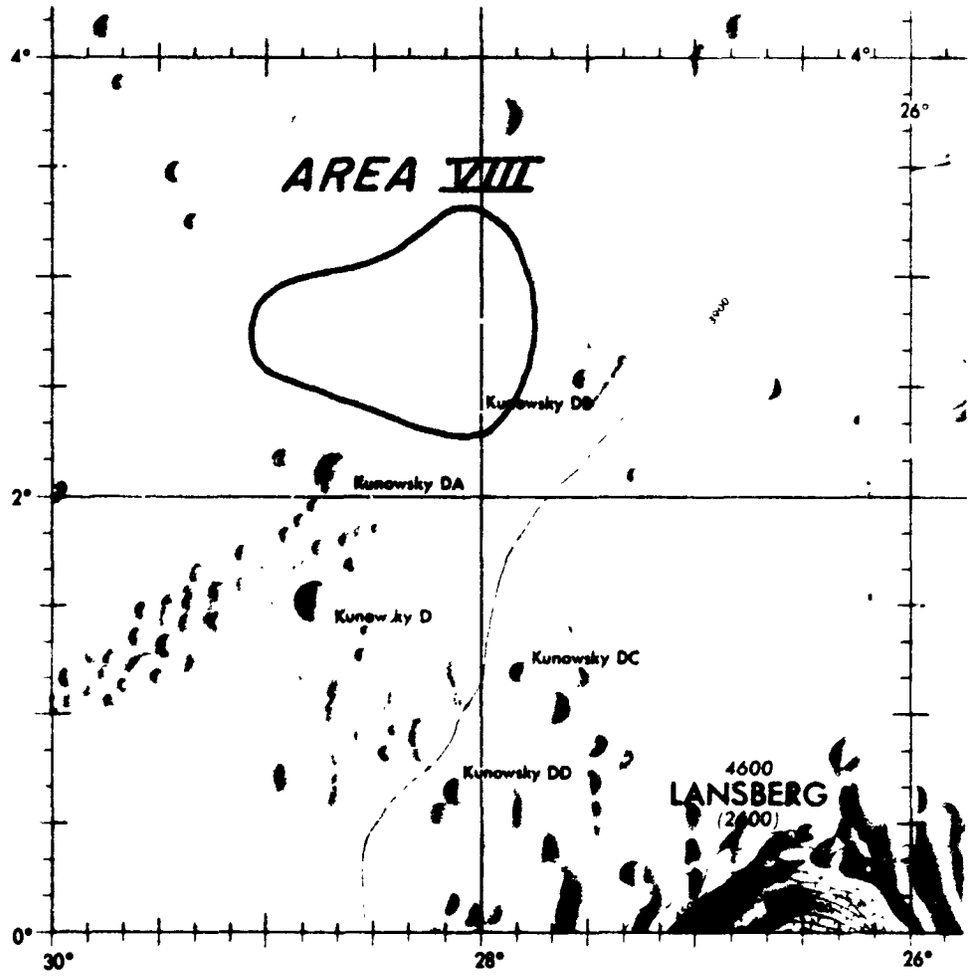

LUNAR CHART

SCALE 1:1,000,000

Published for
UNITED STATES AIR FORCE
and
NATIONAL AERONAUTICS AND SPACE ADMINISTRATION
by
AERONAUTICAL CHART AND INFORMATION CENTER
UNITED STATES AIR FORCE
ST. LOUIS 18, MISSOURI

COPERNICUS

LAC 58

Mercator Projection
Scale 1:1,000 000 at 11°00'45"

1ST EDITION JULY 1961

(h) Area VIII 28°15' W. 2°45' N.

Figure 31.- Recommended lunar landing areas - Continued.

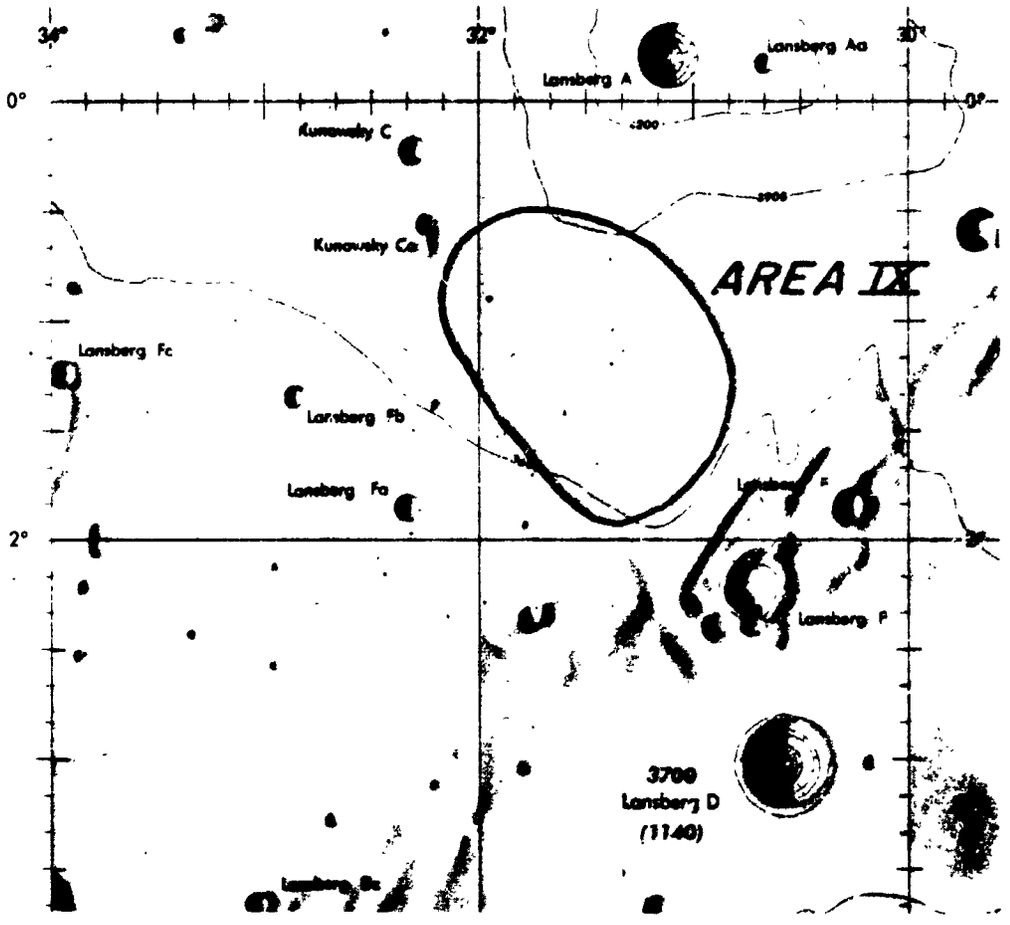

LUNAR CHART

SCALE 1:1,000,000

Published for
UNITED STATES AIR FORCE
and
NATIONAL AERONAUTICS AND SPACE ADMINISTRATION
by
AERONAUTICAL CHART AND INFORMATION CENTER
UNITED STATES AIR FORCE
ST LOUIS 18, MISSOURI

LETRONNE

LAC 75

Mercator Projection
Scale 1:1,000,000 at 11°00'45"

2ND EDITION JUNE 1962

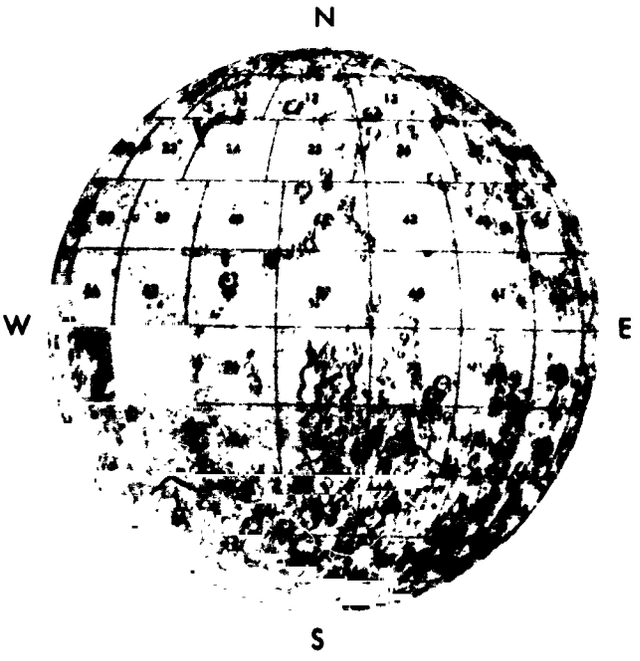

(i) Area IX 31°30' W. 1°05' S.

Figure 31.- Recommended lunar landing areas - Continued.

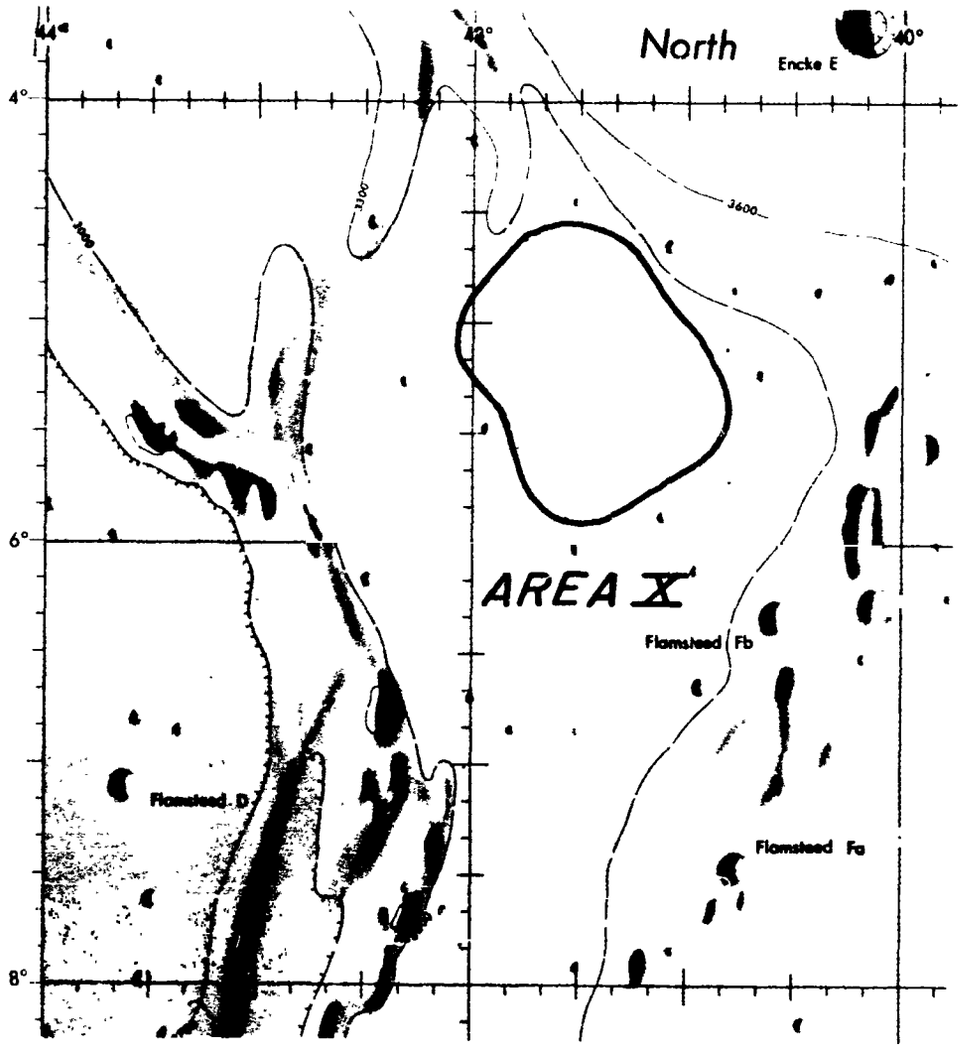

LUNAR CHART

SCALE 1:1,000,000

Published for
UNITED STATES AIR FORCE
and
NATIONAL AERONAUTICS AND SPACE ADMINISTRATION
by
AERONAUTICAL CHART AND INFORMATION CENTER
UNITED STATES AIR FORCE
ST LOUIS 18, MISSOURI

LETRONNE

LAC 75

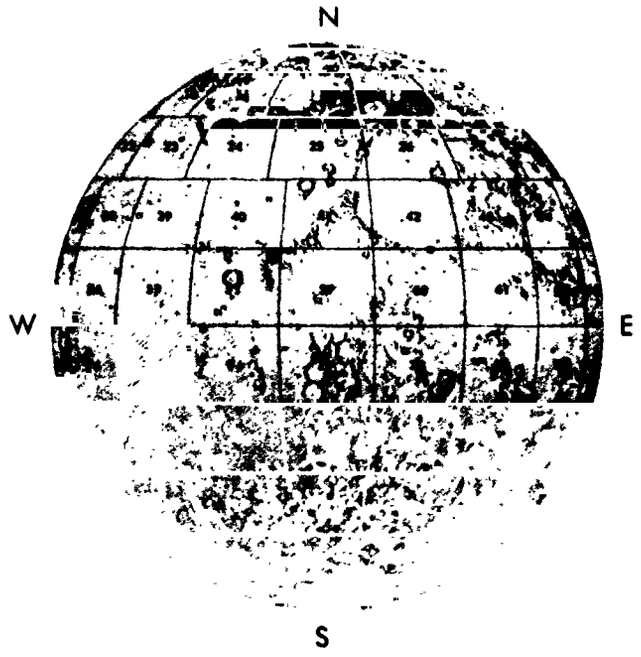

(j) Area X 41°30' W. 1°10' S.

Figure 31.- Recommended lunar landing areas - Concluded.

2307-63